ROYAL AIRCRAFT ESTABLISHMENT
BEDFORD.

R. & M. No. 3264

MINISTRY OF AVIATION

AERONAUTICAL RESEARCH COUNCIL
REPORTS AND MEMORANDA

Wind Tunnel Tests and Theoretical Investigations on the Effect of a Localised Mass on the Flutter of a Delta Wing with Fixed Root

By G. F. Donno, B.Sc.(Eng.), A.F.R.Ae.S.
Design Department, Westland Aircraft Ltd., Saunders-Roe Division.

LONDON: HER MAJESTY'S STATIONERY OFFICE
1962
PRICE £1 7s. 6d. NET

Wind Tunnel Tests and Theoretical Investigations on the Effect of a Localised Mass on the Flutter of a Delta Wing with Fixed Root

By G. F. Donno

*Reports and Memoranda No. 3264**
March, 1959

Summary.—Wind tunnel tests and theoretical investigations have been carried out to study the effect of a localised mass on the flutter characteristics of a delta wing. The experimental work covered a wide range of spanwise and chordwise positions of the mass c.g., variation of the magnitude and radius of gyration of the mass itself, and the effect of the stiffness distribution of the wing. The theoretical work was more limited in its scope and was primarily intended to investigate the reliability of the theoretical approach to this kind of problem.

These investigations have shown that the flutter characteristics of a delta wing carrying a localised mass are primarily dependent on the location of the mass, its magnitude and the stiffness distribution of the wing itself. The flutter speed with a localised mass judiciously placed may be from three to four times that obtained with the same mass in a bad position.

A localised mass in the region around the structural axis generally has an adverse effect on the flutter characteristics, while locations well aft, towards the trailing edge, are usually favourable. Particularly high flutter speeds are often associated with a localised mass close to the leading edge, but some caution is necessary, especially around the mid-span position, as the flutter characteristics in this region are very sensitive to variations in actual mass.

A fair measure of success was obtained in the theoretical investigations, the calculated flutter characteristics being in reasonable agreement with experimental results in most cases. Calculations based on resonance test modes gave remarkably good results in certain cases, but in general, this method showed only a slight superiority over the arbitrary mode approach.

1. *Introduction.* Earlier work carried out in connection with the design of the SR.53 had shown that the fitting of a considerable localised mass to a delta wing could produce changes in the flutter characteristics which are of the same order of magnitude as those which occur in the case of wings of higher aspect ratio. The work on the SR.53, however, was restricted to a study of the effects of a localised mass at the wing tip, whereas the present investigations have covered variations in both the spanwise and chordwise location of a localised mass, together with variations in its magnitude and radius of gyration. The effects of a variation in the wing stiffness distribution, corresponding to the effect of a large cut-out, *e.g.*, undercarriage bay, have also been investigated.

* Previously issued as Westland Aircraft Ltd., Saunders-Roe Division, Report No. Structure /0/37—A.R.C. 21,234.

Both wind tunnel flutter tests and theoretical investigations were carried out in the course of the programme. The former covered a wide range of parameter variations and a total of approximately one hundred and fifty separate cases were investigated. It was impracticable, of course, to cover anything like this range in the course of the theoretical work and ten representative cases were therefore selected for flutter calculations. These ten cases were investigated using both arbitrary modes and resonance modes, the latter being obtained from tests on the model.

2. *Description of the Model.* The model wing used for these investigations was of the now familiar segmented construction, comprising an aluminium alloy plate spar carrying a number of wooden box segments having the required aerofoil shape.

The spar was adapted from the taper-machined plate spar used in the SR.53 wing flutter model. As the latter had a high 'bare wing' flutter speed, however, it was necessary to reduce the stiffness of the spar quite drastically in order to permit investigation of those cases in which the localised mass increases the flutter speed above that of the bare wing. This was achieved by means of saw-cuts from the front and rear edges of the spar, thereby reducing its effective width and stiffness but without appreciably reducing its weight or interfering with the arrangements for attaching the box segments. (*See* Fig. 2.) For the first series of tests (*i.e.*, for a wing without a cut-out) the depth of these saw-cuts was graduated so as to give a fairly smooth grading of stiffness from root to tip. To simulate the cut-out for the second part of the programme, the cuts in the inner portion of the wing were increased in depth so as to reduce the effective width of the spar to about one half its previous value. (*See* Fig. 2.)

The root of the spar was clamped between two substantial angle section members so as to provide a 'fixed root' when set up in the wind tunnel for flutter tests or bolted to a rig for resonance testing.

The aerodynamic form of the flutter model was made up of nine box segments and a tip fairing. These were constructed of balsa and thin plywood and carried a small amount of lead ballast to simulate the inertia properties of a typical aircraft wing of this type. To prevent this shell from making any significant contribution to the overall stiffness of the wing, each segment was bolted to the spar at one spanwise position only, and for the same reason the gaps between the segments were not sealed. Very thin rubber sealing strips were originally fitted to the SR.53 flutter model but it was found that, at the tunnel speeds involved, their removal made no sensible difference to the flutter characteristics. The geometry of the assembled wing is shown in Fig. 1, and the leading particulars are as follows:

Semi-span (overall)	23·5 in.
Root Chord	29·5 in.
Tip Chord (Projected)	8·22 in.
L.E. Sweepback	42 deg
T.E. Sweepback	0 deg
Thickness/Chord Ratio	6 per cent

3. *Stiffness and Resonance Tests.* 3.1. *Stiffness Tests.* Torsional and flexural stiffness tests were carried out to provide basic structural data for arbitrary mode flutter calculations. The model was tested when it was assembled for the first series of tests and again after the spar had been modified to simulate the effect of a large cut-out.

3.2. *Resonance Tests.* Resonance tests were carried out to obtain the modes for use in the theoretical flutter investigations. Of the total of ten cases investigated, seven were for the original wing and three for the wing with its stiffness modified to simulate a large cut-out. Details of these cases are given below in Section 5 'Theoretical Investigations'.

The wing was rigidly mounted at the root and the localised masses were applied through the remote loading rig as in wind tunnel tests. Excitation in these tests was provided by means of a variable eccentric driven by a d.c. electric motor operated as part of a Ward-Leonard set. The actual connection on to the model was made with a length of rubber shock-absorber cord.

Because of the extreme flexibility of the model, no method for determining vibration amplitudes that involved any mechanical connection to the model could be considered. Fortunately, however, a photographic method, originally developed in connection with work on the SR.53 flutter models was available. A series of small white markers or 'flags', were fitted along the leading and trailing edges of the model and a white grid was constructed to cover the whole of one surface of the wing. By making time exposures with the model resonating it was possible to derive the amplitude of vibration and the location of the nodal lines.

4. *Wind Tunnel Tests.* Experimental flutter investigations were carried out in a low speed wind tunnel with a 6 ft by 4 ft elliptical open working section. The maximum speed obtainable was approximately 120 ft/sec.

The model was mounted vertically in the tunnel to avoid large static displacements under gravity (its stiffness being very low) and a plate incorporated in the root mounting acted as a reflector to simulate symmetric flow conditions.

The localised masses were applied to the wing through a remote loading rig of the type described in Ref. 1. With this arrangement there is less possibility of the results being influenced by aerodynamic effects than with localised masses of different shapes and sizes fitted directly to the wings. Other advantages over the fitting of large concentrated weights to the wing are that large gravitational forces on the model are avoided, while the loading platform of the rig makes a good safety device that can be held should the flutter motion become too violent.

Flutter frequencies were obtained from analysis of cine-film records of the flutter motion. By this means it was also possible to study the motion in detail without risking loss of the model by prolonged running above the flutter speed.

(A detailed account of these wind tunnel flutter tests is given in Appendix I.)

4.1. *Programme of Flutter Tests.* 4.1.1. *Tests on the model with original spar (i.e., no cut-out).* After an initial run to determine the flutter characteristics of the bare wing, the following series of investigations were carried out to determine the effect of various parameters relating to the localised mass:

(*a*) *Detailed investigation of the effect of spanwise and chordwise location of the localised mass.* Flutter characteristics were determined with the mass located at each of six evenly spaced stations, across the chord from L.E. to T.E., at 25, 50, 75 and 100 per cent of the semi-span.

This investigation was carried out in full for three different localised masses, representing 40, 70 and 100 per cent of the bare wing weight. The radius of gyration of the localised mass was kept constant throughout, at 30 per cent of the wing mean chord. A more detailed investigation of the effects of varying the magnitude of the localised mass at four selected stations was carried out later. (*See* paragraph (*c*) below.)

(*b*) *Investigations of the effect of variation of the radius of gyration without change of mass.* In this part of the programme, the localised mass was kept constant and equal to the weight of the bare wing, while the radius of gyration was increased in five equal steps from 20 per cent to 40 per cent of the wing mean chord.

This procedure was repeated for four different positions of the localised mass, namely, wing-tip L.E., wing-tip T.E., 50 per cent semi-span L.E. and 50 per cent semi-span T.E.

(*c*) *Investigation of the effect of variation of mass without change of radius of gyration.* The tests already noted in paragraph (*a*) above, involved the investigation of broad variations of this kind, but for certain selected locations the effect of variation of the localised mass was investigated in greater detail. The radius of gyration of the localised mass was kept constant at 30 per cent of the mean chord while the mass was increased in five equal increments from 40 per cent to 100 per cent of the bare wing weight.

The stations selected for these investigations were the same as those chosen in the work described in paragraph (*b*).

4.1.2. *Tests on the model with a modified spar, simulating a large cut-out.* The programme of tests carried out on the model after modification was not so extensive as in the previous series described above.

Following an initial test to determine the flutter characteristics of the bare wing, the effects of the spanwise and chordwise position of the localised mass were investigated. The investigations were essentially similar to those described in paragraph (*a*) of Section 3.1.1, but only two sections, at mid-span and the wing-tip, were considered.

5. *Theoretical Investigations.* Theoretical investigations on the flutter model have covered ten selected cases, comprising:

(*a*) *Investigation on model wing with original spar (i.e., no cut-out).*

Case 1. Bare wing with no localised mass.

Case 2. Localised mass (70 per cent of bare wing weight) at 75 per cent semi-span on L.E.

Case 3. Localised mass (70 per cent of bare wing weight) at 75 per cent semi-span on 40 per cent chord line.

Case 4. Localised mass (70 per cent of bare wing weight) at 75 per cent semi-span on T.E.

Case 5. Localised mass (70 per cent of bare wing weight) at wing-tip on L.E.

Case 6. Localised mass (70 per cent of bare wing weight) at wing-tip on 40 per cent chord line.

Case 7. Localised mass (70 per cent of bare wing weight) at wing-tip on T.E.

(*b*) *Investigations on model with modified spar, simulating a large cut-out.*

Case 1A. Bare wing with no localised mass.

Case 5A. Localised mass (70 per cent of bare wing weight) at wing-tip on L.E.

Case 6A. Localised mass (70 per cent of bare wing weight) at wing-tip on 40 per cent chord line.

In all cases, the flutter characteristics were calculated using both arbitrary modes and modes obtained from resonance tests on the model. Equivalent constant strip derivatives were used throughout, these being estimated from steady motion data in accordance with the procedure given in Ref. 2.

5.1. *Arbitrary Mode Flutter Calculations.* Three bending modes and three torsion modes were used in these flutter calculations. All of these modes were simple polynomial functions of the spanwise position and were defined as follows:

Mode 1	$f_1 = \eta^2$	Bending Modes.
Mode 2	$f_2 = \eta^2 - \eta^3$	
Mode 3	$f_3 = \eta^2 - 3\eta^3 + 2\eta^4$	
Mode 4	$f_4 = \eta$	Torsion Modes.
Mode 5	$f_5 = \eta - \eta^2$	
Mode 6	$f_6 = \eta - 3\eta^2 + 2\eta^3$	

'η' being the spanwise co-ordinate (y/s).

These forms were chosen in the hope that the resulting flutter equations would be sufficiently well-conditioned for solution on an analogue computer, while the fact that, with the localised mass located at the wing-tip, any changes in the parameters relating to the mass affected only the 1–4 binary, reduced the amount of computation involved. The first of these objects was not achieved, however, and before satisfactory solutions could be obtained from the analogue computer it was found necessary to transform the co-ordinates to improve the conditioning. (Ref. 3.)

5.2. *Flutter Calculations based on Resonance Test Modes.* Resonance modes from the tests described in Section 4.2 were used in these investigations. The tests had covered the frequency range 0 to 20 c.p.s. and the number of resonances found within this range varied from four in Case 1, to six in some of the other cases.

In general, the modes were not strictly orthogonal, and the flutter equations were solved with and without inertia couplings included in them. The possibility of orthogonalising the modes to get rid of these inertia couplings was considered but rejected, since the existence of a cross-inertia implies the existence of a cross-stiffness as well and there seems to be no reliable means of evaluating the latter.

(Further details of both these and the arbitrary mode flutter calculations, including the matrices of coefficients, are given in Appendix II.)

6. *Results.* 6.1. *Results of Wind Tunnel Flutter Tests.* The results of wind tunnel tests to determine the effects of the spanwise and chordwise position of a localised mass are presented in the form of flutter 'contours' drawn on the plan form of the wing. These contours, which are lines of constant flutter speed and spaced at intervals of 10 per cent of the bare wing flutter speed, are based on the detailed wind tunnel test results given in Appendix I. The shaded areas are those in which the positioning of a localised mass will reduce the flutter speed below that of the bare wing. Figs. 3, 4 and 5, show the contours for the original delta wing with localised masses equal to 40, 70 and 100 per cent of the bare wing weight. For the wing with the spar modified to simulate a large cut-out, the relevant contour plots are given in Figs. 6, 7 and 8 respectively.

6.1.1. *Investigation of the effects of spanwise and chordwise location of a localised mass on the original delta wing.* Flutter 'contours' for a *localised mass equal to* 40 *per cent of the bare wing weight* are shown in Fig. 3. It will be seen that, with the exception of a small region of the leading edge towards the tip, the placing of such a mass anywhere forward of the mid-chord position will lower the flutter speed below that of the bare wing. There are two areas in which the placing of the mass will produce

particularly low flutter speeds, one centred on the leading edge at mid-span and one on the spar axis at the wing-tip. Flutter speeds appreciably in excess of that of the bare wing are associated with the mass very close to the leading edge from about 70 per cent semi-span outboard to the wing-tip, and with it well aft, towards the trailing edge. These regions in which the presence of the localised mass improves the flutter characteristics are by no means synonymous with those in which the placing of the mass produces overtone type flutter, the latter being limited to a small part of the leading edge in the immediate vicinity of the wing-tip.

When the localised mass is increased to 70 *per cent of the bare wing weight* the contours assume the form shown in Fig. 4. There is little change in the wing-tip region, but further inboard there are significant alterations. At mid-span, the area in which the localised mass will produce a low flutter speed has moved back from the leading edge towards the spar axis and there is now a narrow region along the entire leading edge in which the localised mass improves the flutter characteristics. This improvement is most marked for positions towards mid-span, the flutter speeds being more than 50 per cent above that of the bare wing and above the maximum obtainable in the wind tunnel. For this reason the only direct evidence that the flutter is of the overtone type has been obtained with the localised mass at the wing-tip, but, from the form of the chordwise plots of flutter speed and frequency in Appendix I there seems little doubt but that the flutter will be of this type with the mass anywhere in the region.

Aft of the spar axis, the changes in the form of the contours associated with the increase in the localised mass from 40 to 70 per cent of the bare wing weight are not very significant. Locations well down towards the trailing edge raise the flutter speed appreciably above that of the bare wing and in this respect the mid-span position seems particularly favourable. Generally speaking, the flutter motion is of the fundamental type, but with the mass at the wing-tip trailing edge the transition to the overtone type has occurred. It is suspected that a similar transition may occur with the mass on the trailing edge at mid-span, but the corresponding flutter speed was above the maximum that could be obtained in the wind tunnel.

With a *localised mass equal to the bare wing weight*, the flutter contours are as shown in Fig. 5. Comparison with those corresponding to the smaller masses shows that while the pattern remains much the same for a localised mass in the region of the wing-tip, the situation further inboard is much improved. Along almost the entire leading edge the addition of a localised mass of this magnitude will give a flutter speed well above that of the bare wing. The highest flutter speed appears to be associated with the mid-span position and at this section the mass may be located as much as 35 per cent of the chord aft of the leading edge without the speed falling below that of the bare wing. Overtone flutter occurs with the mass located in part of this leading edge sector, but the transition is not coincidental with the unit contour and flutter speeds in excess of that of the bare wing have been found with motion that is still of the fundamental type.

Behind the spar axis, the situation is much the same as with the smaller masses, at least so far as the flutter speed is concerned. As regards the type of flutter motion, however, there has been a reversion to the fundamental form for a localised mass at the wing-tip trailing edge. The overtone type may persist further inboard, but the associated flutter speeds were too high for satisfactory investigation in the wind tunnel.

6.1.2. *Investigation of the effects of spanwise and chordwise location of a localised mass on the modified delta wing.* (Structural stiffness modified to simulate a large cut-out.) Although this part of the programme was carried out at a later stage than the investigations described in Sections 6.1.3

and 6.1.4, the work was of the same type as that which gave the results described in Section 6.1.1 (above), and it seems convenient to deal with it at this point.

The results obtained with a *localised mass equal to* 40 *per cent of the bare wing weight* are shown as flutter contours in Fig. 6. Comparing this plot with that given for the same mass on the original wing (Fig. 4), it is seen that there is a broad similarity between them. The unfavourable region around the mid-span leading edge is slightly larger, however, and the reduction in flutter speed associated with it is much more drastic. In contrast, the area near the wing-tip where the localised mass lowers the flutter speed appreciably below that of the bare wing is reduced in size. The wing-tip leading edge position is still a favourable one for the positioning of a localised mass but the other good region, aft of the spar axis, has been reduced to a narrow strip along the trailing edge. The flutter motion is of the fundamental type, except in the case of the mass in the wing-tip leading edge region.

Fig. 7 shows the contours for a *localised mass equal to* 70 *per cent of the bare wing weight*. The low flutter speed region centred on the mid-span leading edge has extended further aft and further outboard and in its 'depths' the attachment of a localised mass can reduce the flutter speed to less than half that of the bare wing. The unfavourable region at the wing-tip seems to have almost disappeared, however, and there is now an appreciable area towards the trailing edge in which the localised mass raises the flutter speed above that of the bare wing. The wing-tip leading edge position is again favourable and is associated with overtone flutter. Elsewhere, the fundamental type motion is general, regardless of the flutter speed.

When the localised mass is increased to *equal the weight of the bare wing* the flutter contours change to the form shown in Fig. 8. The lowest flutter speeds are now associated with a mass close to the spar axis, while locations towards either the leading edge or trailing edge, give speeds in excess of that of the bare wing. The flutter motion is of the fundamental type for all positions of the localised mass, however, except for a small area adjacent to the wing-tip leading edge.

An unexpected feature of these results is the apparent falling-off of the flutter speed for a mass close to the leading edge at mid-span (after the initial rise from the flutter 'valley' on the spar axis). The drop is quite small, however, and may not have any particular significance.

6.1.3. *Investigation of the effects of variations in the radius of gyration of a localised mass* (*see* Figs. 9 and 10). As described in Section 4.1.1, paragraph (*b*), these investigations were carried out on the original wing with a localised mass equal to the bare wing weight. The radius of gyration was varied from 20 per cent to 40 per cent of the wing mean chord with the mass located at four different stations, *viz*:

(i) Wing-tip leading edge.

(ii) Wing-tip trailing edge.

(iii) Mid-span leading edge.

(iv) Mid-span trailing edge.

With the mass at both of the wing-tip stations it was found that the changes in the flutter characteristics associated with the specified variation of the radius of gyration were quite negligible.

In the case of the stations at mid-span, the results are of limited value, but as far as they go, they largely support those obtained with the mass at the wing-tip. When the programme of wind tunnel tests was drawn up, the choice of the mid-span section seemed reasonable enough. Unfortunately, however, the flutter speeds associated with a mass of this magnitude at both the leading and

trailing edges proved to be very high. In the case of the mass at the leading edge, the flutter speed was above the maximum obtainable in the tunnel, regardless of the radius of gyration.

With the mass at the trailing edge, flutter did occur with radii of gyration equal to 0·20, 0·24 and 0·32 times c_m, but not in the other three cases. The flutter speeds were so close to maximum tunnel speed, however, that it seems unlikely that this represents any significant trend.

6.1.4. *Investigation of the effects of variations in the magnitude of a localised mass* (*see* Figs. 11 and 12). Although the effects of variations in the magnitude of the localised mass were studied in a broad manner in the part of the programme that produced the data for the flutter 'contours', the effects of such variations were also investigated in detail for certain stations on the wing. The stations selected were the same as those chosen for the radius of gyration investigations (*see* Section 6.1.3 above), and the tests were carried out on the original wing before the spar was modified to simulate a large cut-out. The smallest localised mass considered was 40 per cent of the bare wing weight, and the largest, 100 per cent (*i.e.*, the same as in the flutter 'contour' investigations).

For the wing-tip leading edge position, it was found that the size of the localised mass had no significant effect on the flutter speed or frequency, the overtone type motion being maintained over the entire range. At the trailing edge, the magnitude of the mass had little effect on the flutter speed but large and significant changes occurred in the frequency. With the smallest localised mass, low frequency fundamental type flutter occurred, but, when the mass was increased above half the weight of the bare wing, this was replaced by the higher frequency overtone type. Further increases in the magnitude of the mass produced no sensible change in the flutter frequency until, with a mass equal to the bare wing weight, there was a sudden reversion to the low frequency fundamental type.

With the localised mass at mid-span, it was not possible to determine the actual flutter characteristics for the full range of mass variations because in some cases the flutter speed was above the maximum speed of the tunnel. However, the number of instances in which this occurred was less than in the case of the investigation into the effects of varying the radius of gyration of the mass (*see* Section 6.1.3 above).

The general trend from the results is for the flutter speed to increase with increased mass on either the leading or trailing edges at this mid-span section. In the case of the leading-edge location, the flutter speed was well below that of the bare wing for the smaller localised masses, but, beyond a mass ratio of about one-half, the speed increased very rapidly and soon exceeded the maximum obtainable in the wind tunnel. It seems probable that this increase in speed was accompanied by a transition from fundamental to overtone type flutter.

With the mass on the trailing edge the increase in the flutter speed with increasing weight was far more gradual. It seems possible that a transition to overtone flutter also occurred here when the localised mass became fairly large but there appears to be some scatter in the recorded frequencies which would mask such an effect.

6.2. *Results of Theoretical Investigations.* Theoretical flutter investigations were carried out for ten selected cases as described in Section 5. Seven of these cases were for the wing with its original spar and three for the wing with the spar modified to simulate a large cut-out. In all cases theoretical results have been obtained using both arbitrary modes and modes obtained from resonance tests.

6.2.1. *Results of arbitrary mode flutter calculations.* The results of these flutter calculations are set out in Table 1, together with the corresponding flutter speeds and frequencies as given by wind tunnel tests. The results in each case include the speeds and frequencies given by both the complete

six degree-of-freedom problem and the dominant binary or ternary. (The degrees-of-freedom, comprising three bending and three torsion modes, are defined in Section 5.1.)

The measure of agreement between theoretical and experimental flutter speeds varies considerably, but in all cases the speed from the six degrees-of-freedom problem is lower than that obtained from tunnel tests. One peculiar feature of these calculations is the fact that the dominant binary or ternary usually gives a flutter speed closer to the experimental results than does the complete senary.

In the case of the flutter frequencies, the values from calculations and tunnel tests for the wing with its original spar are generally in very good agreement, although there is a notable exception in Case 7, where the calculations failed to predict overtone flutter. For the wing with the modified spar, however, there are only two cases in which comparison is possible and in these the agreement is rather indifferent.

6.2.2. *Results of flutter calculations based on resonance test modes.* The results of these flutter calculations, together with the corresponding experimental results, are set out in Table 2. In each case, results are given for the complete problem, involving four, five or six degrees-of-freedom, with the inertia couplings included in the flutter equations. The results obtained without the inertia couplings and the results for the principal constituents of the problems (*e.g.*, binaries etc.) are also given in most cases.

Generally speaking, the agreement with tunnel tests is quite fair for both flutter speeds and frequencies. However, in a few instances (notably case 2) there are appreciable discrepancies which will be considered later in Section 7 of this Report.

In most cases where the inertia couplings between the dominant degrees-of-freedom are such that $(a_{RS}/\sqrt{a_{RR}a_{SS}})$ does not exceed 0·25, the results obtained without the inertia couplings are closer to the test results than the solutions obtained with the couplings included. The foregoing holds good for Case 7 which has inertia couplings larger than 0·25, but fails for Case 6A which also has large inertia couplings. However, for what it is worth it may be observed that in each of these cases the higher of the two flutter speeds is closer to the wind tunnel test result.

7. *Discussion of Results.* 7.1. *Wind Tunnel Test Results.* 7.1.1. *Investigations on the wing with the original spar.* Comparison of the flutter contours of Figs. 3, 4 and 5 shows that the flutter characteristics of a delta wing carrying a localised mass are strongly influenced by both its position and magnitude. At the wing-tip, the position of the mass seems to be the dominant parameter, at least so far as flutter speed is concerned, and there is little difference between the contours for a localised mass equal to 40 per cent of the bare wing weight and those corresponding to a mass equal to the bare wing.

For sections further inboard, however, the magnitude of the localised mass becomes increasingly important, especially if the location is forward of the spar axis. Thus in the leading-edge mid-span position, a localised mass equal to 40 per cent of the wing weight reduces the flutter speed some 20 to 30 per cent below that of the bare wing, whereas for masses of 70 per cent of the wing weight and above, the flutter speed is more than one and a half times that of the bare wing. With the localised mass behind the spar axis, however, the effects of variations in its magnitude are much smaller and there is a general similarity between the contours for all three cases.

Flutter speeds well above that of the bare wing are not necessarily associated with overtone type flutter motion. It is true that most of the favourable areas towards the leading edge involve this kind of flutter but aft of the spar axis it is the exception rather than the rule.

7.1.2. *Investigations on the wing with the spar modified to simulate a large cut-out.* Despite differences in detail, which will be considered later, the results for the wing with the modified spar show a broad similarity to those discussed above in Section 7.1.1. The wing-tip leading-edge position is favourable in all cases, regardless of the mass involved, but further inboard everything depends on the magnitude of the mass. At about mid-span, a mass equal to the wing weight gives flutter characteristics that compare favourably with those of the bare wing, whereas a mass of 70 per cent of the wing weight brings the flutter speed right down to less than half that of the bare wing. With the localised mass well aft, the flutter contours for the three localised mass weights show rather more variation than in the case of those for the original spar, but the overall picture remains the same.

Although a localised mass near the trailing edge can raise the flutter speed well above that of the bare wing, the flutter motion remains fundamental in type. Overtone flutter is limited to cases involving high flutter speeds with the mass close to the leading edge.

Differences between the results obtained for the wing with its original spar and those for the wing with the modified spar, are mainly associated with the extent of the adverse flutter regions and the minimum flutter speeds that occur when a localised mass is placed within them. Generally speaking, the overall effect of these differences is that a localised mass at the tip of the wing with the modified spar is less likely to produce trouble than a mass in a similar position on the original wing, but further inboard the positions are reversed.

7.1.3. *Effect of variation of the radius of gyration of the localised mass.* Although a special series of tests were carried out to study in detail the effects of variations in both the magnitude and radius of gyration of the localised mass, the powerful influence of the actual weight on the flutter characteristics, together with the fact that a broad variation of mass had been covered in the main series of investigations, made it convenient to include the effects of mass variation in Section 7.1.1 and 7.1.2 above.

In contrast to the powerful effect of variations of the mass itself, it seems that variations in the radius of gyration have no appreciable effect on the flutter characteristics. This result is consistent with that given for wings of higher aspect ratio in Ref. 1.

7.2. *Appraisal of Theoretical Results.* In this section it is proposed to consider the results of the theoretical investigations in detail and to discuss possible reasons for the discrepancies that exist between them and the experimental results in certain cases.

Cases 1 to 7 inclusive relate to calculations on the wing with its original spar and cases 1A, 5A and 6A to the wing with the spar modified to simulate a large cut-out. In all cases except 1 and 1A, which relate to the bare wing with no localised mass, the mass was equal to 70 per cent of the bare wing weight.

7.2.1. *Discussion of Individual Cases. Case* 1: *Bare wing.* Arbitrary mode calculations gave results that are in reasonable agreement with those from wind tunnel tests.

In the case of calculations based on resonance test modes the agreement is very good and it appears that the moderate inertia couplings that existed between modes had no significant effect.

Case 2: *Mass at* 75 *per cent semi-span, L.E.* No direct comparison is possible in this case as the only information available from the tunnel tests is that the flutter speed is above 120 ft/sec. This is consistent with the results of arbitrary mode flutter calculations, however, which indicate overtone flutter at approximately 130 ft/sec.

In contrast, the work based on resonance test modes gives a very low speed fundamental type flutter. The trouble is due to the fundamental bending—fundamental torsion binary and if the latter mode is removed from the flutter equations the resulting quaternary gives flutter characteristics that agree quite well with those given by the arbitrary mode calculations.

The effects of varying the coefficients in the binary have been investigated in the hope that some clues to the problem might be forthcoming but no justification can be found for the modifications that would be necessary to push the flutter speed up.

Case 3: *Mass at* 75 *per cent semi-span,* 40 *per cent chord aft of L.E.* There is a tolerable measure of agreement between the results of both sets of flutter calculations and the tunnel test results in this case.

The flutter is of the fundamental type and both sets of calculations are dominated by the first bending—first torsion mode binary.

Case 4: *Mass at* 75 *per cent semi-span, T.E.* Although the results from arbitrary and resonance mode calculations agree quite well in this case, both appreciably under-estimate the flutter speed as given by wind tunnel tests.

The flutter motion is of the fundamental type and the effects of coefficient variation in the dominant fundamental binaries have been investigated for both sets of calculations.

Case 5: *Mass at wing tip, L.E.* The agreement between the results of arbitrary mode flutter calculations and those from wind tunnel tests is fairly satisfactory in this case. The calculations were successful in predicting the overtone type of flutter, the solution being dominated by the second bending—second torsion mode binary. This binary gave a flutter speed closer to the experimental result than the complete senary but the frequency was not so good.

The calculations based on resonance modes also gave reasonably good results in this case, although the fact that the theoretical flutter speed is higher than the experimental result is an undesirable feature. Investigations into the effect of coefficient variations in the dominant ternary have shown the most effective modification to bring down the flutter speed would be a reduction in the structural stiffness coefficients but no valid reason can be found to justify such changes.

Case 6: *Mass at wing tip,* 40 *per cent chord aft of L.E.* The agreement between the results of arbitrary mode flutter calculations and tunnel test results is indifferent in this case. Although the flutter frequencies agreed very well, the flutter speed was badly under-estimated in the calculations. An investigation of the constituent binaries and ternaries showed that neither the 1–4 (fundamental) or 2–5 (first overtone) binaries gave anything like the complete senary solution and the nearest approximation to it was given by the 1–4–5 ternary. This ternary gave a flutter speed appreciably closer to the tunnel test result than the complete set of flutter equations and the variations in the coefficients to give still better agreement were investigated. It may be significant that the flutter speeds for both the 1–4 and 2–5 binaries were close together in this case but it is not clear why this should affect the solution given by the full set of modes.

In the case of the resonance mode flutter calculations, however, the agreement with experimental results is quite satisfactory. The inertia couplings between the modes are very small and make no significant difference to the result of the dominant fundamental bending—fundamental torsion binary.

Case 7: *Mass at wing tip T.E.* The arbitrary mode flutter calculations in this case gave rather unsatisfactory results. The flutter speed was appreciably under-estimated and fundamental type flutter was obtained instead of the overtone type found in wind tunnel tests. It appears from the

investigations that were carried out on the constituent binaries that the solution was dominated by the fundamental 1–4 binary, whereas the 2–5 overtone binary would give flutter characteristics in reasonable agreement with the tunnel test results. Modifications corresponding to a rearward shift of the mass c.g. were tried in an attempt to suppress the 1–4 binary but without success.

In the case of the resonance mode flutter calculations there is an appreciable difference between the results obtained with and without the inertia couplings included in the flutter calculations. This was to be expected, however, as the set of modes in this case was poor, with large inertia couplings. The flutter frequencies were in fair agreement with the tunnel test results, as was the flutter speed for the solution without cross-inertias, but the speed with the couplings included was low.

Case 1A: Bare wing; modified spar with cut-out. Arbitrary mode flutter calculations gave a flutter speed that is in fair agreement with that obtained in wind tunnel tests but the frequency appeared to be badly over-estimated. The experimental frequency recorded in this case seems extremely low, however, and is regarded with some suspicion.

In the case of the calculations based on resonance test modes, the complete set of equations gave a very low flutter speed. The solution was dominated by a binary comprising the fundamental bending mode and a mode that looks like fundamental torsion. However, the frequency of this torsion mode seems unreasonably low compared with that obtained for the model with the original spar and it is badly coupled with some of the other modes. If this mode is rejected as spurious, the solution of the resulting quinary gives a flutter speed that agrees quite well with the tunnel test and arbitrary mode results, while the flutter frequency is close to that given by the arbitrary mode calculations.

Case 5A: Mass at wing tip, 40 per cent chord aft of L.E.; modified spar with cut-out. In this case, the arbitrary mode calculations gave a flutter speed that agrees reasonably well with the tunnel test result, although the calculated flutter frequency is rather high.

The results of the resonance mode flutter calculations are particularly good in this case. The dominant overtone binary gave a fair approximation to the flutter speed but the frequency was much improved by the inclusion of the other modes.

Case 6A: Mass at wing tip, 40 per cent chord aft of L.E.; modified spar with cut-out. The agreement between the results of arbitrary mode flutter calculations and wind tunnel tests is poor in this case. Investigation of the constituent binaries and the dominant ternary revealed a situation similar to that existing in Case 6.

In the case of the calculations based on resonance test modes the position is also unsatisfactory although the trouble here is only too plainly due to poor modes with large inertia couplings. The solution with the inertia couplings included in the flutter equations agrees quite well with the tunnel test results but the speed obtained with the couplings excluded was very low and close to the arbitrary mode result.

7.2.2. *General discussion of theoretical results.* Although there are a few unfortunate exceptions, the results of the arbitrary mode flutter calculations are generally in fair agreement with the wind tunnel test results. In all cases the flutter speeds have been under-estimated, which suggests either that the structural stiffness coefficients are inclined to be rather low or that there is appreciable damping in the actual model.* However, the fact that there is no general trend for the flutter speeds

* It has been suggested that the aerodynamic derivatives, based on Minhinnick Rules, may also contribute to conservative estimates of flutter speeds.

obtained from calculations based on resonance modes to be low seems to disprove the damping hypothesis. It seems probable, therefore, that the trouble is due to the stiffness coefficients, these being notoriously difficult to calculate to a high degree of accuracy, especially in the case of swept and delta wings (Ref. 4).

The calculations based on resonance test modes generally yield better results than the arbitrary mode calculations, subject, of course, to the proviso that the initial set of modes should be fairly good and free from large inertia couplings. It seems questionable, however, whether the superiority of the results obtained using these modes is really sufficient to justify the time and labour necessary to carry out the tests and analyse the results, especially since there is always the possibility that the set may prove to be poor, with the modes not really orthogonal.

In contrast, the ease with which variations in the basic parameters can be introduced into calculations based on simple arbitrary modes makes this approach very attractive in a research programme or in the early stages of the design of a new aircraft. Whether or not the use of such modes is desirable beyond the project stage involves other factors outside the range of this Report however, and the question has, in any case, been dealt with very fully in Ref. 4.

8. *Conclusions.* The investigations carried out in this research programme have shown that the effect of a localised mass on the flutter characteristics of a delta wing are dependent mainly on (*a*) the magnitude of the mass, (*b*) its spanwise and chordwise positions and (*c*) the stiffness distributions of the wing itself. Variation of the radius of gyration of the mass seems to have no significant effect on the flutter characteristics.

In a favourable position, a localised mass can raise the flutter speed to more than 1·5 times that of the bare wing, while in an unfavourable position, the mass may reduce it to less than 0·5 times the bare wing speed. The position and extent of these favourable and unfavourable regions is dependent, however, on the mass value and the stiffness distribution of the wing. A localised mass placed close to the leading edge between, say, 0·7 semi-span and the wing-tip generally improves the flutter characteristics, but, further inboard, it seems that the leading edge region should be regarded with caution. If the mass is very large (of the order of the bare wing weight), the flutter speed is likely to be higher than that of the bare wing, but for smaller masses in this position the speed may be very low. This effect was accentuated by the modification of the wing spar to simulate a large cut-out.

As in the case of wings of higher aspect ratio, the positioning of a localised mass in the vicinity of the structural axis always seems to have an adverse effect on the flutter characteristics. For positions well aft of the structural axis, however, the effects of a localised mass on the flutter characteristics are far more favourable for the delta wing. Flutter speeds well in excess of the bare wing speed have been obtained and there is evidence of a transition to overtone type flutter with the mass right down on the trailing edge.

A fair measure of success has been obtained with the theoretical part of the programme. The agreement between flutter calculations and wind tunnel test results is reasonably close in many cases, while in most of those where appreciable differences have occurred, it has been possible to find a reasonable explanation for the discrepancies.

REFERENCES

No.	*Author*	*Title, etc.*
1	D. R. Gaukroger	Wind tunnel tests on the effect of a localised mass on the flutter of a swept-back wing with fixed root. A.R.C. R. & M. 3141. December, 1953.
2	I. T. Minhinnick	A symposium on the flutter problem in aircraft design. Paper No. 4. A.R.C. 16,081. May, 1953.
3	E. G. Broadbent	Ill-conditioned flutter equations and their improvement for simulator use. A.R.C. C.P. 298. June, 1956.
4	E. G. Broadbent	Research on wing and control surface flutter with particular reference to the choice of co-ordinates. A.R.C. 17,872. June, 1955.

BIBLIOGRAPHY

In addition to those reports to which direct reference has been made herein, the following have also been referred to in the course of these investigations.

No.	*Author*	*Title, etc.*
1	D. R. Gaukroger, E. W. Chapple and A. Milln.	Wind tunnel flutter tests on a model delta wing under fixed and free root conditions. A.R.C. R. & M. 2826. September, 1950.
2	D. R. Gaukroger and D. Nixon ..	Wind tunnel tests on anti-symmetric flutter of a delta wing with rolling body freedom. A.R.C. C.P. 259. February, 1955.
3	D. R. Gaukroger	Wind tunnel tests on the effect of spar variations on the flutter of a model wing. A.R.C. 18,937. July, 1956.
4	W. G. Molyneux	Flutter of wings with localised masses. A.R.C. 19,062. July, 1956.
5	D. R. Gaukroger	A theoretical treatment of the flutter of a wing with a localised mass. *J. R. Ae. Soc.* Vol. 63. No. 2. p.95. February, 1959.
6	H. Hall and W. A. Coles	Wind tunnel tests on the effects of an added mass on the flutter of a model delta wing. A.R.C. R. & M. 3255. September, 1958.

TABLE 1

Results of Arbitrary Mode Flutter Calculations (With Experimental Results Included for Comparison)

Case	Particulars of localised mass			Results of arbitrary mode flutter calculations					Experimental results	
	Mass as percentage of bare wing weight	Location		Flutter speed (ft/sec)	Frequency (c.p.s.)	Binaries and ternaries			Flutter speed (ft/sec)	Frequency (c.p.s.)
		Semi-span (per cent)	Chord aft of L.E. (per cent)			Description	Flutter speed (ft/sec)	Frequency (c.p.s.)		
WING WITH ORIGINAL SPAR										
1	None	—	—	69	6·05	1–4 Binary	81	6·05	85	6·5
2	70	75	0	131	15·1	2–6 Binary	140	15·1	No flutter up to 120 ft/sec	
3	70	75	40	56·5	2·8	1–4 Binary	81	3·03	75	2·5
4	70	75	100	68·6	2·33	1–4 Binary* 2–5 Binary 2–6 Binary	72 159 141	2·88 14·1 15·1	115	2·55
5	70	100	0	85·2	9·9	2–5 Binary	93·5	10·3	106	8·12
6	70	100	40	29·5	1·37	1–4 Binary 2–5 Binary 1–4–5 Ternary*	93·0 103·5 40·0	2·14 9·68 1·79	62	1·33
7	70	100	100	76·5	1·12	1–4 Binary 2–5 Binary	74·0 108·5	2·08 10·59	116	8·12
WING WITH SPAR MODIFIED TO SIMULATE A LARGE CUT-OUT										
1A	None	—	—	58·5	4·84	1–4 Binary	65·5	5·19	77	2·56†
5A	70	100	0	81·0	8·75	2–5 Binary	91·5	9·68	96	5·82
6A	70	100	40	36·0	1·36	1–4 Binary 2–5 Binary 1–4–5 Ternary*	79·0 99·0 39·0	1·79 9·68 —	80·5	—

* In the case of binaries and ternaries marked with an asterisk, the effects of variations in the coefficients have been investigated. The results are shown in graphical form in Appendix II.

† This figure is regarded with suspicion.

TABLE 2

Results of Flutter Calculations Based on Resonance Test Modes (With Experimental Results Included for Comparison)

Case	Particulars of localised mass			Results of resonance mode flutter calculations								Experimental results	
	Mass as percentage of bare wing weight	Semi-span (per cent)	Chord aft of L.E. (per cent)	Number of degrees-of-freedom	Without inertia coupling		With inertia coupling		Binaries, ternaries, etc.			Flutter speed (ft/sec)	Flutter frequency (c.p.s.)
					Flutter speed (ft/sec)	Flutter frequency (c.p.s.)	Flutter speed (ft/sec)	Flutter frequency (c.p.s.)	Description	Flutter speed (ft/sec)	Flutter frequency (c.p.s.)		
WING WITH ORIGINAL SPAR													
1	None	—	—	4	87·0	6·35	83·0	6·9				85·0	6·5
2	70	75	0	5	31·0	2·08	Just unstable		1–2 Binary without × inertias 1–2 Binary with × inertias* 1–3–4–5 Quaternary no × inertias 1–3–4–5 Quaternary with × inertias	30·0 37·0 144·4 174·8	2·06 2·08 14·90 13·30	No flutter up to 120 ft/sec	
3	70	75	40	5	68·0	2·68	57·0	2·90				75·0	2·50
4	70	75	100	5	82·0	1·89	80·0	1·98	1–2 Binary with × inertias*	81·2	2·07	115·0	2·55
5	70	100	0	5	129·0	7·25	120·4	8·76	2–3–4 Ternary with × inertias* 2–3 Binary with × inertias 2–4 Binary with × inertias	121·2 149·2 159·2	9·67 8·45 9·43	106·0	8·12
6	70	100	40	6	Not investigated Couplings very small		54·2	1·31	1–2 Binary with × inertias*	53·0	1·37	62·0	1·33
7	70	100	100	5	104·4	8·92	76·0	8·92	2–3–4 Ternary no × inertias 2–3–4 Ternary with × inertias*	107·2 132·4	8·82 11·12	116·0	8·12
WING WITH SPAR MODIFIED TO SIMULATE A LARGE CUT-OUT													
1A	None	—	—	6	Senary not investigated		30·6	3·02	1–3–4–5–6 Quinary no × inertias 1–3–4–5–6 Quinary with × inertias 1–3–4 Ternary no × inertias 1–3–4 Ternary with × inertias	71·0 66·4 71·8 65·8	5·31 5·31 4·83 5·31	77·0	2·56†
5A	70	100	0	6	Senary not investigated		98·4	6·04	3–4 Binary without × inertias 3–4 Binary with × inertias	108·2 105·3	8·37 8·26	96·0	5·82
6A	70	100	40	5	37·0	1·26	68·8	1·21	1–2 Binary without × inertias 1–2 Binary with × inertias	36·6 71·0	1·26 1·29	80·5	—

* In the case of binaries and ternaries marked with an asterisk, the effects of variations in the coefficients have been investigated. The results are shown in graphical form in Appendix II.

† This figure is regarded with suspicion.

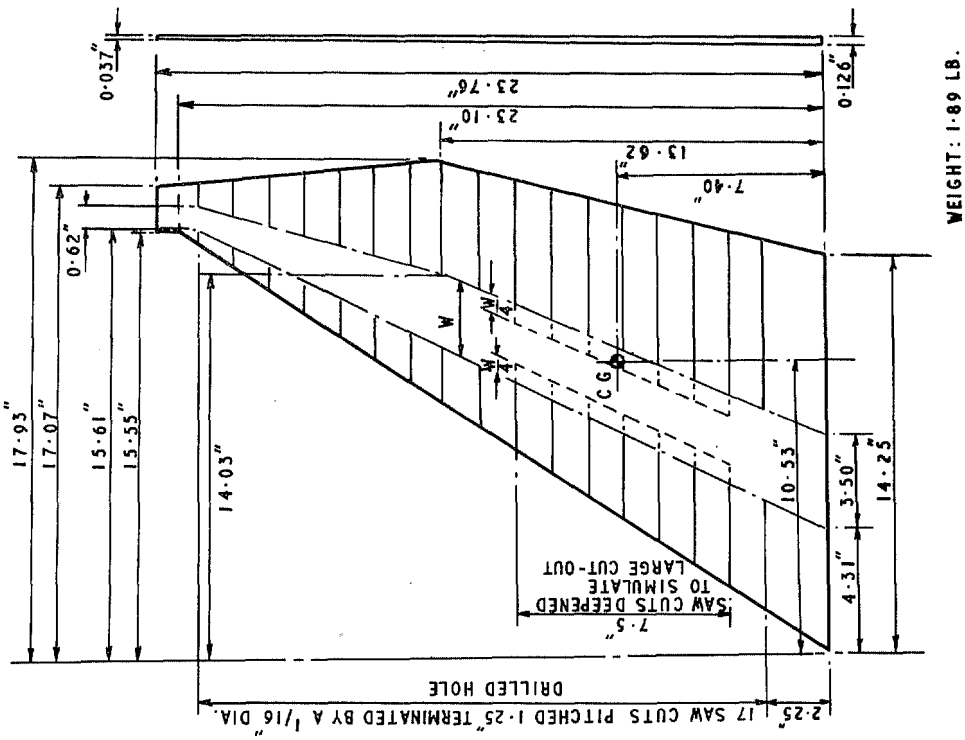

FIG. 2. Spar geometry.

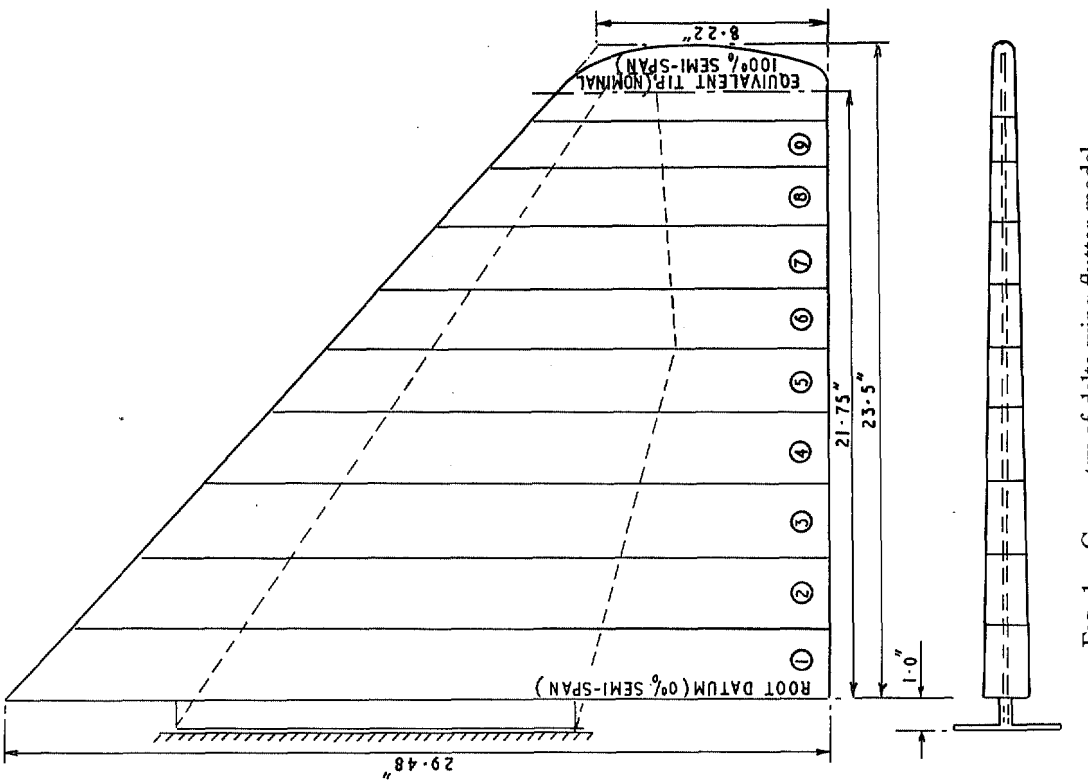

FIG. 1. Geometry of delta wing flutter model.

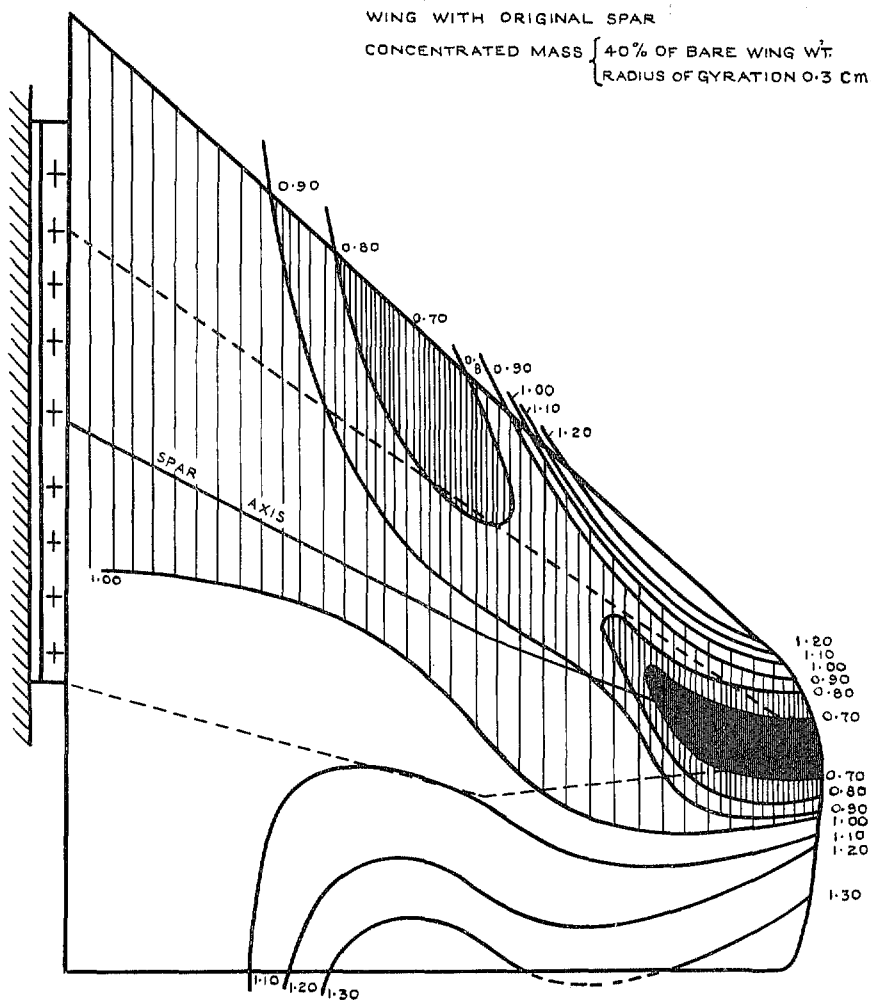

FIG. 3. Effect of location of a localised mass on the flutter of a delta wing.

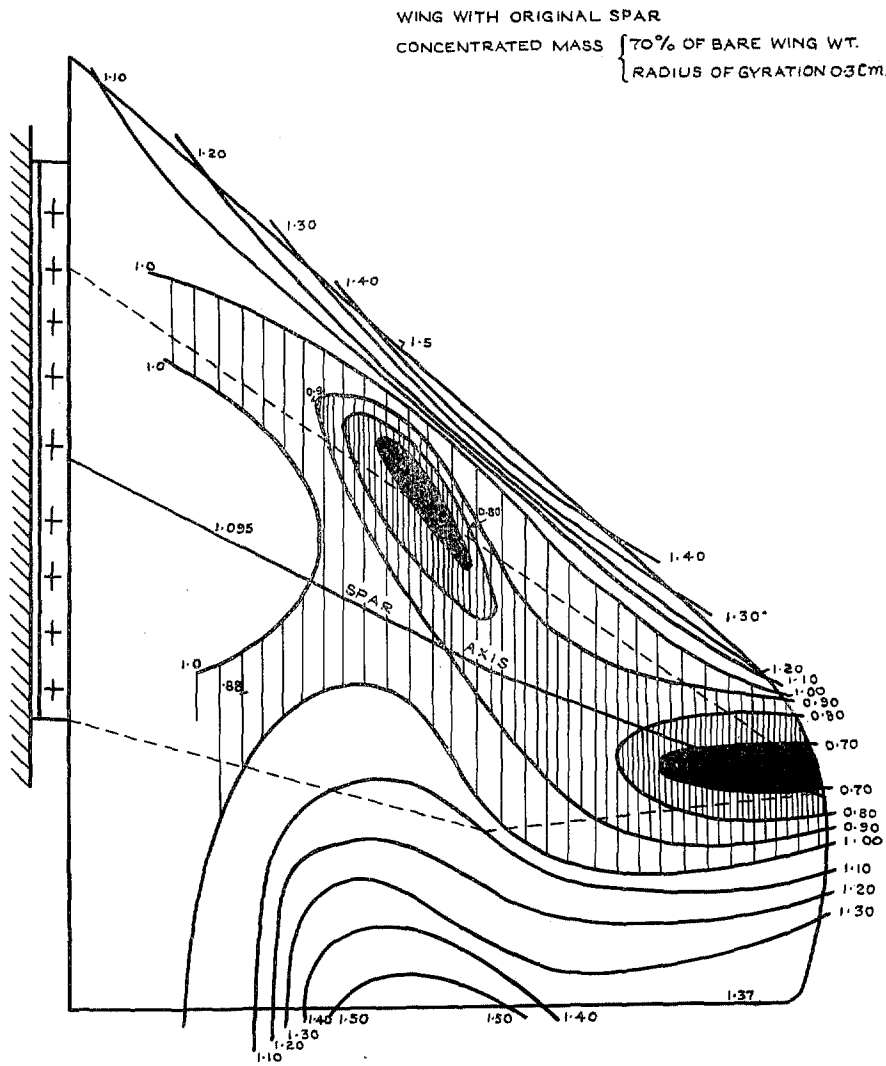

FIG. 4. Effect of location of a localised mass on the flutter of a delta wing.

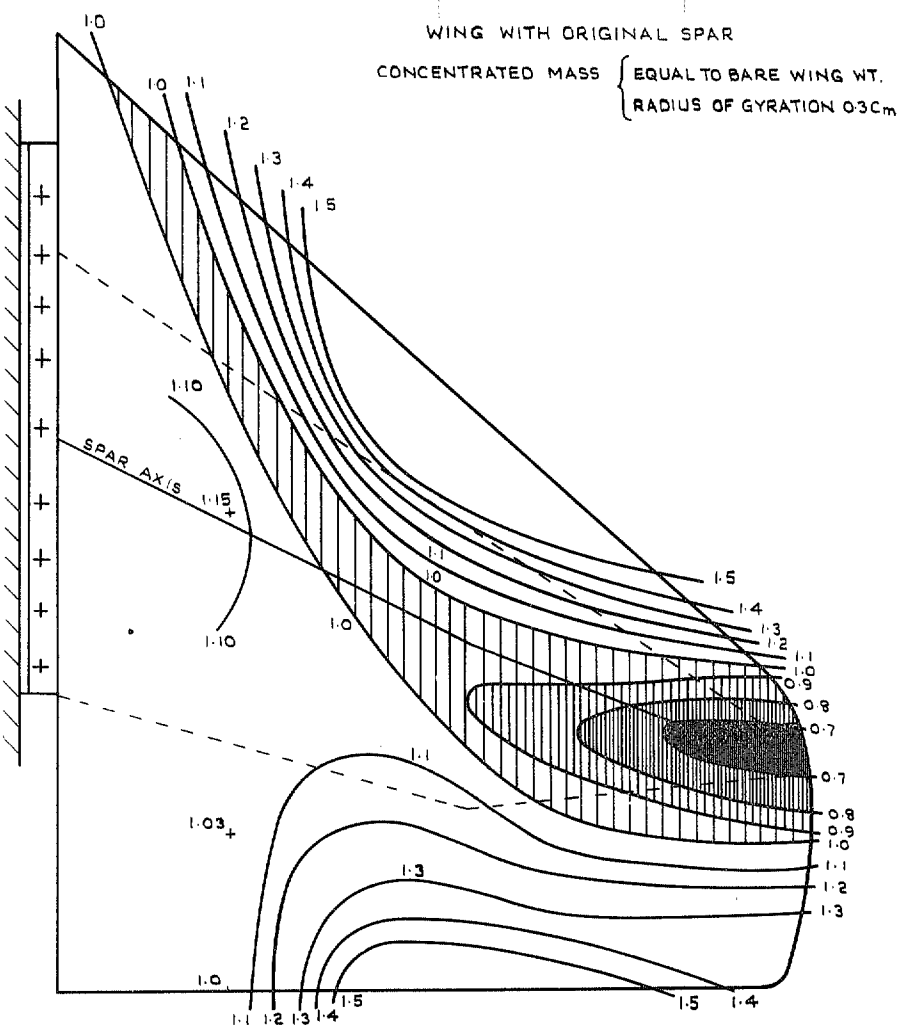

FIG. 5. Effect of location of a localised mass on the flutter of a delta wing.

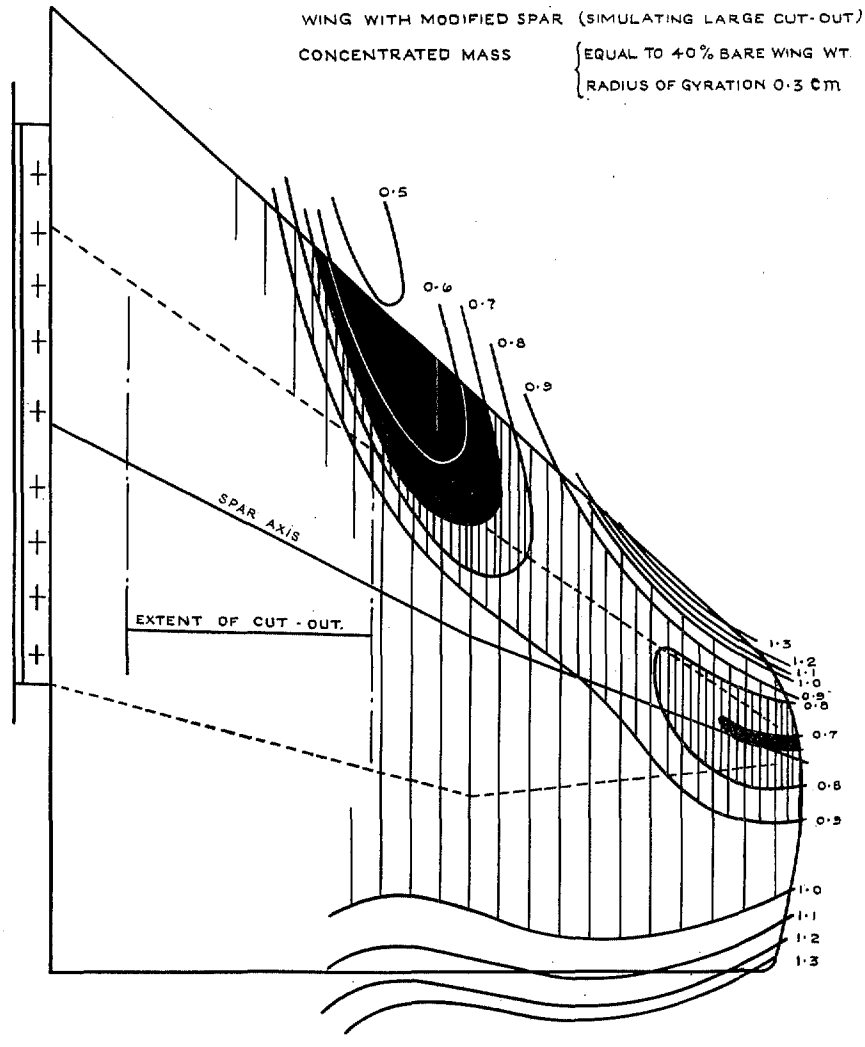

FIG. 6. Effect of location of a localised mass on the flutter of a delta wing.

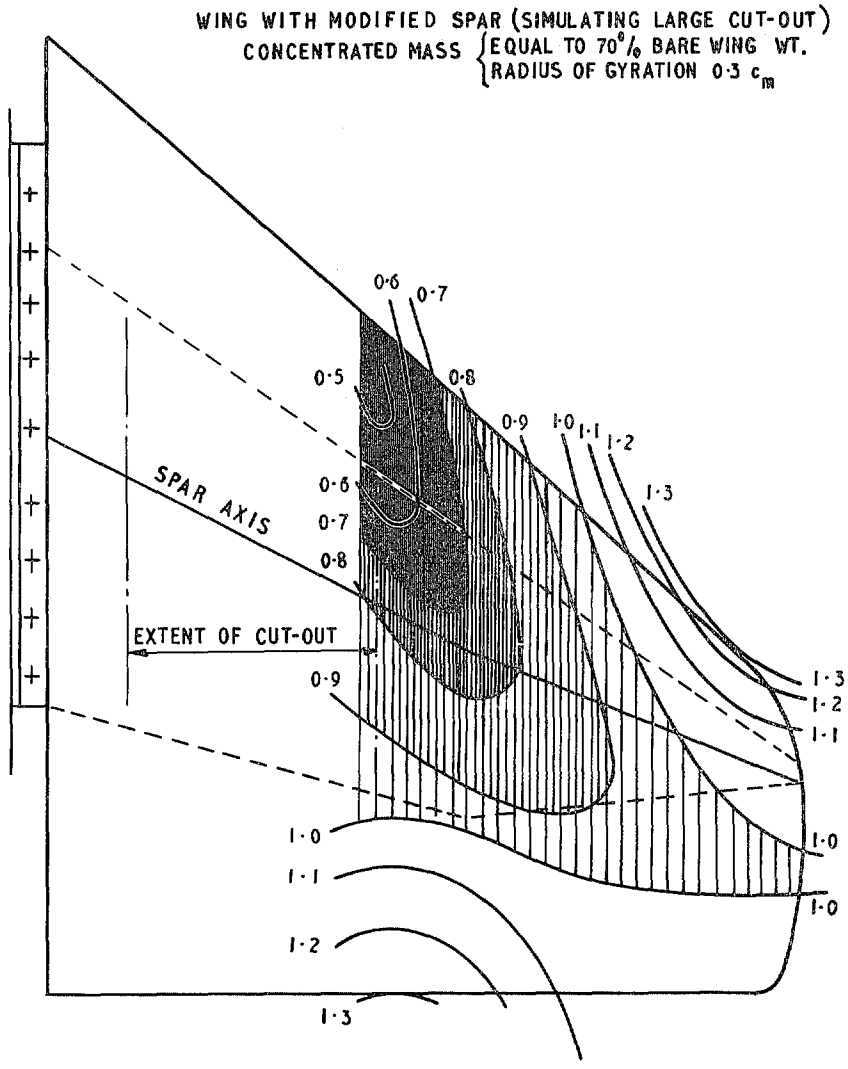

FIG. 7. Effect of location of a localised mass on the flutter of a delta wing.

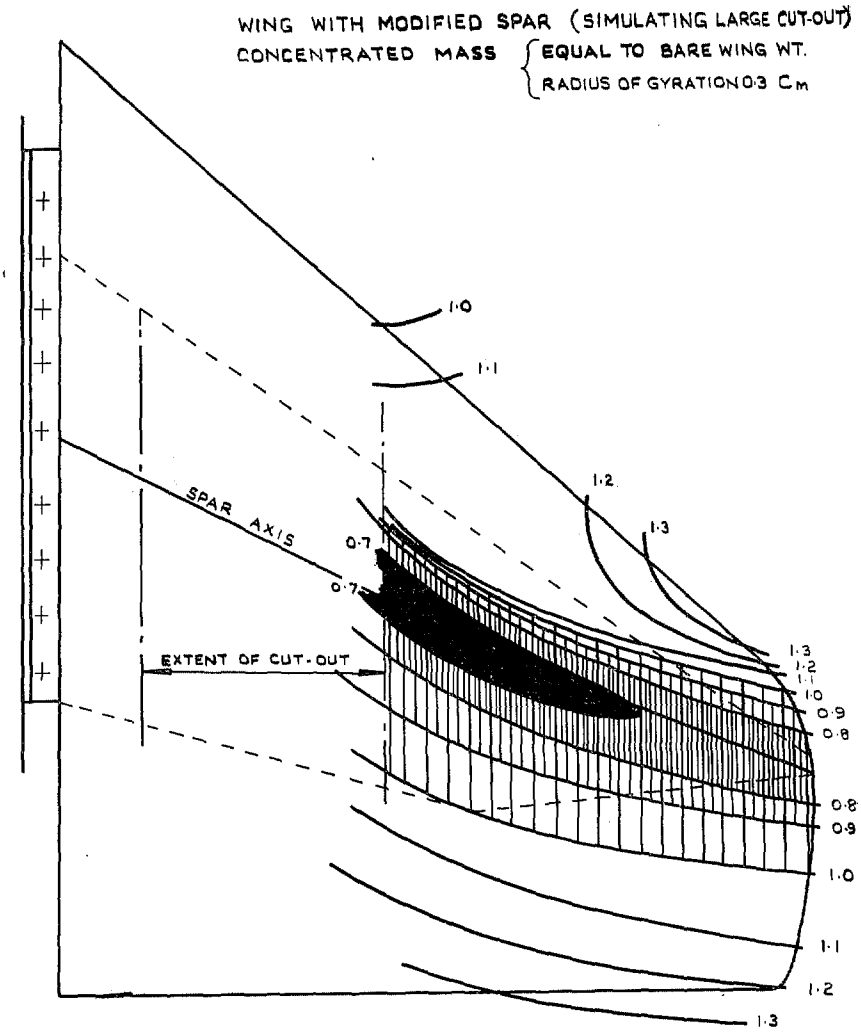

FIG. 8. Effect of location of a localised mass on the flutter of a delta wing.

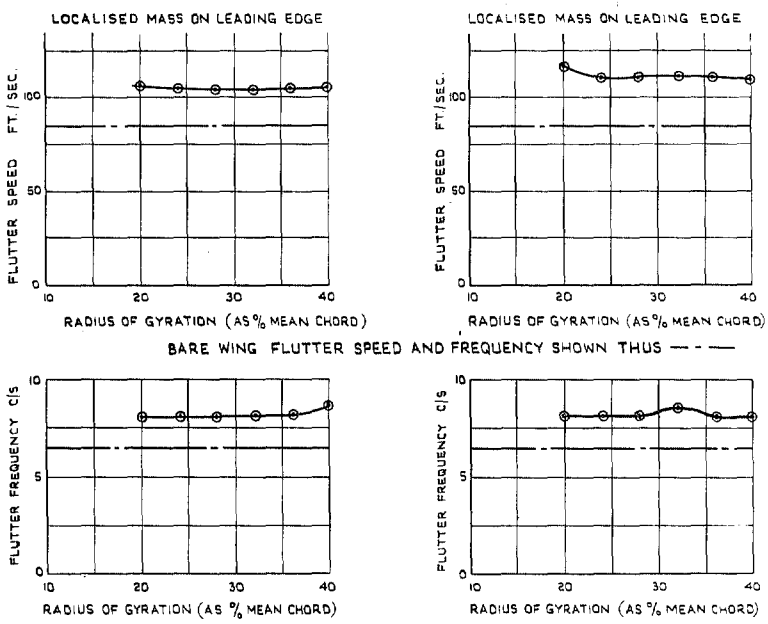

FIG. 9. Flutter of a delta wing carrying a localised mass. Variation of flutter speed and frequency with radius of gyration of a localised mass equal to the bare wing weight. Localised mass at wing-tip.

FOR THE CASE WITH LOCALISED MASS ON THE LEADING EDGE FLUTTER WAS NOT OBTAINED WITHIN THE SPEED RANGE OF THE WIND TUNNEL

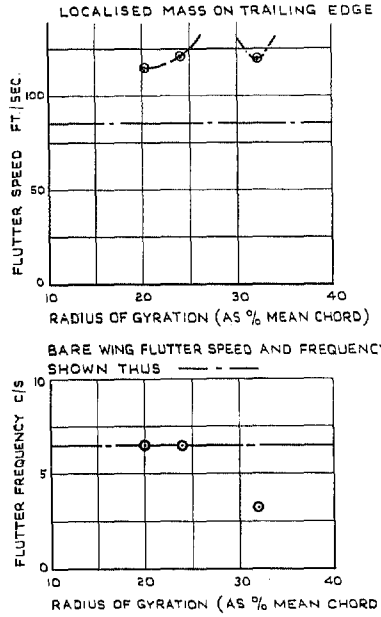

FIG. 10. Flutter of a delta wing carrying a localised mass. Variation of flutter speed and frequency with radius of gyration of a localised mass equal to the bare wing weight. Localised mass at 50 per cent at semi-span.

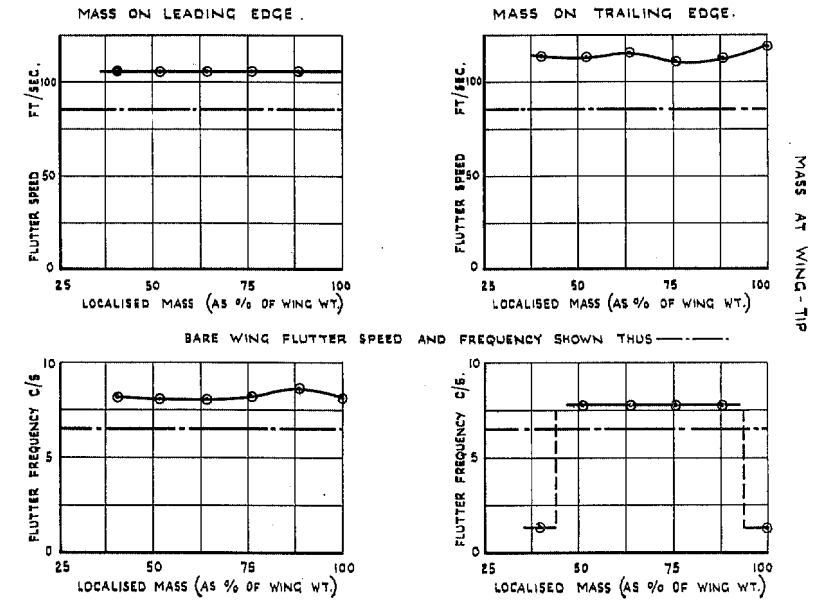

FIG. 11. Flutter of a delta wing carrying a localised mass. Variation of flutter speed and frequency with magnitude of localised mass. (Constant radius of gyration equal to 30 per cent wing mean chord.) Mass at wing-tip.

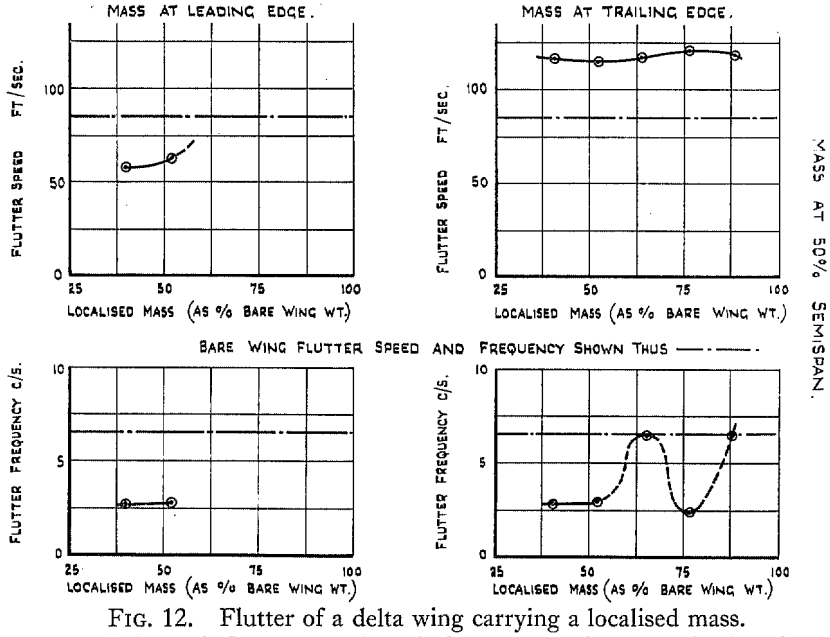

FIG. 12. Flutter of a delta wing carrying a localised mass. Variation of flutter speed and frequency with magnitude of localised mass. (Constant radius of gyration equal to 30 per cent wing mean chord.) Mass at 50 per cent semi-span.

APPENDIX I

Wind Tunnel Flutter Tests

1. *Introduction.* The experimental part of the research programme has already been briefly described in Section 4 of the main part of this Report. However, in this Appendix the actual test procedure will be considered in more detail and the results obtained will be given in full.

2. *Range of Investigations.* The wind tunnel flutter test programme included an extensive range of investigations on the effect of a localised mass on the flutter of the original wing and a more restricted series of tests on the model after the spar was modified to simulate the effect of a large cut-out, such as an undercarriage bay.

In the work on the original wing, a detailed investigation was carried out with the localised mass at each of a series of chordwise stations at four sections on the wing. Three different mass values were covered in these investigations, while a more detailed study of the effects of variations in the mass value and the radius of gyration was carried out at certain selected stations.

In the case of the wing with the modified spar, the investigations were limited to study of the effect of the chordwise position of the localised mass at the mid-span and wing-tip sections. Three mass values were covered in this work.

Full details of the tests that were carried out are given in the Tables at the end of this Appendix.

3. *Description of the Model.* The model wing was of segmented construction, comprising an aluminium alloy plate spar carrying nine wooden box segments and a tip fairing to give the required aerodynamic form (*see* Fig. 1).

The spar was adapted from the taper-machined plate spar used in the SR.53 wing flutter model. The latter had a high 'bare-wing' flutter speed, however, and the stiffness of the spar had to be drastically reduced so as to permit investigation of those cases in which the localised mass increases the flutter speed above that of the bare wing. This reduction in stiffness was achieved by reducing the effective width of the spar with saw-cuts from the front and rear edges of the plate. For the first series of tests, *i.e.*, for a wing without a cut-out, the depth of these saw-cuts was graduated so as to give a fairly smooth grading of stiffness from root to tip. To simulate the cut-out for the second part of the programme, the cuts in the inboard part of the wing were increased in depth so as to reduce the effective width of the spar to about one half its previous value. (Details of the spar are given in Fig. 2.)

All tests on the model were to be carried out under 'fixed root' conditions, so the spar root was clamped between two substantial angle section members which were bolted to a rigid support for wind tunnel and resonance tests.

The box segments that provided the aerodynamic form of the wing were constructed of balsa and thin plywood. A small amount of lead ballast was fitted in these segments to give the required mass distribution. (Particulars of the weights and c.g. positions of these box segments are given in

Note. This Appendix is based on Westland Aircraft Ltd., Saunders-Roe Division Wind Tunnel Reports Nos. A/2/326a and A/2/326b. The first of these Reports covered tests on the model with its original spar stiffness and the second the tests carried out after the spar was modified to simulate the effect of a large cut-out.

the Table below.) To prevent the shell from making any appreciable contribution to the wing stiffness, each segment was bolted to the spar at one spanwise position only and the gaps between the segments were not sealed, as experience with the SR.53 wing flutter model had shown that such sealing had no appreciable effect on the results.*

Inertia Data for Box Segments

Segment No.	Weight (lb)	Distance of c.g. Forward of T.E. (inches)
1	0·607	12·0
2	0·542	11·25
3	0·546	10·72
4	0·482	9·45
5	0·433	8·50
6	0·326	7·10
7	0·348	6·40
8	0·277	5·75
9	0·225	5·20
Tip Fairing	0·054	5·50

Total weight of segments and tip fairing	3·84 lb
Weight of spar (excluding clamped portion inboard of root datum)	1·71 lb
Bare wing weight	5·55 lb

4. *Test Procedure.* Tests were carried out in a low speed wind tunnel (120 ft/sec max) with a 6 ft by 4 ft open working section.

The model was mounted hanging vertically downwards from the top of the tunnel to avoid large static displacements under gravity and the localised masses were applied indirectly through a remote loading rig of the type described in Ref. 1. The loading platform was suspended by wires from a beam approximately twenty feet above the model and was connected to the model through two light weight tubes through universal joints, as shown in Fig. I.1. A shield was fitted round the tubes to eliminate adverse wind tunnel effects and a drag restrainer was fitted to hold these rods in alignment with the drag shield.

During the tests the tunnel speed was increased until the model commenced to flutter. The flutter motion was then photographed with a cine-camera running at 64 frames per second for subsequent analysis and frequency determination. By this means it was possible to study the motion in detail without risking loss of the model by prolonged running above the critical speed.

In the analysis of the film record, the cine film was projected on to a screen at 2 frames per second, and the number of frames to each flutter cycle counted. In most cases four or five cycles were counted to obtain a mean and the flutter frequency was then obtained from the relationship:

$$\text{Frequency (Cycles/second)} = \frac{\text{Frames/second (normally 64)}}{\text{Frames/cycle}}$$

* It has since been suggested that, in some cases, the effect of sealing may be more significant than was originally supposed.

5. *Results.* The results of these wind tunnel flutter tests have already been presented and discussed in the main part of this Report (Sections 6.1; 7.1 and Figs. 3 to 12 inclusive). In the case of the main series of investigations, however, the results were reduced and given in the form of 'flutter contours' (Figs. 3 to 8) without details of frequency or type of flutter motion, although the general characteristics in these respects were noted and discussed in the text.

In this Appendix, full details of the results of the main series of investigations on the wing with its original stiffness distribution and with its stiffness modified to simulate a large cut-out are given in Tables I.1 and I.4 respectively. The variation in flutter speed and frequency with chordwise location of the localised mass is shown in Figs. I.2 to I.7. These diagrams cover the three mass values at the four spanwise sections on the wing with its original stiffness distribution, and the two on the modified wing.

The results for the detailed investigations on the effects of variation in radius of gyration and magnitude of the localised mass are given in Tables I.2 and I.3 respectively. These results were presented diagramatically in Figs. 9 to 12 in the main part of this Report.

TABLE I.1

Results of Tests on Model with Original Stiffness Distribution

Detailed Investigation of the Effect of Spanwise and Chordwise Position of a Localised Mass

Run No.	Flutter		Loading			Rad. Gyr. per cent $\bar{c}$	Type of Flutter and Remarks
	ft/sec	c.p.s.	span (per cent)	chord (per cent)	B.W. (per cent)		
0	85	6·5	—	Bare Wing		—	Large torsional amplitude, small bending amplitude
1	82	3·82	25	0	40	30·1	Large torsional amplitude, moderate bending amplitude. Wing motion unsteady
2	103	8·12	25	0	70	30·1	Very large torsional amplitude developing violently; no appreciable bending
3	98	6·5	25	0	100	30·1	Moderate torsional amplitude, no appreciable bending
4	83	5·0	25	20	40	30·1	Torsional and bending amplitudes both small
5	81	3·94	25	20	70	30·1	Torsional and bending amplitudes both small
6	81	4·06	25	20	100	30·1	Torsional and bending amplitudes both small
7	81	5·91	25	40	40	30·1	Torsional and bending amplitudes both small
8	92	6·2	25	40	70	30·1	Large torsional and bending amplitudes
9	98	5·41	25	40	100	30·1	Large torsional and bending amplitudes
10	88	7·23	25	60	40	30·1	Small torsional amplitude with no appreciable bending
11	84	7·23	25	60	70	30·1	Small torsional amplitude with no appreciable bending
12	85	6·5	25	60	100	30·1	Large torsional amplitude, bending amplitude very small
13	88	6·5	25	80	40	30·1	Large torsional amplitude, bending amplitude very small
14	86	6·85	25	80	70	30·1	Moderate torsional amplitude, small bending amplitude
15	88	6·85	25	80	100	30·1	Moderate torsional amplitude, small bending amplitude
16	87	6·5	25	100	40	30·1	Moderate torsional amplitude, small bending amplitude
17	87	6·5	25	100	70	30·1	Moderate torsional amplitude, small bending amplitude

TABLE I.1—*continued*

Run No.	Flutter		Loading			Rad. Gyr. per cent $\bar{c}$	Type of Flutter and Remarks
	ft/sec	c.p.s.	span (per cent)	chord (per cent)	B.W. (per cent)		
18	86	6·85	25	100	100	30·1	Moderate torsional amplitude, small bending amplitude
19	59	2·84	50	0	40	30·1	Small torsional amplitude, with some bending outboard of the localised mass
20	—	—	50	0	70	30·1	Above tunnel speed (120 ft/sec)
21	—	—	50	0	100	30·1	Above tunnel speed (120 ft/sec)
22	69	3·61	50	20	40	30·1	Moderate torsional amplitude, large bending amplitude*
23	59	2·84	50	20	70	30·1	Moderate torsional amplitude, large bending amplitude*
24	—	—	50	20	100	30·1	Above tunnel speed (120 ft/sec)
25	79	4·65	50	40	40	30·1	Large torsional amplitude, moderate bending amplitude
26	79	3·61	50	40	70	30·1	Large torsional amplitude, moderate bending amplitude*
27	81	3·43	50	40	100	30·1	Moderate torsional amplitude, small bending amplitude
28	86	4·65	50	60	40	30·1	Moderate torsional and bending amplitudes. The action of the connecting rod broke a rib
29	89	3·83	50	60	70	30·1	Moderate torsional amplitude with large amount of bending; the two not in phase
30	91	3·17	50	60	100	30·1	Large torsional and bending amplitudes
31	100	4·2	50	80	40	30·1	Small torsional amplitude, large bending amplitude
32	108	2·84	50	80	70	30·1	Small torsional amplitude, moderate bending amplitude
33	108	2·5	50	80	100	30·1	Small torsional amplitude, moderate bending amplitude
34	116	2·96	50	100	40	30·1	Small torsional amplitude with large amount of bending, the two out of phase
35	—	—	50	100	70	30·1	Above tunnel speed (120 ft/sec)
36	—	—	50	100	100	30·1	Above tunnel speed (120 ft/sec)
37	105	1·86	75	0	40	30·1	No appreciable torsion, moderate bending amplitude
38	—	—	75	0	70	30·1	Above tunnel speed (120 ft/sec)

* In these cases the wing was seen to be striking the drag shield.

TABLE I.1—*continued*

Run No.	Flutter		Loading			Rad. Gyr. per cent $\bar{c}$	Type of Flutter and Remarks
	ft/sec	c.p.s.	span (per cent)	chord (per cent)	B.W. (per cent)		
39	—	—	75	0	100	30·1	Above tunnel speed (120 ft/sec)
40	74	2·77	75	20	40	30·1	Small torsional amplitude, large bending amplitude
41	78	2·32	75	20	70	30·1	Small torsional amplitude, large bending amplitude
42	105	2·06	75	20	100	30·1	Small torsional amplitude, moderate bending amplitude
43	76	3·25	75	40	40	30·1	Moderate torsional amplitude, no appreciable bending
44	75	2·5	75	40	70	30·1	Moderate torsional amplitude, no appreciable bending. Section of wing outboard of the localised mass simply follows motion of the latter
45	77	2·06	75	40	100	30·1	Moderate torsional amplitude, no appreciable bending. Section of wing outboard of the localised mass simply follows motion of the latter
46	78	3·61	75	60	40	30·1	Moderate torsional amplitude, no appreciable bending
47	75	2·84	75	60	70	30·1	Moderate torsional amplitude, no appreciable bending
48	78	2·1	75	60	100	30·1	Moderate torsional amplitude, no appreciable bending
49	95	3·1	75	80	40	30·1	Moderate torsional and bending amplitudes
50	101	2·6	75	80	70	30·1	Moderate torsional and bending amplitudes
51	104	2·45	75	80	100	30·1	Moderate torsional and bending amplitudes
52	105	2·71	75	100	40	30·1	Moderate torsional and bending amplitudes
53	115	2·55	75	100	70	30·1	Moderate torsional amplitudes, large bending amplitude
54	117	—	75	100	100	30·1	No film
55	104	8·12	100	0	40	30·1	Moderate torsional amplitude inboard of the tip with no appreciable bending. Tip remained stationary

TABLE I.1—*continued*

Run No.	Flutter		Loading			Rad. Gyr. per cent $\bar{c}$	Type of Flutter and Remarks
	ft/sec	c.p.s.	span (per cent)	chord (per cent)	B.W. (per cent)		
56	106	8·12	100	0	70	30·1	Moderate torsional amplitude inboard of the tip with no appreciable bending. Tip remained stationary
57	106	8·12	100	0	100	30·1	Moderate torsional amplitude inboard of the tip with no appreciable bending
58	62	1·51	100	20	40	30·1	Small torsional amplitude, large bending amplitude*
59	61	1·14	100	20	70	30·1	Small torsional amplitude, large bending amplitude*
60	61	1·07	100	20	100	30·1	Torsional and bending amplitudes both small
61	59	1·61	100	40	40	30·1	Moderate torsional amplitude, no appreciable bending
62	62	1·33	100	40	70	30·1	Large torsional amplitude, no appreciable bending
63	63	1·1	100	40	100	30·1	Large torsional amplitude, no appreciable bending
64	87	1·51	100	60	40	30·1	Large torsional amplitude, moderate bending amplitude*
65	85	1·51	100	60	70	30·1	Large torsional amplitude, small bending amplitude*
66	87	1·28	100	60	100	30·1	Large torsional amplitude, small bending amplitude*
67	108	2·04	100	80	40	30·1	Large torsional amplitude, small bending amplitude*
68	111	1·36	100	80	70	30·1	Large torsional amplitude, small bending amplitude*
69	111	1·34	100	80	100	30·1	Large torsional amplitude, small bending amplitude*
70	114	1·25	100	100	40	30·1	Large torsional amplitude, small bending amplitude*
71	116	8·12	100	100	70	30·1	Moderate torsional amplitude inboard of the tip with no appreciable bending. Tip unsteady
72	118	1·3	100	100	100	30·1	Large torsional amplitude, moderate bending amplitude

* In these cases the wing was seen to be striking the drag shield.

TABLE I.2

Results of Tests on Model with Original Stiffness Distribution

Investigation of the Effect of Variation of Radius of Gyration without change of Mass

Run No.	Flutter		Loading			Rad. Gyr. per cent $\bar{c}$	Type of Flutter and Remarks
	ft/sec	c.p.s.	span (per cent)	chord (per cent)	B.W. (per cent)		
73	—	—	50	0	100	20	Above tunnel speed (120 ft/sec)
74	—	—	50	0	100	24	Above tunnel speed (120 ft/sec)
75	—	—	50	0	100	28	Above tunnel speed (120 ft/sec)
76	—	—	50	0	100	32	Above tunnel speed (120 ft/sec)
77	—	—	50	0	100	36	Above tunnel speed (120 ft/sec)
78	—	—	50	0	100	40	Above tunnel speed (120 ft/sec)
79	115	6·5	50	100	100	20	Torsion outboard of the localised mass position with a little bending
80	120	6·5	50	100	100	24	Torsion and bending building up to moderate amplitude and damping out again
81	—	—	50	100	100	28	Above tunnel speed (120 ft/sec)
82	120	3·1	50	100	100	32	Torsion and bending building up to moderate amplitude and damping out again
83	—	—	50	100	100	36	Above tunnel speed (120 ft/sec)
84	—	—	50	100	100	40	Above tunnel speed (120 ft/sec)
85	106	8·12	100	0	100	20	Moderate torsional amplitude inboard of tip with no appreciable bending. Tip steady
86	105	8·12	100	0	100	24	Moderate torsional amplitude inboard of tip with no appreciable bending. Tip steady
87	105	8·12	100	0	100	28	Moderate torsional amplitude inboard of tip with no appreciable bending. Tip steady
88	105	8·12	100	0	100	32	Moderate torsional amplitude inboard of tip with no appreciable bending. Tip steady
89	106	8·12	100	0	100	36	Moderate torsional amplitude inboard of tip with no appreciable bending. Tip steady
90	106	8·68	100	0	100	40	Moderate torsional amplitude inboard of tip with no appreciable bending. Tip steady

TABLE I.2—*continued*

Run No.	Flutter		Loading			Rad. Gyr. per cent $\bar{c}$	Type of Flutter and Remarks
	ft/sec	c.p.s.	span (per cent)	chord (per cent)	B.W. (per cent)		
91	116	8·12	100	100	100	20	Moderate torsional amplitude inboard of tip with large amount of bending
92	110	8·12	100	100	100	24	Small torsional amplitude inboard of tip with moderate bending and torsion of tip
93	112	8·12	100	100	100	28	Moderate torsional and bending amplitudes inboard of tip. Tip unsteady
94	112	8·68	100	100	100	32	Moderate torsional amplitude inboard of tip with no appreciable bending. Tip unsteady
95	111	8·12	100	100	100	36	Large torsional amplitude inboard of tip with no appreciable bending. Tip steady
96	110	8·12	100	100	100	40	Large torsional amplitude inboard of tip with no appreciable bending. Tip steady

TABLE I.3

Results of Tests on Model with Original Stiffness Distribution

Investigation of the Effect of Variation of Mass without change of Radius of Gyration

Run No.	Flutter		Loading			Rad. Gyr. per cent $\bar{c}$	Type of Flutter and Remarks
	ft/sec	c.p.s.	span (per cent)	chord (per cent)	B.W. (per cent)		
97	59	2·84	50	0	40	30·1	Small torsional and bending amplitudes outboard of localised mass
98	63	2·96	50	0	52	30·1	Small torsional amplitude, large bending amplitude
99	—	—	50	0	64	30·1	Above tunnel speed (120 ft/sec)
100	—	—	50	0	76	30·1	Above tunnel speed (120 ft/sec)
101	—	—	50	0	88	30·1	Above tunnel speed (120 ft/sec)
102	—	—	50	0	100	30·1	Above tunnel speed (120 ft/sec)

TABLE I.3—*continued*

Run No.	Flutter		Loading			Rad. Gyr. per cent $\bar{c}$	Type of Flutter and Remarks
	ft/sec	c.p.s.	span (per cent)	chord (per cent)	B.W. (per cent)		
103	116	2·96	50	100	40	30·1	Small torsional amplitude with large bending amplitudes, the motions being out of phase
104	115	2·96	50	100	52	30·1	Small torsional amplitude, large bending amplitude
105	117	6·5	50	100	64	30·1	Moderate torsional amplitude with large bending amplitude, the motions being out of phase
106	120	2·36	50	100	76	30·1	Moderate torsional amplitude with large bending amplitude, the motions being out of phase
107	118	6·5	50	100	88	30·1	Moderate torsional amplitude with large bending amplitude, the motions being out of phase
108	—	—	50	100	100	30·1	Above tunnel speed (120 ft/sec)
109	104	8·12	100	0	40	30·1	Moderate torsional amplitude inboard of tip with no appreciable bending. Tip steady
110	105	8·12	100	0	52	30·1	Large torsional amplitude inboard of tip. Tip steady
111	106	8·12	100	0	64	30·1	Moderate torsional amplitude inboard of tip. Tip steady
112	105	8·12	100	0	76	30·1	Moderate torsional amplitude inboard of tip. Tip steady
113	106	8·68	100	0	88	30·1	Moderate torsional amplitude inboard of tip. Tip steady
114	106	8·12	100	0	100	30·1	Moderate torsional amplitude inboard of tip. Tip steady
115	114	1·25	100	100	40	30·1	Large torsional amplitude, moderate bending amplitude*
116	114	8·12	100	100	52	30·1	Moderate torsional amplitude inboard of tip. Tip unsteady
117	115	8·12	100	100	64	30·1	Moderate torsional amplitude inboard of tip. Tip steady
118	110	8·12	100	100	76	30·1	Moderate torsional amplitude inboard of tip. Tip unsteady
119	111	8·12	100	100	88	30·1	Moderate torsional amplitude inboard of tip. Tip unsteady
120	118	1·3	100	100	100	30·1	Large torsional amplitude, moderate bending amplitude

* In these cases the wing was seen to be striking the drag shield.

TABLE I.4

Results of Tests on Model with Stiffness Distribution Modified to Simulate the Effect of a Large Cut-Out

Detailed Investigation of the Effects of Spanwise and Chordwise Position of a Localised Mass

Run No.	Flutter		Loading			Rad. Gyr. per cent $\bar{c}$	Type of Flutter and Remarks
	ft/sec	c.p.s.	span (per cent)	chord (per cent)	B.W. (per cent)		
121	77	2·56	Bare Wing		—	—	Large torsional amplitude with only a little bending
122	39	—	50	0	40	30·1	No film
123	43	—	50	0	70	30·1	No film
124	79	2·21	50	0	100	30·1	Small torsional amplitude with moderate to large bending amplitude
125	50	2·46	50	20	40	30·1	Small torsional amplitude, moderate bending amplitude
126	39·5	2·37	50	20	70	30·1	Moderate torsional amplitude, small bending amplitude
127	90	4·27	50	20	100	30·1	Small torsional amplitude, large bending amplitude
128	73	2·29	50	40	40	30·1	Large torsional amplitude, moderate bending amplitude
129	58	2·95	50	40	70	30·1	Moderate to large torsional amplitude with only a little bending
130	48·5	4·00	50	40	100	30·1	Moderate torsional amplitude with only a little bending
131	73·5	3·56	50	60	40	30·1	Large torsional amplitude, small bending amplitude
132	67	3·37	50	60	70	30·1	Torsional and bending amplitudes both small
133	71	2·67	50	60	100	30·1	Moderate torsional amplitude, small bending amplitude
134	73·5	3·05	50	80	40	30·1	Large torsional amplitude with no appreciable bending
135	83	3·37	50	80	70	30·1	Moderate torsional amplitude, small bending amplitude
136	86	3·76	50	80	100	30·1	Small torsional amplitude, large bending amplitude
137	87	2·46	50	100	40	30·1	Small torsional amplitude, large or very large bending amplitude
138	101	3·05	50	100	70	30·1	Small torsional amplitude, large or very large bending amplitude
139	106	2·91	50	100	100	30·1	Small torsional amplitude, large or very large bending amplitude

TABLE I.4—*continued*

Run No.	Flutter		Loading			Rad. Gyr. per cent $\bar{c}$	Type of Flutter and Remarks
	ft/sec	c.p.s.	span (per cent)	chord (per cent)	B.W. (per cent)		
140	100	4·92	100	0	40	30·1	Large torsional amplitude commencing at mid-span L.E. No appreciable bending
141	96	5·82	100	0	70	30·1	Moderate torsional amplitude commencing at mid-span L.E. No appreciable bending
142	98	6·40	100	0	100	30·1	Large torsional amplitude commencing at mid-span L.E. No appreciable bending
143	58	1·50	100	20	40	30·1	Torsional and bending amplitudes both moderate
144	83	1·03	100	20	70	30·1	Small torsional amplitude, large bending amplitude
145	63	1·39	100	20	100	30·1	Small torsional amplitude, large bending amplitude
146	57·5	1·46	100	40	40	30·1	Large torsional amplitude with only a little bending
147	80·5	—	100	40	70	30·1	No film
148	59	—	100	40	100	30·1	No film
149	70	2·78	100	60	40	30·1	Moderate torsional amplitude with only a little bending
150	71·5	1·52	100	60	70	30·1	Moderate torsional amplitude with only a little bending
151	74·5	2·29	100	60	100	30·1	Moderate torsional amplitude with only a little bending
152	75	—	100	80	40	30·1	No film
153	80	1·80	100	80	70	30·1	Large torsional amplitude, small bending amplitude. Violent but intermittent
154	82	1·19	100	80	100	30·1	Moderate torsional amplitude with only a little bending
155	91·5	1·88	100	100	40	30·1	Large torsional amplitude, moderate bending amplitude
156	78	1·60	100	100	70	30·1	Torsional and bending amplitudes both moderate
157	92	—	100	100	100	30·1	No film

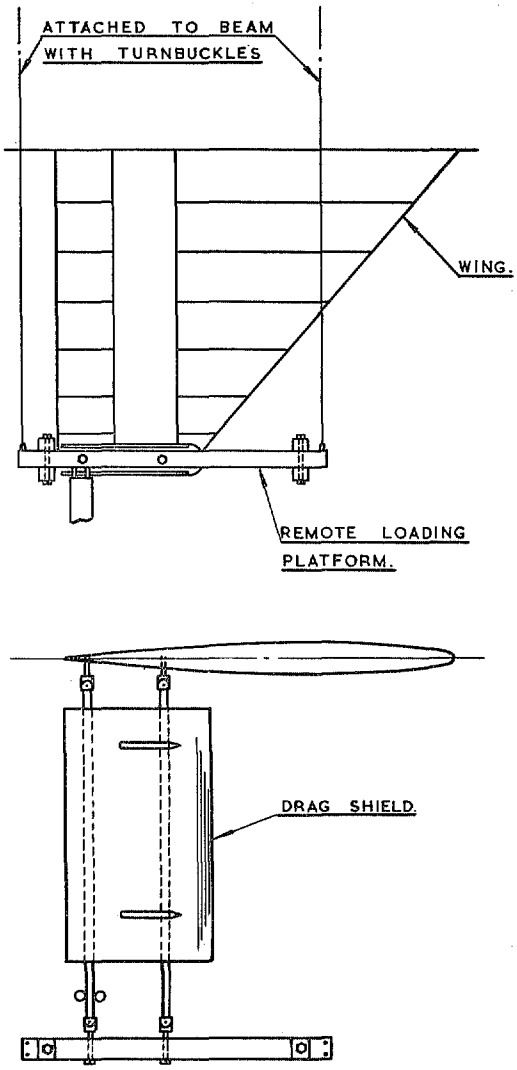

FIG. I.1. General arrangement of model and remote loading rig.

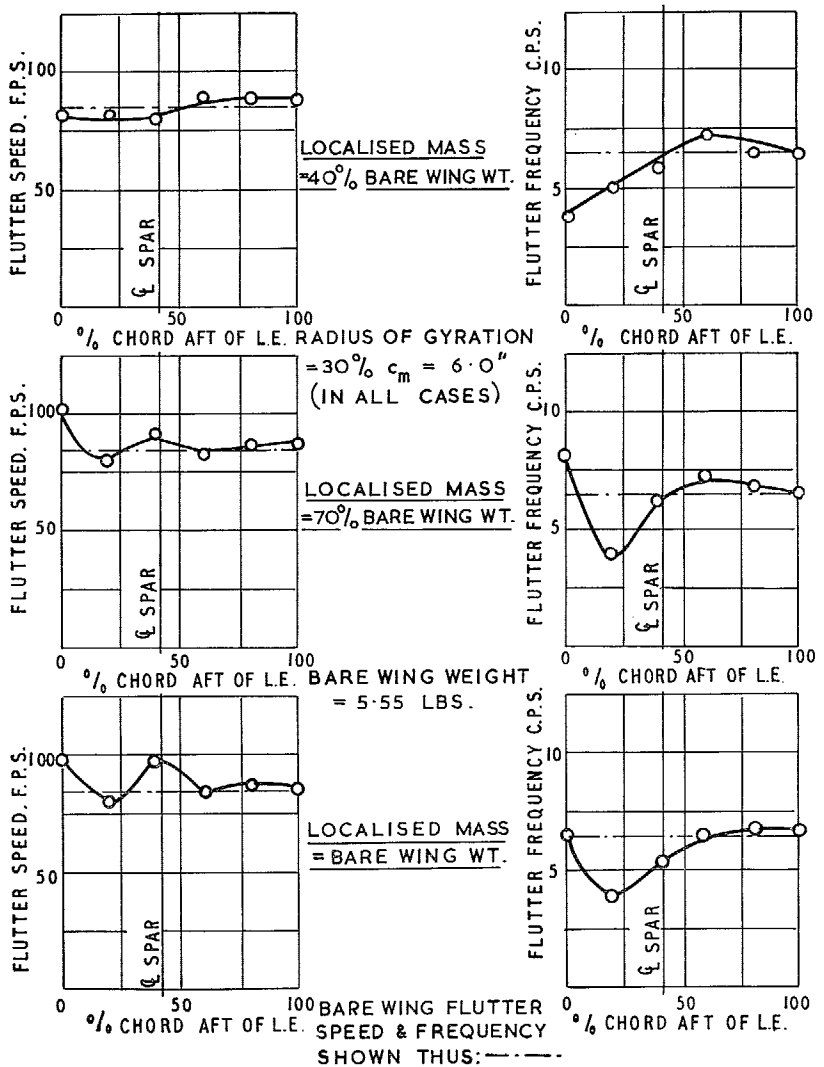

FIG. I.2. Wind tunnel tests on model with original stiffness distribution. The effect of chordwise position of a localised mass at 25 per cent semi-span.

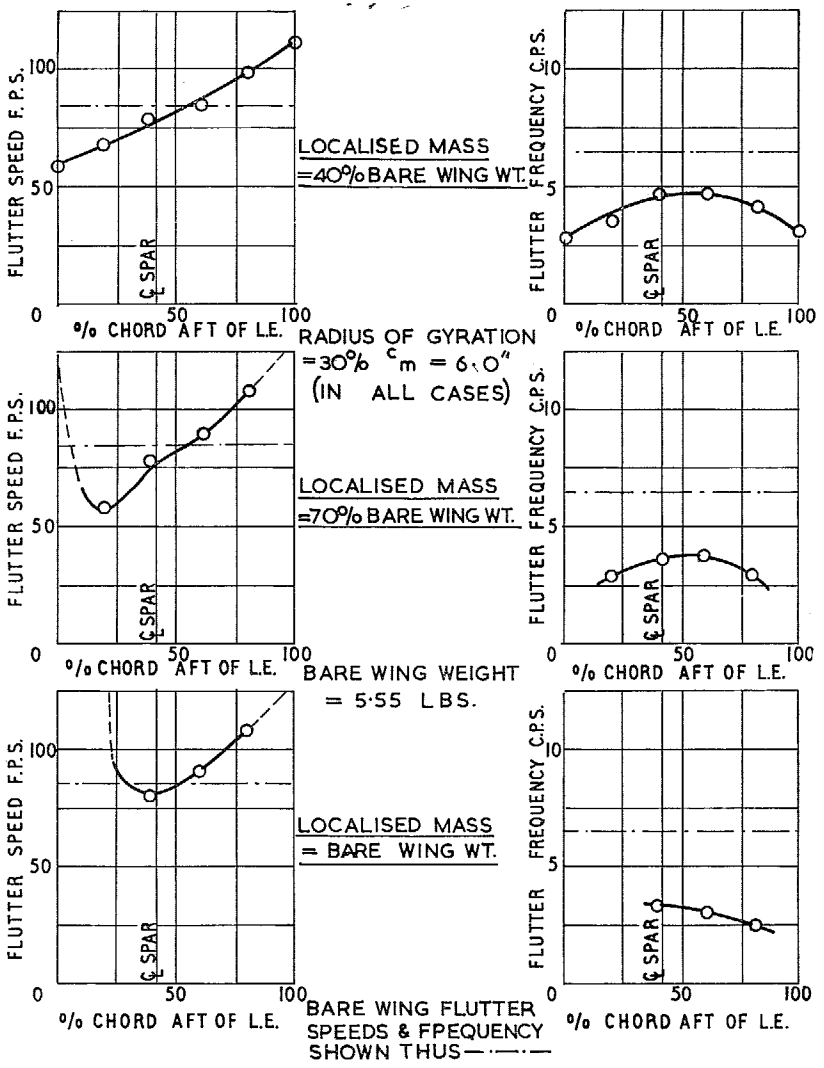

FIG. I.3. Wind tunnel tests on model with original stiffness distribution. The effect of chordwise position of a localised mass at 50 per cent semi-span.

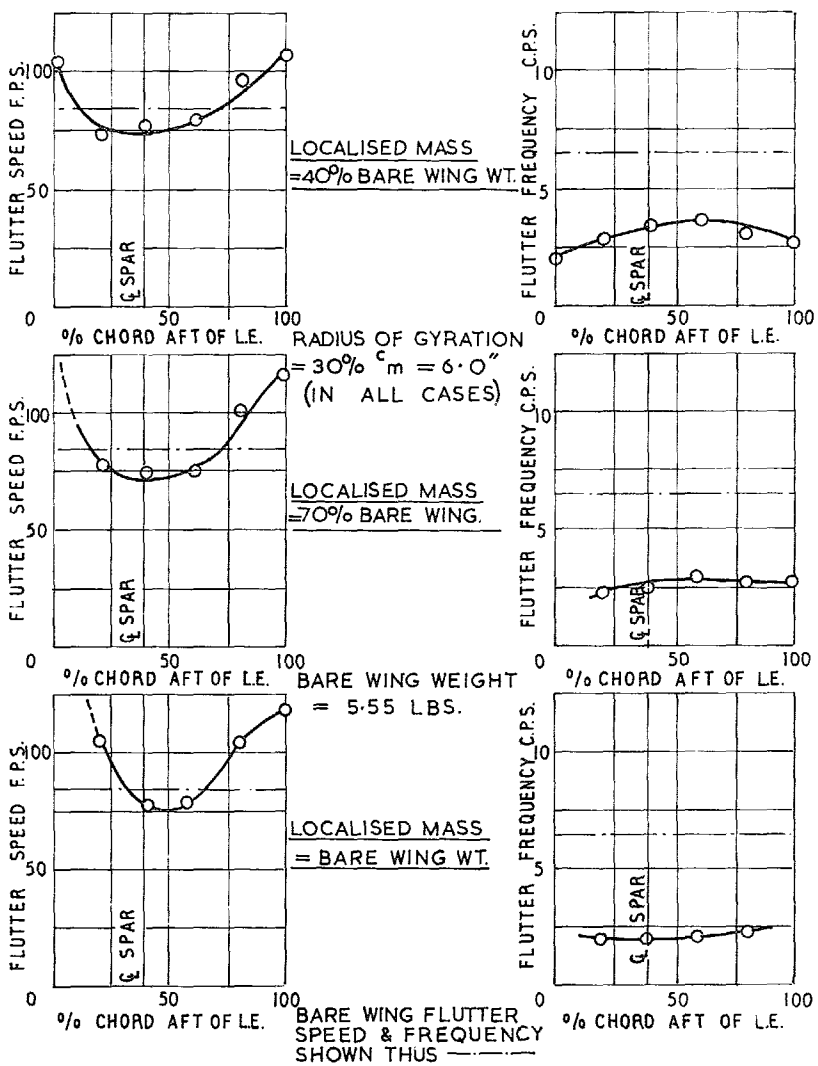

FIG. I.4. Wind tunnel tests on model with original stiffness distribution. The effect of chordwise position of a localised mass at 75 per cent semi-span.

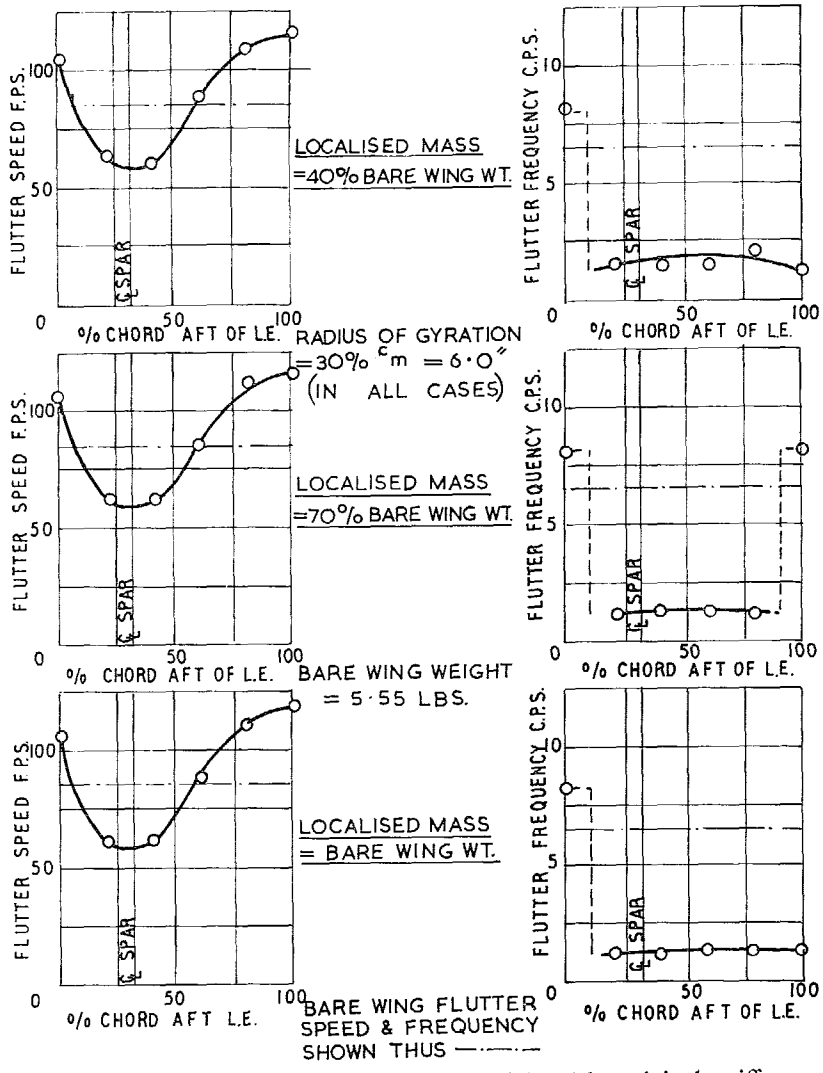

FIG. I.5. Wind tunnel tests on model with original stiffness distribution. The effect of chordwise position of a localised mass at wing-tip.

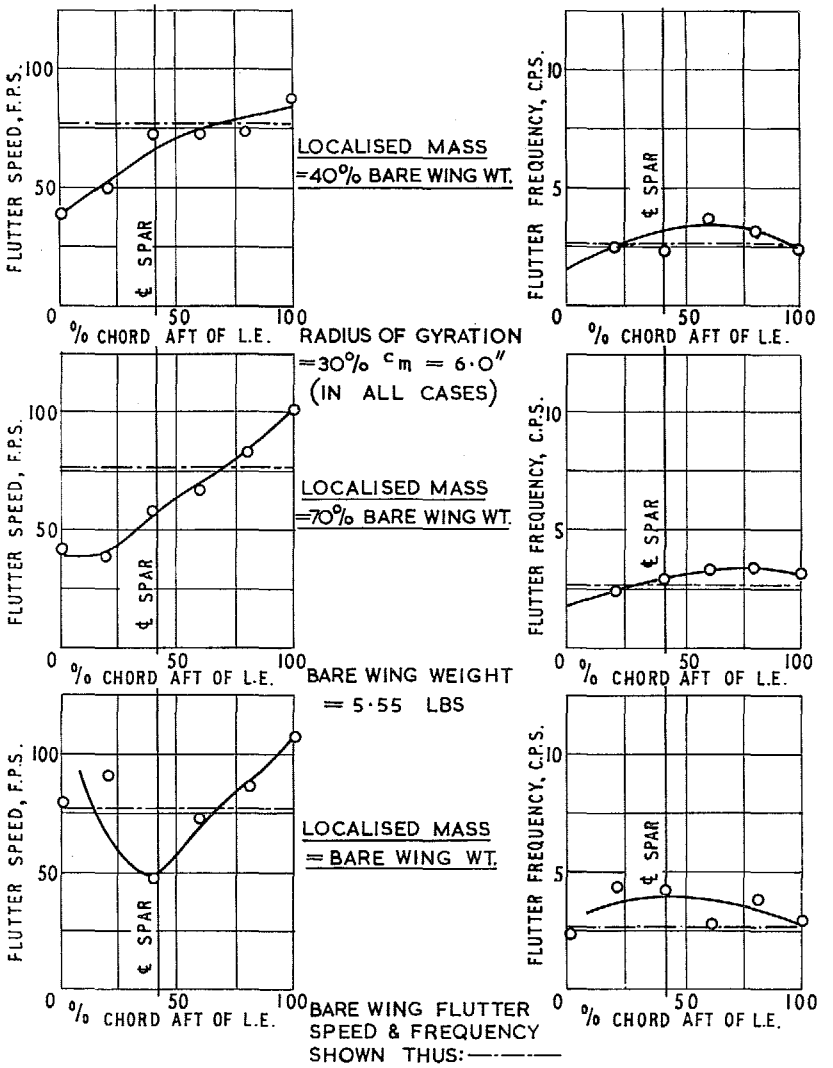

FIG. I.6. Wind tunnel tests on model with modified stiffness distribution. The effect of chordwise position of a localised mass at 50 per cent semi-span.

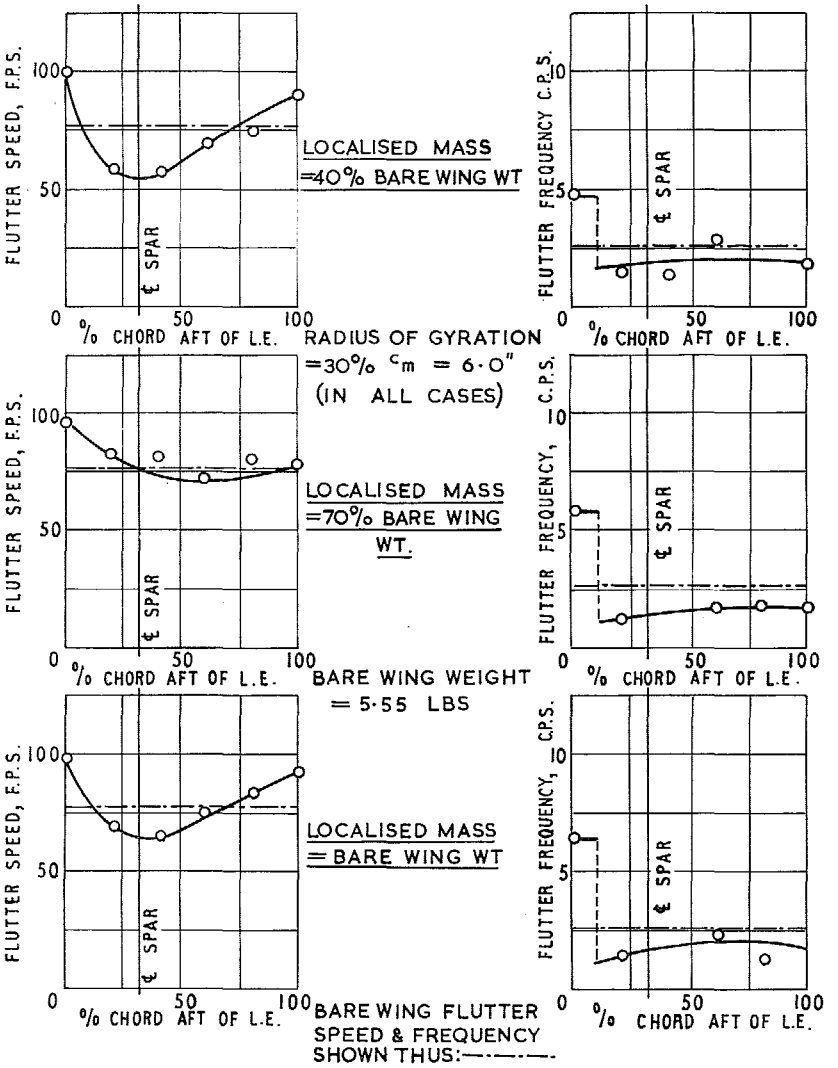

FIG. I.7. Wind tunnel tests on model with modified stiffness distribution. The effect of chordwise position of a localised mass at wing-tip.

APPENDIX II

Theoretical Flutter Investigations

1. *Introduction.* In certain cases the flutter characteristics of the model wing were determined from theoretical investigations as well as by wind tunnel tests. This work was carried out, partly with a view to examining the reliability of theoretical methods in handling this kind of flutter problem and partly with the object of obtaining a better understanding of the different kinds of flutter associated with different positions of the localised mass.

A total of ten cases were covered in the course of these theoretical investigations, seven of them being for the model with its original wing stiffness distribution and three for the model with the spar modified to simulate the effect of a large cut-out. In all cases, the flutter speeds and frequencies were obtained from calculations based on both simple arbitrary modes and modes obtained from resonance tests.

2. *Range of Theoretical Investigations.* The cases covered by these theoretical investigations have been designated as follows:

Model with the original spar.

Case 1	Bare wing with no localised mass.
Case 2	Wing with localised mass equal to 70 per cent of the bare wing weight, at 75 per cent semi-span, on leading edge.
Case 3	Mass and spanwise position similar to Case 2, but with mass c.g. 40 per cent chord aft of the leading edge.
Case 4	Mass and spanwise position similar to Case 2, but with mass c.g. on the trailing edge.
Case 5	Wing with localised mass equal to 70 per cent of the bare wing weight, at wing-tip, on leading edge.
Case 6	Mass and spanwise position similar to Case 5, but with mass c.g. 40 per cent chord aft of the leading edge.
Case 7	Mass and spanwise position similar to Case 5, but with mass c.g. on trailing edge.

Model with spar modified to simulate a large cut-out.

Case 1A	Bare wing with no localised mass.
Case 5A	Wing with localised mass equal to 70 per cent of the bare wing weight, at wing-tip, on leading edge.
Case 6A	Mass and spanwise position similar to Case 5A, but with mass c.g. 40 per cent chord aft of the leading edge.

Although the two bare wing cases do not strictly fulfill the purposes set out in the Introduction, it was considered necessary to include them so as to get a general indication of the reliability of the basic data and the assumptions that had been made, without the additional complication of a localised mass.

3. *Basic Data.* 3.1. *Aerodynamic Derivatives.* 'Equivalent Constant Strip' derivatives were used throughout in these investigations. These were derived from overall steady motion data and two-dimensional flutter derivatives in accordance with the procedure given in Ref. 2.

The numerical values of the derivatives were as follows:

Stiffness Derivatives:

1_z	0	m_z	0
1_α	1·43	m_α	− 0·393

Damping Derivatives:

$1_{\dot{z}}$	1·43	$m_{\dot{z}}$	− 0·393
$1_{\dot{\alpha}}$	1·29	$m_{\dot{\alpha}}$	− 0·641

Acceleration Derivatives:

$1_{\ddot{z}}$	0·7854	$m_{\ddot{z}}$	− 0·3927
$1_{\ddot{\alpha}}$	0·3927	$m_{\ddot{\alpha}}$	− 0·2208

These acceleration derivatives are simply the two-dimensional values.

3.2. *Structural Inertia.* As far as possible, the inertia data used in these theoretical investigations was based on actual weighed weights and c.g. positions. Each of the box segments was weighed and its c.g. determined, while in the case of the plate spar, its weighed weight and experimentally determined c.g. position were used to check the calculated distribution.

3.3. *Structural Stiffness.* Structural stiffness tests were carried out to provide data for the calculation of the structural stiffness coefficients in the arbitrary mode investigations. (The structural stiffness coefficients in the resonance mode calculations were derived directly from the inertia coefficients and the mode frequencies; *see* Section 5 below.)

Comparison of the experimentally determined stiffness with results obtained by calculation showed general agreement in the form of the stiffness distribution although the actual structure was stiffer than calculated. However, the calculations were based on the assumption that only the material between roots of the saw-cuts was effective as structure, whereas a greater width was probably effective in between the cuts. It was found that if the effective width was increased by about 30 per cent, quite good agreement could be obtained between calculations and test results.

Apart from its main use in providing data for the actual flutter calculations, the stiffness test results were also used to estimate the flutter speed of the bare wing by substitution in the formula given in Section 8 of A.R.C. R. & M. 3231. The results obtained, 76 ft/sec for the original wing and 65 ft/sec for the wing with the spar modified to simulate the effect of a large cut-out are in quite good agreement with the results obtained from wind tunnel tests and detailed theoretical investigations (*cf.*, Tables 1 and 2).

3.4. *Resonance Test Results.* As the discussion of this part of the data for the theoretical investigations is specifically related to the resonance mode calculations, it seems desirable to defer such discussion to Section 5.

4. *Arbitrary Mode Flutter Calculations.* 4.1. *Arbitrary Modes.* Six arbitrary modes, three bending and three torsion, were used in these calculations. The modes were simple polynomial functions of the spanwise co-ordinate η ($= y/s$) and were defined as follows:

Bending Modes

Mode 1 $\quad f_1 = \eta^2$

Mode 2 $\quad f_2 = \eta^2 - \eta^3$

Mode 3 $\quad f_3 = \eta^2 - 3\eta^3 + 2\eta^4$

Torsion Modes

Mode 4 $\quad f_4 = \eta$

Mode 5 $\quad f_5 = \eta - \eta^2$

Mode 6 $\quad f_6 = \eta - 3\eta^2 + 2\eta^3$

Modes 1 and 4 have no nodes, modes 2 and 5 one node and modes 3 and 6 two nodes each. By having modes that did not resemble each other, it was hoped that the resulting flutter equations would be sufficiently well conditioned for solution by an analogue computer. In the event, however, this hope was not realised and it was necessary to change the co-ordinates using the procedure given in Ref. 3. Further details of this work are given in Section 4.3 below.

4.2. *Calculations of Flutter Coefficients.* The calculation of the aerodynamic coefficients corresponding to a set of simple arbitrary modes is a very straightforward procedure and calls for no comment. As the same modes were used throughout, the same set of aerodynamic coefficients served for all ten cases. The contribution of the wing structure to the structural inertia coefficients also remained unchanged and it was only necessary to include the appropriate contribution from the localised mass in each case.

With regard to structural stiffness coefficients, however, there is no wholly satisfactory procedure for evaluating them except in the simplest cases, and it seems probable that at least part of the discrepancies between the results of these flutter calculations and the wind tunnel test results is due to trouble with these coefficients.

4.3. *Improvement of the Equations for Solution by Analogue Computer.* As has already been mentioned in Section 4.1, the flutter equations obtained from the chosen arbitrary modes were too ill-conditioned for satisfactory solutions to be obtained from an analogue computer. It was necessary, therefore, to transform the equations so as to improve the conditioning.

To effect this improvement, the co-ordinates were changed in accordance with the procedure given in Ref. 3, the inertia couplings between modes of like kind being reduced to zero. The original flutter coefficients, as obtained directly from the specified arbitrary modes, and the transformed coefficients for analogue computer solution are given at the end of this Appendix in Tables II.1 and II.2 respectively.

4.4. *Results of Arbitrary Mode Flutter Calculations.* The results of these arbitrary mode flutter calculations have been set out in Table 1, and discussed in Sections 6.2.1 and 7.2 in the main part of this Report.

Recapitulating, the theoretical flutter speeds are all lower than the corresponding results obtained in wind tunnel flutter tests. In six of the cases, the experimental flutter speed is of the order

of 20 to 30 per cent higher than the theoretical estimate, while in the remaining four cases, the experimental speed exceeds the theoretical results by 50 per cent in Case 7, 70 per cent in Case 4, and more than 100 per cent in Cases 6 and 6A.

The flutter frequencies for those cases relating to the wing with its original spar stiffness are generally quite good, although in Case 7, the calculations failed to give the overtone type of flutter obtained in tunnel tests (and resonance mode flutter calculations). For the wing with the modified spar, however, the flutter frequencies obtained by calculation were higher than those recorded in the wind tunnel tests.

In the four cases in which the agreement between the calculations and tunnel test results was indifferent, further investigations were carried out to try to account for the discrepancies. These investigations are discussed below:

Case 4. The theoretical solution, which was dominated by the 1–4 fundamental binary, gave a flutter speed that is well below the experimental result but in fair agreement with the result obtained from calculations based on resonance test modes. The effect of varying the coefficients in the 1–4 binary was investigated (*see* Figs. II.1 and II.2) but there appears to be no justification for altering any of the coefficients to the extent necessary to raise the flutter speed up to experimental result.

Cases 6 *and* 6*A*. The same general characteristics are apparent in the theoretical solutions for both these cases. The result in each case was dominated by the 1–4–5 ternary, while the 1–4 and 2–5 binaries gave flutter speeds much higher than either the ternary or the complete six degree-of-freedom problem. It is suspected that the small difference between the flutter speeds obtained for the 1–4 and 2–5 binaries may have something to do with the trouble in these two cases.

The effects of varying the coefficients in the ternary were investigated in both cases and the results are shown graphically in Figs. II.3 and II.4 for Case 6 and in Figs. II.5 and II.6 for Case 6A.

Case 7. The explanation of the trouble in this case is basically straightforward, the solution for the complete six degree-of-freedom problem being dominated by the wrong binary. If the 1–4 binary could be eliminated, the 2–5 binary would give a result that would agree very well with the experimental result and the flutter would be of the right type. However, investigations in which arbitrary chordwise movements of the localised mass c.g. were assumed failed to eliminate the 1–4 binary.

5. *Flutter Calculations Based on Resonance Test Modes.* 5.1. *Resonance Test Modes.* The frequency range covered in these tests was approximately 0 to 20 c.p.s., which sufficed to give four modes (fundamental and overtone bending and torsion) for the original wing with no localised mass. With the addition of a localised mass the frequencies were generally reduced and more resonances were found within the frequency range. Thus in all of the other nine cases that were investigated, five or six resonance modes were available as degrees-of-freedom in the flutter calculations.

The inclusion of these extra modes in the flutter calculations did not generally give superior results, however, and the best result was obtained, in fact, from the quaternary in Case 1. In fairness, however, it should be added that there is reason to suspect that in at least some of the cases one or more of the additional modes may be spurious.

In this connection, the check on the orthogonal properties of the modes, set out in Table II.4, is quite revealing. While in many cases the inertia couplings are generally rather larger than is really desirable, certain modes stand out as being particularly bad. Thus in Cases 2, 3 and 4, the fourth mode is notably poor. Further examination of this mode shows that in all three cases the form and the

frequency have a considerable resemblance to the fundamental torsion mode of the bare wing. This looks suspiciously like the effect of backlash in the remote loading rig and seems fair grounds for rejecting the mode as spurious. Fortunately, however, the fourth mode is fairly passive in all three cases and is unlikely to influence the results.

Of the remaining cases for the wing with its original spar stiffness, the modes for Cases 5 and 6 are generally quite good while those for Case 7 are poor. Surprisingly enough, the largest inertia couplings in Case 7 are associated with the first mode.

Turning to the results obtained in the tests on the model with its spar stiffness modified to simulate a large cut-out, most of the modes for Cases 1A and 5A are fairly good. Both these cases involve one bad mode, however, as may be seen from inspection of Table II.4. In Case 1A, the second mode is definitely peculiar and gives a low flutter speed if it is included in the flutter equations (*see* later). The mode is of fundamental torsion form but the frequency is unreasonably low and it is probably spurious.

The fifth mode in Case 5A is also spurious. In Table II.4 the large coupling between modes four and five is readily apparent but it is not clear from the couplings with the other modes which one of them is at fault. In fact, however, the form of the fifth mode was very distorted and it was finally discarded.

In Case 6A, the results are generally poor with quite large inertia couplings, between nearly all of the modes. The effects of this are reflected in the results from the flutter calculations.

5.2. *Calculation of Flutter Coefficients.* The coefficients, set out in full in Table II.3, were computed by the usual matrix multiplication procedure.

5.3. *Results of Flutter Calculations based on Resonance Test Modes.* The results of these flutter calculations have already been given in Table 2 in the main part of this Report, and have been discussed in Sections 6.2.2 and 7.2.

Of the ten cases investigated, Cases 1, 3, 5A and 6 have given results that are in quite good agreement with those obtained from wind tunnel tests, while the agreement is also fair for Cases 4 and 5. These six cases will not be considered further, therefore, and our attention here will be confined to the remaining four cases in which the agreement is indifferent or poor.

In *Case* 2 the theoretical investigations gave a very low flutter speed which conflicts with the evidence from wind tunnel tests. The results from the investigations on the constituents of the complete quinary leave little doubt but that mode 2 is the source of the trouble, yet there is no evidence from either the form of the mode, or from the inertia couplings in Table II.4 that it is unsatisfactory. The effects of varying the coefficients in the dominant 1–2 binary were investigated (*see* Figs. II.7 and II.8) in an attempt to resolve the problem but no clear-cut explanation was obtained. It seems probable, however, that the anomalous result is due to the fact that the flutter characteristics are acutely sensitive to precise positioning of a localised mass in the region concerned.

A very similar situation arose in the results obtained for *Case* 1*A*. Here again a very low flutter speed was given by the complete set of flutter equations. However, there seems to be a straightforward explanation in this case as there is good reason to believe that the mode which causes the trouble is spurious. (*See* Section 5.1 of this Appendix.)

In the remaining two cases, Numbers 6A and 7, the shortcomings in the theoretical results are quite clearly attributable to lack of orthogonality in the resonance modes. In both cases the solutions obtained with and without the inertia couplings included in the flutter equations showed little

difference in frequency but a wide variation in flutter speed. The possibility of normalising the modes was considered but abandoned in view of the difficulties involved in making reliable estimates of the cross-structural stiffnesses.

Tables of Coefficients Used in Theoretical Flutter Investigations

The following tables contain the matrices of flutter coefficients calculated in the course of the theoretical investigations on the delta wing flutter model.

Coefficients for Arbitrary Mode Flutter Calculations (Prior to Transformation).	Table II.1
Transformed Coefficients for Arbitrary Mode Flutter Calculations	Table II.2
Coefficients for Flutter Calculations based on Resonance Test Modes	Table II.3
Magnitude of Inertia Couplings between the Resonance Test Modes	Table II.4

All of the coefficients given in Tables II.1, II.2 and II.3, are expressed in non-dimensional form, the relevant reference dimensions, speed, etc., being as follows:

Reference Length	1·788 ft
Reference Chord	1·656 ft
Reference Speed	100 ft/sec
Air Density	0·00238 slugs/ft^3

TABLE II.1

Arbitrary Mode Flutter Calculations

Matrices of Coefficients (Prior to Transformation)

1. *Inertia Coeficients* [*A*].

Cases 1 and 1A.

1·650120	0·353605	−0·118312	0·246873	0·062627	−0·014433
0·353605	0·118320	−0·018500	0·062656	0·024110	−0·001203
−0·118312	−0·018500	0·015781	−0·014619	−0·001254	0·002996
0·246873	0·062656	−0·014619	0·192462	0·078046	0·004317
0·062627	0·024110	−0·001254	0·078046	0·041173	0·008219
−0·014433	−0·001203	0·002996	0·004317	0·008219	0·007392

Case 2.

5·239259	1·214278	−0·543158	−1·059089	−0·267803	0·148864
1·214278	0·324737	−0·120370	−0·250506	−0·055123	0·037953
−0·543158	−0·120370	0·066064	0·139964	0·037860	−0·016330
−1·059089	−0·250506	0·139964	1·197055	0·332220	−0·121288
−0·267803	−0·055123	0·037860	0·332220	0·105484	−0·023562
0·148864	0·037953	−0·016330	−0·121288	−0·023562	0·023097

Case 3.

5·239259	1·214278	−0·543158	0·258330	0·065530	−0·015864
1·214278	0·324737	−0·120370	0·065405	0·024805	−0·001547
−0·543158	−0·120370	0·066064	−0·015976	−0·001597	0·003165
0·258330	0·065405	−0·015976	0·721195	0·211822	−0·061791
0·065530	0·024805	−0·001597	0·211822	0·075021	−0·008508
−0·015864	−0·001547	0·003165	−0·061791	−0·008508	0·015658

Note that elements in 1 to 3 block are identical to those in Case 2.

TABLE II.1—*continued*

Case 4.

5·239259	1·214278	−0·543158	2·406956	0·609128	−0·284521
1·214278	0·324737	−0·120370	0·580629	0·155162	−0·065967
−0·543158	−0·120370	0·066064	−0·270301	−0·065946	0·034966
2·406956	0·580629	−0·270301	2·021878	0·540911	−0·224417
0·609128	0·155162	−0·065946	0·540911	0·158287	−0·049655
−0·284521	−0·065967	0·034966	−0·224417	−0·049655	0·035993

Note that elements in 1 to 3 block are identical to those in Case 2.

Cases 5 and 5A.

12·031040	0·353605	−0·118312	−1·358933	0·062627	−0·014433
0·353605	0·118320	−0·018500	0·062656	0·024110	−0·001203
−0·118312	−0·018500	0·015781	−0·014619	−0·001254	0·002996
−1·358933	0·062656	−0·014619	1·390144	0·078046	0·004317
0·062627	0·024110	−0·001254	−0·078046	0·041173	0·008219
−0·014433	−0·001203	0·002996	0·004317	0·008219	0·007392

Cases 6 and 6A.

12·031040	0·353605	−0·118312	0·782539	0·062627	−0·014433
0·353605	0·118320	−0·018500	0·062656	0·024110	−0·001203
−0·118312	−0·018500	0·015781	−0·014619	−0·001254	0·002996
0·782539	0·062656	−0·014619	1·139995	0·078046	0·004317
0·062627	0·024110	−0·001254	0·078046	0·041173	0·008219
−0·014433	−0·001203	0·002996	0·004317	0·008219	0·007392

Note that all elements except a_{14}, a_{41} and a_{44} are identical to Cases 5 and 5A.

Case 7.

12·031040	0·353605	−0·118312	3·997936	0·062627	−0·014433
0·353605	0·118320	−0·018500	0·062656	0·024110	−0·001203
−0·118312	−0·018500	0·015781	−0·014619	−0·001254	0·002996
3·997936	0·062656	−0·014619	2·496862	0·078046	0·004317
0·062627	0·024110	−0·001254	0·078046	0·041173	0·008219
−0·014433	−0·001203	0·002996	0·004317	0·008219	0·007392

Note that all elements except a_{14}, a_{41} and a_{44} are identical to Cases 5 and 5A.

2. *Structural Stiffness Coefficients* [*E*].

Cases 1 to 7 inclusive.

0·288090	0·081270	−0·014966	0	0	0
0·081270	0·112563	0·018029	0	0	0
−0·014966	0·018029	0·080941	0	0	0
0	0	0	0·109625	0·056440	0·011526
0	0	0	0·056440	0·044235	0·019680
0	0	0	0·011526	0·019680	0·021150

Cases 1A, 5A and 6A.

0·208628	0·065390	0·019856	0	0	0
0·065390	0·102901	0·021005	0	0	0
0·019856	0·021005	0·062745	0	0	0
0	0	0	0·078485	0·041835	0·015141
0	0	0	0·041835	0·036263	0·020015
0	0	0	0·015141	0·020015	0·019035

TABLE II.1—*continued*

3. *Aerodynamic Damping Coefficients* [*B*].

Applicable to All Cases.

0·194923	0·038302	−0·014400	0·101385	0·026726	−0·005595
0·038302	0·012033	−0·002324	0·026739	0·010571	−0·000303
−0·014400	−0·002324	0·001760	−0·005674	−0·000327	0·001335
−0·019137	−0·006622	0·000652	0·035671	0·013595	0·000374
−0·006618	−0·002992	−0·000141	0·013595	0·006983	0·001314
0·000637	−0·000129	−0·000348	0·000374	0·001314	0·001159

4. *Aerodynamic Stiffness Coefficients* [*C*].

Applicable to All Cases.

0	0	0	0·255589	0·060666	−0·015910
0	0	0	0·060693	0·022391	−0·001657
0	0	0	−0·016107	−0·001706	0·002941
0	0	0	−0·033237	−0·014101	−0·000869
0	0	0	−0·014101	−0·007483	−0·001507
0	0	0	−0·000869	−0·001507	−0·001481

TABLE II.2

Arbitrary Mode Flutter Calculations

Transformed Coefficients

Case 1. (Case 1A is identical, apart from its structural stiffness matrix.)

Inertia Matrix [*A*].

1·650120	0	0	0·246873	−0·037483	0·005486
0	0·042546	0	0·009754	0·006735	−0·002902
0	0	0·006194	0·001511	0·000901	0·001011
0·246873	0·009754	0·001511	0·192462	0	0
−0·037483	0·006735	0·000901	0	0·009524	0
0·005486	−0·002902	0·001010	0	0	0·002902

Aerodynamic Damping Matrix [*B*].

0·194923	−0·003468	0·000134	0·101385	−0·014387	0·001902
−0·003468	0·004568	−0·000222	0·005013	0·002811	−0·001126
0·000134	−0·000223	0·000650	0·000788	0·000489	0·000440
−0·019137	−0·002521	−0·000314	0·035671	−0·000870	0·000165
0·001142	−0·000552	−0·000234	−0·000870	0·001823	−0·000056
0·000290	0·000166	−0·000093	0·000165	−0·000056	0·000395

Aerodynamic Stiffness Matrix [*C*].

0	0	0	0·255589	−0·042979	0·007546
0	0	0	0·005923	0·006989	−0·003128
0	0	0	0·001265	0·000618	0·001070
0	0	0	−0·033237	−0·000623	0·000300
0	0	0	−0·000623	−0·001512	−0·000114
0	0	0	0·000300	−0·000114	−0·000607

TABLE II.2—*continued*

Case 1. (*continued*)

Structural Stiffness Matrix [*E*].

0·288090	0·019535	0·002543	0	0	0
0·019535	0·090962	0·007985	0	0	0
0·002543	0·007985	0·075343	0	0	0
0	0	0	0·109625	0·011986	0·000927
0	0	0	0·011986	0·016488	0·003540
0	0	0	0·000927	0·003540	0·008275

Structural Stiffness Matrix [*E*] *for Case* 1*A*.

0·208628	0·020683	0·031483	0	0	0
0·020683	0·084457	0·004629	0	0	0
0·031483	0·004630	0·062983	0	0	0
0	0	0	0·078485	0·010008	0·006583
0	0	0	0·010008	0·015240	0·003301
0	0	0	0·006583	0·003301	0·006883

Case 2.

Inertia Matrix [*A*].

5·239259	0	0	−1·059089	0·026127	0·021691
0	0·043310	0	−0·005046	0·008344	−0·003403
0	0	0·009052	0·030810	0·000662	0·001281
−1·059089	−0·005046	0·030810	1·197055	0	0
0·026127	0·008345	0·000662	0	0·013283	0
0·021691	−0·003404	0·001282	0	0	0·003130

Aerodynamic Damping Matrix [*B*].

0·194923	−0·006874	0·006683	0·101385	−0·001411	0·005751
−0·006874	0·004749	−0·000304	0·003242	0·003477	−0·001321
0·006683	−0·000304	0·000870	0·004424	0·000658	0·000576
−0·019137	−0·002187	−0·001054	0·035671	0·003695	0·001179
−0·001307	−0·000851	−0·000349	0·003695	0·002185	−0·000076
−0·000308	0·000149	−0·000088	0·001179	−0·000076	0·000454

Aerodynamic Stiffness Matrix [*C*].

0	0	0	0·255589	−0·010268	0·017793
0	0	0	0·001456	0·007927	−0·003849
0	0	0	0·010205	0·000691	0·001542
0	0	0	−0·033237	−0·004877	−0·000529
0	0	0	−0·004877	−0·002216	−0·000075
0	0	0	−0·000529	−0·000075	−0·000603

Structural Stiffness Matrix [*E*].

0·288090	0·014501	0·013054	0	0	0
0·014501	0·090366	0·011495	0	0	0
0·013054	0·011495	0·076542	0	0	0
0	0	0	0·109625	0·026016	0·002854
0	0	0	0·026016	0·021351	0·002884
0	0	0	0·002854	0·002884	0·007884

TABLE II.2—*continued*

Case 3.

Inertia Matrix [*A*].

5·239259	0	0	0·258330	−0·010344	0·014059
0	0·043310	0	0·005533	0·007992	−0·003414
0	0	0·009052	0·010101	0·001005	0·001358
0·258330	0·005533	0·010101	0·721195	0	0
−0·010344	0·007992	0·001005	0	0·012807	0
0·014059	−0·003414	0·001358	0	0	0·003104

Aerodynamic Damping Matrix [*B*].

0·194923	−0·006874	0·006683	0·101385	−0·003052	0·005389
−0·006874	0·004749	−0·000304	0·003242	0·003425	−0·001307
0·006683	−0·000304	0·000870	0·004424	0·000587	0·000565
−0·019137	−0·002187	−0·001054	0·035671	0·003118	0·001083
−0·000997	−0·000816	−0·000331	0·003118	0·002074	−0·000091
−0·000252	0·000150	−0·000087	0·001083	−0·000091	0·000445

Aerodynamic Stiffness Matrix [*C*].

0	0	0	0·255589	−0·014403	0·016835
0	0	0	0·001456	0·007903	−0·003796
0	0	0	0·010205	0·000526	0·001512
0	0	0	−0·033237	−0·004339	−0·000450
0	0	0	−0·004339	−0·002067	−0·000067
0	0	0	−0·000450	−0·000067	−0·000601

Structural Stiffness Matrix [*E*].

0·288090	0·014501	0·013054	0	0	0
0·014501	0·090366	0·011495	0	0	0
0·013054	0·011495	0·076542	0	0	0
0	0	0	0·109625	0·024242	0·002665
0	0	0	0·024242	0·020538	0·002907
0	0	0	0·002665	0·002907	0·007907

Case 4.

Inertia Matrix [*A*].

5·239259	0	0	2·406956	−0·034803	0·009247
0	0·043310	0	0·022781	0·007893	−0·003532
0	0	0·009052	−0·023672	0·001754	0·001503
2·406956	0·022781	−0·023672	2·021878	0	0
−0·034803	0·007893	0·001754	0	0·013578	0
0·009247	−0·003532	0·001503	0	0	0·003144

Aerodynamic Damping Matrix [*B*].

0·194923	−0·006874	0·006683	0·101385	−0·000397	0·005962
−0·006874	0·004749	−0·000304	0·003242	0·003510	−0·001330
0·006683	−0·000304	0·000870	0·004424	0·000702	0·000582
−0·019137	−0·002187	−0·001054	0·035671	0·004052	0·001235
−0·001498	−0·000873	−0·000359	0·004052	0·002262	−0·000066
−0·000341	0·000148	−0·000088	0·001235	−0·000066	0·000460

TABLE II.2—*continued*

Case 4. (*continued*)

Aerodynamic Stiffness Matrix [*C*].

0	0	0	0·255589	−0·007711	0·018355
0	0	0	0·001456	0·007941	−0·003881
0	0	0	0·010205	0·000793	0·001559
0	0	0	−0·033237	−0·005209	−0·000575
0	0	0	−0·005209	−0·002317	−0·000081
0	0	0	−0·000575	−0·000081	−0·000605

Structural Stiffness Matrix [*E*].

0·288090	0·014501	0·013054	0	0	0
0·014501	0·090366	0·011495	0	0	0
0·013054	0·011495	0·076542	0	0	0
0	0	0	0·109625	0·027112	0·002961
0	0	0	0·027112	0·021883	0·002872
0	0	0	0·002961	0·002873	0·007870

Case 5. (Case 5A is identical, apart from its structural stiffness matrix.)

Inertia Matrix [*A*].

12·031040	0	0	−1·358933	0·138920	−0·040304
0	0·107927	0	0·102596	0·016509	−0·004675
0	0	0·012526	−0·013702	0·003231	0·002088
−1·358933	0·102596	−0·013702	1·390144	0	0
0·138920	0·016509	0·003231	0	0·036791	0
−0·040304	−0·004675	0·002088	0	0	0·005650

Aerodynamic Damping Matrix [*B*].

0·194923	0·032573	−0·007949	0·101385	0·021034	−0·010468
0·032573	0·009950	−0·000195	0·023759	0·008451	−0·002044
−0·007949	−0·000195	0·001249	−0·001370	0·001375	0·000967
−0·019137	−0·006060	−0·000380	0·035671	0·011592	−0·002249
−0·005544	−0·002457	−0·000575	0·011592	0·005569	0·000050
0·001898	0·000403	−0·000237	−0·002249	0·000050	0·000874

Aerodynamic Stiffness Matrix [*C*].

0	0	0	0·255589	0·046317	−0·026740
0	0	0	0·053181	0·017622	−0·005173
0	0	0	−0·006191	0·002107	0·002182
0	0	0	−0·033237	−0·012235	0·001885
0	0	0	−0·012235	−0·006004	−0·000119
0	0	0	0·001885	−0·000119	−0·001142

Structural Stiffness Matrix [*E*].

0·288090	0·072803	−0·001999	0	0	0
0·072803	0·108034	0·034223	0	0	0
−0·001999	0·034223	0·088109	0	0	0
0	0	0	0·109625	0·050285	0·000290
0	0	0	0·050285	0·038243	0·010591
0	0	0	0·000290	0·010591	0·014694

TABLE II.2—*continued*

Case 5. (*continued*)

Structural Stiffness Matrix [*E*] *for Case* 5*A*.

0·208626	0·059258	0·030156	0	0	0
0·059258	0·099237	0·034818	0	0	0
0·030156	0·034818	0·070926	0	0	0
0	0	0	0·078485	0·037429	0·006787
0	0	0	0·037429	0·031813	0·012156
0	0	0	0·006787	0·012156	0·012181

Case 6. (Case 6A is identical, apart from its structural stiffness matrix.)

Inertia Matrix [*A*].

12·031040	0	0	0·782539	0·009053	−0·019410
0	0·107927	0	0·039656	0·019554	−0·005254
0	0	0·012526	−0·001404	0·002558	0·002186
0·782539	0·039656	−0·001404	1·139995	0	0
0·009053	0·019554	0·002558	0	0·035830	0
−0·019410	−0·005254	0·002186	0	0	0·005624

Aerodynamic Damping Matrix [*B*].

0·194923	0·032573	−0·007949	0·101385	0·019785	−0·010355
0·032573	0·009950	−0·000195	0·023759	0·008158	−0·002033
−0·007949	−0·000195	0·001249	−0·001370	0·001392	0·000958
−0·019137	−0·006060	−0·000380	0·035671	0·011153	−0·002228
−0·005308	−0·002383	−0·000570	0·011153	0·005288	0·000077
0·001883	0·000402	−0·000235	−0·002228	0·000077	0·000865

Aerodynamic Stiffness Matrix [*C*].

0	0	0	0·255589	0·043168	−0·026427
0	0	0	0·053181	0·016967	−0·005143
0	0	0	−0·006191	0·002183	0·002160
0	0	0	−0·033237	−0·011826	0·001872
0	0	0	−0·011826	−0·005708	−0·000140
0	0	0	0·001872	−0·000140	−0·001134

Structural Stiffness Matrix [*E*].

0·288090	0·072803	−0·001999	0	0	0
0·072803	0·108034	0·034223	0	0	0
−0·001999	0·034223	0·088109	0	0	0
0	0	0	0·109625	0·048935	0·000289
0	0	0	0·048935	0·037021	0·010519
0	0	0	0·000289	0·010519	0·014602

Structural Stiffness Matrix [*E*] *for Case* 6*A*.

0·208628	0·059258	0·030156	0	0	0
0·059258	0·099237	0·034818	0	0	0
0·030156	0·034818	0·070926	0	0	0
0	0	0	0·078485	0·036462	0·006781
0	0	0	0·036462	0·030903	0·012007
0	0	0	0·006781	0·012007	0·012100

TABLE II.2—*continued*

Case 7.

Inertia Matrix [*A*].

$$\begin{bmatrix} 12{\cdot}031040 & 0 & 0 & 3{\cdot}997936 & -0{\cdot}062340 & -0{\cdot}008365 \\ 0 & 0{\cdot}107927 & 0 & -0{\cdot}054847 & 0{\cdot}023983 & -0{\cdot}005689 \\ 0 & 0 & 0{\cdot}012526 & 0{\cdot}017062 & 0{\cdot}001929 & 0{\cdot}002314 \\ 3{\cdot}997936 & -0{\cdot}054847 & 0{\cdot}017062 & 2{\cdot}496862 & 0 & 0 \\ -0{\cdot}062340 & 0{\cdot}023983 & 0{\cdot}001928 & 0 & 0{\cdot}038733 & 0 \\ -0{\cdot}008365 & -0{\cdot}005689 & 0{\cdot}002314 & 0 & 0 & 0{\cdot}005697 \end{bmatrix}$$

Aerodynamic Damping Matrix [*B*].

$$\begin{bmatrix} 0{\cdot}194923 & 0{\cdot}032573 & -0{\cdot}007949 & 0{\cdot}101385 & 0{\cdot}023557 & -0{\cdot}010687 \\ 0{\cdot}032573 & 0{\cdot}009950 & -0{\cdot}000195 & 0{\cdot}023759 & 0{\cdot}009042 & -0{\cdot}002067 \\ -0{\cdot}007949 & -0{\cdot}000195 & 0{\cdot}001249 & -0{\cdot}001370 & 0{\cdot}001341 & 0{\cdot}000984 \\ -0{\cdot}019137 & -0{\cdot}006060 & -0{\cdot}000380 & 0{\cdot}035671 & 0{\cdot}012480 & -0{\cdot}002292 \\ -0{\cdot}006020 & -0{\cdot}002608 & -0{\cdot}000583 & 0{\cdot}012480 & 0{\cdot}006168 & -0{\cdot}000006 \\ 0{\cdot}001927 & 0{\cdot}000407 & -0{\cdot}000239 & -0{\cdot}002292 & -0{\cdot}000006 & 0{\cdot}000892 \end{bmatrix}$$

Aerodynamic Stiffness Matrix [*C*].

$$\begin{bmatrix} 0 & 0 & 0 & 0{\cdot}255589 & 0{\cdot}052677 & -0{\cdot}027347 \\ 0 & 0 & 0 & 0{\cdot}053181 & 0{\cdot}018946 & -0{\cdot}005235 \\ 0 & 0 & 0 & -0{\cdot}006191 & 0{\cdot}001953 & 0{\cdot}002222 \\ 0 & 0 & 0 & -0{\cdot}033237 & -0{\cdot}013062 & 0{\cdot}001915 \\ 0 & 0 & 0 & -0{\cdot}013062 & -0{\cdot}006634 & -0{\cdot}000073 \\ 0 & 0 & 0 & 0{\cdot}001915 & -0{\cdot}000073 & -0{\cdot}001159 \end{bmatrix}$$

Structural Stiffness Matrix [*E*].

$$\begin{bmatrix} 0{\cdot}288090 & 0{\cdot}072803 & -0{\cdot}001999 & 0 & 0 & 0 \\ 0{\cdot}072803 & 0{\cdot}108034 & 0{\cdot}034223 & 0 & 0 & 0 \\ -0{\cdot}001999 & 0{\cdot}034223 & 0{\cdot}088109 & 0 & 0 & 0 \\ 0 & 0 & 0 & 0{\cdot}109625 & 0{\cdot}053013 & 0{\cdot}000272 \\ 0 & 0 & 0 & 0{\cdot}053013 & 0{\cdot}040814 & 0{\cdot}010710 \\ 0 & 0 & 0 & 0{\cdot}000272 & 0{\cdot}010710 & 0{\cdot}014862 \end{bmatrix}$$

TABLE II.3

Case 1.

Inertia Coefficients [*A*].

$$\begin{bmatrix} 1{\cdot}8961 & -0{\cdot}6036 & -0{\cdot}1328 & -0{\cdot}0838 \\ -0{\cdot}6036 & 5{\cdot}2244 & 0{\cdot}0668 & -0{\cdot}2758 \\ -0{\cdot}1328 & 0{\cdot}0668 & 0{\cdot}4482 & 0{\cdot}0482 \\ -0{\cdot}0838 & -0{\cdot}2758 & 0{\cdot}0482 & 0{\cdot}2141 \end{bmatrix}$$

Aerodynamic Damping Coefficients [*B*].

$$\begin{bmatrix} 0{\cdot}2507 & -0{\cdot}1357 & -0{\cdot}1555 & -0{\cdot}0366 \\ -0{\cdot}0082 & 0{\cdot}7177 & 0{\cdot}0618 & -0{\cdot}1564 \\ 0{\cdot}0627 & -0{\cdot}0250 & 0{\cdot}0597 & 0{\cdot}0136 \\ 0{\cdot}0056 & 0{\cdot}0350 & 0{\cdot}0077 & 0{\cdot}0285 \end{bmatrix}$$

Aerodynamic Stiffness Coefficients [*C*].

$$\begin{bmatrix} 0{\cdot}1927 & -0{\cdot}1417 & -0{\cdot}3682 & -0{\cdot}1504 \\ 0{\cdot}0754 & 0{\cdot}2076 & -0{\cdot}1894 & -0{\cdot}1903 \\ 0{\cdot}1163 & -0{\cdot}2363 & -0{\cdot}1970 & -0{\cdot}0254 \\ 0{\cdot}0027 & 0{\cdot}1969 & 0{\cdot}0376 & -0{\cdot}0873 \end{bmatrix}$$

TABLE II.3—*continued*

Case 1. (*continued*)

Structural Stiffness Coefficients [*E*].

$$\begin{bmatrix} 0{\cdot}1170 & 0 & 0 & 0 \\ 0 & 3{\cdot}2353 & 0 & 0 \\ 0 & 0 & 0{\cdot}3929 & 0 \\ 0 & 0 & 0 & 0{\cdot}7169 \end{bmatrix}$$

Case 2.

Inertia Coefficients [*A*].

$$\begin{bmatrix} 1{\cdot}0873 & -0{\cdot}2674 & -0{\cdot}0838 & 0{\cdot}0572 & 0{\cdot}0789 \\ -0{\cdot}2674 & 21{\cdot}1997 & 0{\cdot}0607 & -0{\cdot}9812 & -0{\cdot}5364 \\ -0{\cdot}0838 & 0{\cdot}0607 & 0{\cdot}3729 & 0{\cdot}2348 & 0{\cdot}1046 \\ 0{\cdot}0572 & -0{\cdot}9812 & 0{\cdot}2348 & 0{\cdot}2313 & 0{\cdot}1738 \\ 0{\cdot}0789 & -0{\cdot}5364 & 0{\cdot}1046 & 0{\cdot}1738 & 0{\cdot}4260 \end{bmatrix}$$

Aerodynamic Damping Coefficients [*B*].

$$\begin{bmatrix} 0{\cdot}0748 & 0{\cdot}1350 & 0{\cdot}0061 & 0{\cdot}0167 & 0{\cdot}0150 \\ -0{\cdot}0563 & 0{\cdot}1586 & 0{\cdot}0097 & 0{\cdot}0005 & -0{\cdot}0113 \\ -0{\cdot}0024 & -0{\cdot}0122 & 0{\cdot}0511 & 0{\cdot}0428 & 0{\cdot}0618 \\ 0{\cdot}0040 & 0{\cdot}0087 & 0{\cdot}0278 & 0{\cdot}0280 & 0{\cdot}0470 \\ 0{\cdot}0040 & 0{\cdot}0079 & -0{\cdot}0117 & 0{\cdot}0049 & 0{\cdot}0483 \end{bmatrix}$$

Aerodynamic Stiffness Coefficients [*C*].

$$\begin{bmatrix} 0{\cdot}0568 & 0{\cdot}3171 & 0{\cdot}0323 & 0{\cdot}0507 & 0{\cdot}0791 \\ -0{\cdot}1040 & -0{\cdot}5532 & 0{\cdot}0108 & -0{\cdot}0225 & -0{\cdot}0249 \\ 0{\cdot}0020 & 0{\cdot}0195 & 0{\cdot}0322 & 0{\cdot}0343 & 0{\cdot}0583 \\ 0{\cdot}0056 & 0{\cdot}0286 & 0{\cdot}0024 & 0{\cdot}0051 & 0{\cdot}0078 \\ 0{\cdot}0122 & 0{\cdot}0189 & -0{\cdot}0871 & -0{\cdot}0793 & -0{\cdot}1389 \end{bmatrix}$$

Structural Stiffness Coefficients [*E*].

$$\begin{bmatrix} 0{\cdot}0313 & 0 & 0 & 0 & 0 \\ 0 & 1{\cdot}0598 & 0 & 0 & 0 \\ 0 & 0 & 0{\cdot}2230 & 0 & 0 \\ 0 & 0 & 0 & 0{\cdot}2376 & 0 \\ 0 & 0 & 0 & 0 & 1{\cdot}2982 \end{bmatrix}$$

Case 3.

Inertia Coefficients [*A*].

$$\begin{bmatrix} 1{\cdot}5753 & 0{\cdot}3721 & -0{\cdot}1563 & 0{\cdot}5694 & 0{\cdot}0219 \\ 0{\cdot}3721 & 4{\cdot}8893 & -0{\cdot}0123 & 0{\cdot}7054 & -0{\cdot}1680 \\ -0{\cdot}1563 & -0{\cdot}0123 & 0{\cdot}3645 & -0{\cdot}3370 & 0{\cdot}1180 \\ 0{\cdot}5694 & 0{\cdot}7054 & -0{\cdot}3370 & 1{\cdot}0004 & -0{\cdot}0404 \\ 0{\cdot}0219 & -0{\cdot}1680 & 0{\cdot}1180 & -0{\cdot}0404 & 0{\cdot}3534 \end{bmatrix}$$

Aerodynamic Damping Coefficients [*B*].

$$\begin{bmatrix} 0{\cdot}0755 & 0{\cdot}1152 & 0{\cdot}0038 & 0{\cdot}0853 & 0{\cdot}0134 \\ -0{\cdot}0342 & 0{\cdot}1033 & 0{\cdot}0125 & 0{\cdot}0064 & 0{\cdot}0023 \\ -0{\cdot}0030 & -0{\cdot}0070 & 0{\cdot}0480 & -0{\cdot}0386 & 0{\cdot}0571 \\ 0{\cdot}0349 & 0{\cdot}1030 & -0{\cdot}0375 & 0{\cdot}1299 & -0{\cdot}0393 \\ 0{\cdot}0055 & 0{\cdot}0044 & -0{\cdot}0093 & 0{\cdot}0152 & 0{\cdot}0434 \end{bmatrix}$$

TABLE II.3—*continued*

Case 3. (*continued*)

Aerodynamic Stiffness Coefficients [*C*].

0·0579	0·2492	0·0266	0·1159	0·0692
−0·0751	−0·3007	0·0179	−0·1609	0·0030
0·0017	0·0172	0·0315	0·0047	0·0583
0·0052	0·0177	0·0045	0·0170	−0·0050
0·0124	0·0153	−0·0736	0·0581	−0·1201

Structural Stiffness Coefficients [*E*].

0·0378	0	0	0	0
0	0·5574	0	0	0
0	0	0·2216	0	0
0	0	0	1·0583	0
0	0	0	0	1·0881

Case 4.

Inertia Coefficients [*A*].

3·4620	0·2932	−0·1451	0·8407	−0·0573
0·2932	1·4448	−0·0216	0·0764	0·1442
−0·1451	−0·0216	0·3828	−0·2847	0·0745
0·8407	0·0764	−0·2847	0·4350	−0·0130
−0·0573	0·1442	0·0745	−0·0130	0·4074

Aerodynamic Damping Coefficients [*B*].

0·0711	0·0193	0·0089	0·0607	0·0708
0·1151	0·1074	0·0061	0·0799	0·1338
−0·0025	0·0024	0·0506	−0·0120	−0·0232
0·0185	−0·0200	−0·0094	0·0451	0·0416
0·0624	0·0170	−0·1049	0·1170	0·2416

Aerodynamic Stiffness Coefficients [*C*].

0·0610	−0·0571	0·0311	0·0866	0·0976
0·1512	−0·1347	0·0457	0·2253	0·2471
0·0012	−0·0006	0·0328	0·0132	0·0282
−0·0090	0·0085	0·0041	−0·0103	−0·0079
0·0428	−0·0096	−0·1234	0·0898	0·0693

Structural Stiffness Coefficients [*E*].

0·0411	0	0	0	0
0	0·2233	0	0	0
0	0	0·2350	0	0
0	0	0	0·4462	0
0	0	0	0	0·9503

Case 5.

Inertia Coefficients [*A*].

8·2886	−0·1533	−0·1454	2·2841	0·2081
−0·1533	7·4898	0·2765	2·0541	−0·3916
−0·1454	0·2765	0·6168	−0·0781	−0·1283
2·2841	2·0541	−0·0781	7·3403	0·6257
0·2081	−0·3916	−0·1283	0·6257	0·4395

TABLE II.3—*continued*

Case 5. (*continued*)

Aerodynamic Damping Coefficients [*B*].

$$\begin{bmatrix} 0{\cdot}0877 & 0{\cdot}2854 & 0{\cdot}0882 & 0{\cdot}1705 & 0{\cdot}0228 \\ 0{\cdot}1307 & 0{\cdot}8555 & 0{\cdot}1913 & 0{\cdot}8905 & -0{\cdot}0374 \\ -0{\cdot}0247 & -0{\cdot}0727 & 0{\cdot}0815 & -0{\cdot}0237 & -0{\cdot}0001 \\ -0{\cdot}1116 & -0{\cdot}0121 & 0{\cdot}0231 & 0{\cdot}8918 & 0{\cdot}0330 \\ 0{\cdot}0218 & 0{\cdot}0336 & 0{\cdot}0057 & 0{\cdot}1088 & 0{\cdot}0582 \end{bmatrix}$$

Aerodynamic Stiffness Coefficients [*C*].

$$\begin{bmatrix} 0{\cdot}0323 & 0{\cdot}3668 & 0{\cdot}2305 & 0{\cdot}4876 & 0{\cdot}0261 \\ 0{\cdot}0445 & 0{\cdot}4982 & 0{\cdot}2266 & 0{\cdot}6016 & -0{\cdot}0278 \\ -0{\cdot}0244 & -0{\cdot}2748 & -0{\cdot}0709 & -0{\cdot}3608 & 0{\cdot}0293 \\ -0{\cdot}0936 & -1{\cdot}0560 & -0{\cdot}3850 & -1{\cdot}3716 & 0{\cdot}0656 \\ 0{\cdot}0072 & 0{\cdot}0996 & 0{\cdot}0603 & 0{\cdot}2096 & 0{\cdot}0356 \end{bmatrix}$$

Structural Stiffness Coefficients [*E*].

$$\begin{bmatrix} 0{\cdot}0986 & 0 & 0 & 0 & 0 \\ 0 & 2{\cdot}2238 & 0 & 0 & 0 \\ 0 & 0 & 0{\cdot}7002 & 0 & 0 \\ 0 & 0 & 0 & 9{\cdot}8851 & 0 \\ 0 & 0 & 0 & 0 & 0{\cdot}9610 \end{bmatrix}$$

Case 6.

Inertia Coefficients [*A*].

$$\begin{bmatrix} 72{\cdot}1952 & -1{\cdot}1067 & -0{\cdot}0123 & 0{\cdot}4662 & -10{\cdot}6606 & -0{\cdot}1960 \\ -1{\cdot}1067 & 4{\cdot}5742 & 0{\cdot}2276 & -0{\cdot}0699 & 2{\cdot}2330 & 0{\cdot}1544 \\ -0{\cdot}0123 & 0{\cdot}2276 & 5{\cdot}3316 & 0{\cdot}1248 & 1{\cdot}6664 & 0{\cdot}0746 \\ 0{\cdot}4662 & -0{\cdot}0699 & 0{\cdot}1248 & 0{\cdot}4896 & -0{\cdot}8025 & 0{\cdot}0011 \\ -10{\cdot}6606 & 2{\cdot}2330 & 1{\cdot}6664 & -0{\cdot}8025 & 23{\cdot}5312 & 0{\cdot}6043 \\ -0{\cdot}1960 & 0{\cdot}1544 & 0{\cdot}0746 & 0{\cdot}0010 & 0{\cdot}6042 & 0{\cdot}4470 \end{bmatrix}$$

Aerodynamic Damping Coefficients [*B*].

$$\begin{bmatrix} 0{\cdot}4386 & -0{\cdot}1987 & -0{\cdot}6294 & -0{\cdot}1137 & -0{\cdot}2692 & 0{\cdot}0522 \\ -0{\cdot}0179 & 0{\cdot}0550 & 0{\cdot}1738 & 0{\cdot}0569 & 0{\cdot}2096 & -0{\cdot}0241 \\ -0{\cdot}0788 & 0{\cdot}1234 & 0{\cdot}6591 & 0{\cdot}1078 & 1{\cdot}2827 & -0{\cdot}0704 \\ 0{\cdot}1153 & 0{\cdot}0001 & -0{\cdot}0461 & 0{\cdot}0608 & -0{\cdot}0633 & -0{\cdot}0230 \\ 0{\cdot}7060 & -0{\cdot}1751 & -0{\cdot}2602 & -0{\cdot}0999 & 2{\cdot}4824 & 0{\cdot}0930 \\ -0{\cdot}0365 & 0{\cdot}0008 & -0{\cdot}0122 & -0{\cdot}0289 & 0{\cdot}0501 & 0{\cdot}0336 \end{bmatrix}$$

Aerodynamic Stiffness Coefficients [*C*].

$$\begin{bmatrix} -0{\cdot}9800 & -0{\cdot}2128 & -0{\cdot}9415 & -0{\cdot}5433 & -2{\cdot}6305 & 0{\cdot}2440 \\ 0{\cdot}2337 & 0{\cdot}0451 & 0{\cdot}1801 & 0{\cdot}1174 & 0{\cdot}5178 & -0{\cdot}0518 \\ 0{\cdot}2177 & 0{\cdot}0752 & 0{\cdot}4340 & 0{\cdot}1758 & 1{\cdot}1605 & -0{\cdot}0857 \\ 0{\cdot}0067 & -0{\cdot}0147 & -0{\cdot}1306 & -0{\cdot}0191 & -0{\cdot}3714 & 0{\cdot}0129 \\ -0{\cdot}8134 & -0{\cdot}2867 & -1{\cdot}7013 & -0{\cdot}6278 & -4{\cdot}6894 & 0{\cdot}3183 \\ 0{\cdot}0513 & 0{\cdot}0082 & 0{\cdot}0302 & 0{\cdot}0115 & 0{\cdot}1678 & 0{\cdot}0047 \end{bmatrix}$$

Structural Stiffness Coefficients [*E*].

$$\begin{bmatrix} 1{\cdot}8731 & 0 & 0 & 0 & 0 & 0 \\ 0 & 0{\cdot}0373 & 0 & 0 & 0 & 0 \\ 0 & 0 & 1{\cdot}5450 & 0 & 0 & 0 \\ 0 & 0 & 0 & 0{\cdot}5487 & 0 & 0 \\ 0 & 0 & 0 & 0 & 32{\cdot}3016 & 0 \\ 0 & 0 & 0 & 0 & 0 & 0{\cdot}6127 \end{bmatrix}$$

TABLE II.3—*continued*

Case 7.

Inertia Coefficients [*A*].

$$\begin{bmatrix} 6\cdot3369 & 3\cdot0712 & -0\cdot5948 & -1\cdot9658 & 0\cdot4094 \\ 3\cdot0712 & 4\cdot8808 & 0\cdot0219 & -3\cdot3098 & -0\cdot0752 \\ -0\cdot5948 & 0\cdot0219 & 0\cdot6420 & 1\cdot3815 & -0\cdot0754 \\ -1\cdot9658 & -3\cdot3098 & 1\cdot3815 & 27\cdot8351 & -0\cdot7405 \\ 0\cdot4094 & -0\cdot0752 & -0\cdot0754 & -0\cdot7405 & 0\cdot3975 \end{bmatrix}$$

Aerodynamic Damping Coefficients [*B*].

$$\begin{bmatrix} 0\cdot2249 & 0\cdot4477 & 0\cdot1223 & -0\cdot1486 & 0\cdot0161 \\ 0\cdot1292 & 0\cdot6463 & 0\cdot1529 & -1\cdot1676 & -0\cdot0439 \\ -0\cdot0620 & -0\cdot0504 & 0\cdot0742 & 0\cdot1228 & 0\cdot0075 \\ 0\cdot4727 & 0\cdot2860 & 0\cdot1621 & 3\cdot1698 & -0\cdot0325 \\ 0\cdot0027 & 0\cdot0031 & -0\cdot0054 & -0\cdot0689 & 0\cdot0530 \end{bmatrix}$$

Aerodynamic Stiffness Coefficients [*C*].

$$\begin{bmatrix} -0\cdot0357 & 0\cdot6774 & 0\cdot3925 & -1\cdot0075 & 0\cdot0701 \\ 0\cdot0204 & 0\cdot3221 & 0\cdot1428 & -0\cdot5382 & -0\cdot0283 \\ -0\cdot0250 & -0\cdot2346 & -0\cdot0594 & 0\cdot5646 & 0\cdot0341 \\ 0\cdot0800 & 2\cdot1332 & 0\cdot8889 & -4\cdot1012 & -0\cdot0612 \\ -0\cdot0021 & 0\cdot0510 & 0\cdot0165 & -0\cdot1482 & 0\cdot0115 \end{bmatrix}$$

Structural Stiffness Coefficients [*E*].

$$\begin{bmatrix} 0\cdot2927 & 0 & 0 & 0 & 0 \\ 0 & 1\cdot5550 & 0 & 0 & 0 \\ 0 & 0 & 0\cdot7205 & 0 & 0 \\ 0 & 0 & 0 & 38\cdot5219 & 0 \\ 0 & 0 & 0 & 0 & 0\cdot9130 \end{bmatrix}$$

Case 1A.

Inertia Coefficients [*A*].

$$\begin{bmatrix} 1\cdot9050 & -0\cdot1883 & -0\cdot4631 & -0\cdot0942 & 0\cdot1751 & 0\cdot0736 \\ -0\cdot1883 & 0\cdot6784 & 0\cdot2901 & 0\cdot7501 & 0\cdot5344 & 0\cdot1386 \\ -0\cdot4631 & 0\cdot2901 & 1\cdot4952 & -0\cdot0326 & -0\cdot1239 & -0\cdot3510 \\ -0\cdot0942 & 0\cdot7501 & -0\cdot0326 & 1\cdot0035 & 0\cdot1758 & 0\cdot2575 \\ 0\cdot1751 & 0\cdot5344 & -0\cdot1239 & 0\cdot1758 & 5\cdot9150 & 0\cdot2404 \\ 0\cdot0736 & 0\cdot1386 & -0\cdot3510 & 0\cdot2575 & 0\cdot2404 & 0\cdot2911 \end{bmatrix}$$

Aerodynamic Damping Coefficients [*B*].

$$\begin{bmatrix} 0\cdot2534 & -0\cdot1864 & -0\cdot1745 & -0\cdot1931 & -0\cdot0142 & -0\cdot0268 \\ 0\cdot0646 & 0\cdot0929 & 0\cdot0190 & 0\cdot1058 & 0\cdot1360 & 0\cdot0451 \\ 0\cdot0283 & 0\cdot0636 & 0\cdot2081 & 0\cdot0386 & -0\cdot0603 & -0\cdot0823 \\ 0\cdot0820 & 0\cdot0965 & -0\cdot0384 & 0\cdot1301 & 0\cdot0896 & 0\cdot0765 \\ 0\cdot0240 & 0\cdot0281 & -0\cdot0304 & -0\cdot0123 & 0\cdot8647 & 0\cdot0750 \\ 0\cdot0280 & 0\cdot0026 & -0\cdot0257 & 0\cdot0068 & 0\cdot0210 & 0\cdot0430 \end{bmatrix}$$

Aerodynamic Stiffness Coefficients [*C*].

$$\begin{bmatrix} 0\cdot1885 & -0\cdot4444 & -0\cdot3103 & -0\cdot4821 & -0\cdot1713 & -0\cdot1710 \\ 0\cdot1215 & -0\cdot2215 & -0\cdot2708 & -0\cdot2287 & 0\cdot1366 & 0\cdot0059 \\ 0\cdot1067 & -0\cdot2542 & -0\cdot1758 & -0\cdot2714 & -0\cdot1784 & -0\cdot1043 \\ 0\cdot1365 & -0\cdot2315 & -0\cdot3266 & -0\cdot2303 & 0\cdot1657 & 0\cdot0367 \\ 0\cdot0205 & -0\cdot0361 & -0\cdot0496 & -0\cdot0274 & 0\cdot0292 & 0\cdot0315 \\ 0\cdot0154 & -0\cdot0802 & 0\cdot0245 & -0\cdot0984 & -0\cdot1314 & -0\cdot0907 \end{bmatrix}$$

TABLE II.3—*continued*

Case 1A. (*continued*)

Structural Stiffness Coefficients [*E*].

0·0750	0	0	0	0	0
0	0·1040	0	0	0	0
0	0	0·6440	0	0	0
0	0	0	0·6310	0	0
0	0	0	0	8·8210	0
0	0	0	0	0	0·8540

Case 5A.

Inertia Coefficients [*A*].

3·9901	0·0093	0·8174	−0·3245	−1·1425	−0·1353
0·0093	2·9112	1·3759	1·2912	1·3460	0·9482
0·8174	1·3759	8·6622	0·3992	−1·3933	−0·2639
−0·3245	1·2912	0·3992	1·3513	2·4970	0·4405
−1·1425	1·3460	−1·3933	2·4970	6·9741	0·4060
−0·1353	0·9482	−0·2639	0·4405	0·4060	0·6751

Aerodynamic Damping Coefficients [*B*].

0·0812	0·0714	0·3061	0·1002	0·1082	0·0267
0·0264	0·0364	0·1570	0·0667	0·0758	0·0112
0·1328	0·1563	1·1580	0·3060	0·3068	−0·1001
−0·0354	0·0048	−0·1238	0·1107	0·2078	0·0295
−0·0723	−0·0219	−0·5190	0·2179	0·6087	0·0490
0·0129	0·0189	−0·0097	0·0027	−0·0194	0·0569

Aerodynamic Stiffness Coefficients [*C*].

0·0422	0·1179	0·3986	0·2583	0·3139	−0·0728
0·0093	0·0261	0·0869	0·0572	0·0697	0·0149
0·0445	0·0909	0·4976	0·2562	0·3154	−0·0077
−0·0401	−0·0685	−0·5239	−0·1765	−0·1873	0·0605
−0·0718	−0·1171	−1·0536	−0·1768	−0·0977	0·1115
0·0104	0·0649	0·1247	0·0386	0·0359	0·0093

Structural Stiffness Coefficients [*E*].

0·0347	0	0	0	0	0
0	0·0581	0	0	0	0
0	0	1·9584	0	0	0
0	0	0	1·1877	0	0
0	0	0	0	6·2970	0
0	0	0	0	0	1·2467

Case 6A.

Inertia Coefficients [*A*].

6·5262	12·8727	0·7011	0·6063	1·7250
12·8727	55·3324	0·9433	6·9126	7·1105
0·7011	0·9433	1·5550	−0·7922	−0·1030
0·6063	6·9126	−0·7922	4·2696	1·1867
1·7250	7·1105	−0·1030	1·1867	1·4550

TABLE II.3—*continued*

Case 6A. (*continued*)

Aerodynamic Damping Coefficients [*B*].

$$\begin{bmatrix} 0{\cdot}1142 & 0{\cdot}1348 & 0{\cdot}1497 & 0{\cdot}1051 & 0{\cdot}0370 \\ -0{\cdot}0941 & 0{\cdot}1575 & 0{\cdot}0077 & 0{\cdot}1345 & -0{\cdot}0634 \\ 0{\cdot}0826 & 0{\cdot}1930 & 0{\cdot}2078 & 0{\cdot}1385 & -0{\cdot}0363 \\ -0{\cdot}1440 & 0{\cdot}0069 & -0{\cdot}2654 & 0{\cdot}3218 & 0{\cdot}0580 \\ 0{\cdot}0250 & 0{\cdot}0387 & -0{\cdot}0034 & 0{\cdot}0293 & 0{\cdot}0697 \end{bmatrix}$$

Aerodynamic Stiffness Coefficients [*C*].

$$\begin{bmatrix} 0{\cdot}0842 & 0{\cdot}4105 & 0{\cdot}1739 & 0{\cdot}3563 & 0{\cdot}0776 \\ -0{\cdot}1276 & -0{\cdot}6393 & -0{\cdot}2319 & -0{\cdot}5330 & -0{\cdot}1597 \\ 0{\cdot}0360 & 0{\cdot}1558 & 0{\cdot}1020 & 0{\cdot}1508 & -0{\cdot}0099 \\ -0{\cdot}1709 & -0{\cdot}6742 & -0{\cdot}5597 & -0{\cdot}5903 & 0{\cdot}0983 \\ 0{\cdot}0230 & 0{\cdot}1142 & 0{\cdot}0481 & 0{\cdot}1056 & 0{\cdot}0134 \end{bmatrix}$$

Structural Stiffness Coefficients [*E*].

$$\begin{bmatrix} 0{\cdot}0483 & 0 & 0 & 0 & 0 \\ 0 & 1{\cdot}0432 & 0 & 0 & 0 \\ 0 & 0 & 0{\cdot}3375 & 0 & 0 \\ 0 & 0 & 0 & 3{\cdot}9746 & 0 \\ 0 & 0 & 0 & 0 & 2{\cdot}6767 \end{bmatrix}$$

TABLE II.4

Flutter Calculations Based on Resonance Test Modes

Check on the Orthogonal Properties of the Resonance Modes:

Matrices showing the Magnitide of the Inertia Couplings expressed in the form $\{a_{RS}/\sqrt{(a_{RR}a_{SS})}\}$

Case 1.

$$\begin{bmatrix} 1{\cdot}000 & -0{\cdot}191 & -0{\cdot}144 & -0{\cdot}131 \\ -0{\cdot}191 & 1{\cdot}000 & 0{\cdot}044 & -0{\cdot}260 \\ -0{\cdot}144 & 0{\cdot}044 & 1{\cdot}000 & 0{\cdot}156 \\ -0{\cdot}131 & -0{\cdot}260 & 0{\cdot}156 & 1{\cdot}000 \end{bmatrix}$$

Case 2.

$$\begin{bmatrix} 1{\cdot}000 & -0{\cdot}056 & -0{\cdot}133 & 0{\cdot}114 & 0{\cdot}116 \\ -0{\cdot}056 & 1{\cdot}000 & 0{\cdot}022 & -0{\cdot}443 & -0{\cdot}178 \\ -0{\cdot}133 & 0{\cdot}022 & 1{\cdot}000 & 0{\cdot}799 & 0{\cdot}263 \\ 0{\cdot}114 & -0{\cdot}443 & 0{\cdot}799 & 1{\cdot}000 & 0{\cdot}553 \\ 0{\cdot}116 & -0{\cdot}178 & 0{\cdot}263 & 0{\cdot}553 & 1{\cdot}000 \end{bmatrix}$$

Case 3.

$$\begin{bmatrix} 1{\cdot}000 & 0{\cdot}134 & -0{\cdot}206 & 0{\cdot}453 & 0{\cdot}029 \\ 0{\cdot}134 & 1{\cdot}000 & -0{\cdot}092 & 0{\cdot}319 & -0{\cdot}127 \\ -0{\cdot}206 & -0{\cdot}092 & 1{\cdot}000 & -0{\cdot}558 & 0{\cdot}329 \\ 0{\cdot}453 & 0{\cdot}319 & -0{\cdot}558 & 1{\cdot}000 & -0{\cdot}068 \\ 0{\cdot}029 & -0{\cdot}127 & 0{\cdot}329 & -0{\cdot}068 & 1{\cdot}000 \end{bmatrix}$$

TABLE II.4—*continued*

Case 4.

1·000	0·131	−0·127	0·685	0·048
0·131	1·000	−0·029	0·096	0·188
−0·127	−0·029	1·000	−0·699	0·188
0·685	0·096	−0·699	1·000	−0·031
0·048	0·188	0·188	−0·031	1·000

Case 5.

1·000	−0·019	−0·064	0·293	0·109
−0·019	1·000	0·129	0·278	0·216
−0·064	0·129	1·000	−0·037	−0·246
0·293	0·278	−0·037	1·000	0·350
0·109	0·216	−0·246	0·350	1·000

Case 6.

1·000	−0·061	−0·001	0·079	−0·258	−0·034
−0·061	1·000	0·046	−0·047	−0·215	0·108
−0·001	0·046	1·000	0·076	0·149	0·047
0·079	−0·047	0·076	1·000	−0·236	0·002
−0·258	0·215	0·149	−0·236	1·000	0·186
−0·034	0·108	0·047	0·002	0·186	1·000

Case 7.

1·000	0·551	−0·294	−0·148	0·258
0·551	1·000	0·012	−0·285	−0·054
−0·294	0·012	1·000	0·327	−0·149
−0·148	−0·285	0·327	1·000	−0·223
0·258	−0·054	−0·149	−0·223	1·000

Case 1A.

1·000	−0·166	−0·274	−0·068	0·052	0·096
−0·166	1·000	0·289	0·910	0·266	0·312
−0·274	0·289	1·000	−0·027	−0·042	−0·533
−0·068	0·910	−0·027	1·000	0·072	0·476
0·052	0·266	−0·042	0·072	1·000	0·183
0·096	0·312	−0·533	0·476	0·183	1·000

Case 5A.

1·000	0·003	0·139	−0·140	−0·217	−0·083
0·003	1·000	0·274	0·651	0·298	0·675
0·139	0·274	1·000	0·117	−0·180	−0·109
−0·140	0·651	0·117	1·000	0·814	0·460
−0·217	0·298	−0·180	0·814	1·000	0·187
−0·083	0·675	−0·109	0·460	0·187	1·000

Case 6A.

1·000	0·676	0·220	0·115	0·560
0·676	1·000	0·102	0·450	0·795
0·220	0·102	1·000	−0·308	−0·069
0·115	0·450	−0·308	1·000	0·476
0·560	0·795	−0·069	0·476	1·000

Theoretical Investigations on the Effect of a Localised Mass on the Flutter of a Delta Wing

The diagrams that follow show the effect of variations in the coefficients involved in the dominant binaries and ternaries for certain specified Cases.

The coefficients were varied individually and only those which have a significant effect upon the flutter speed have been included in the diagrams.

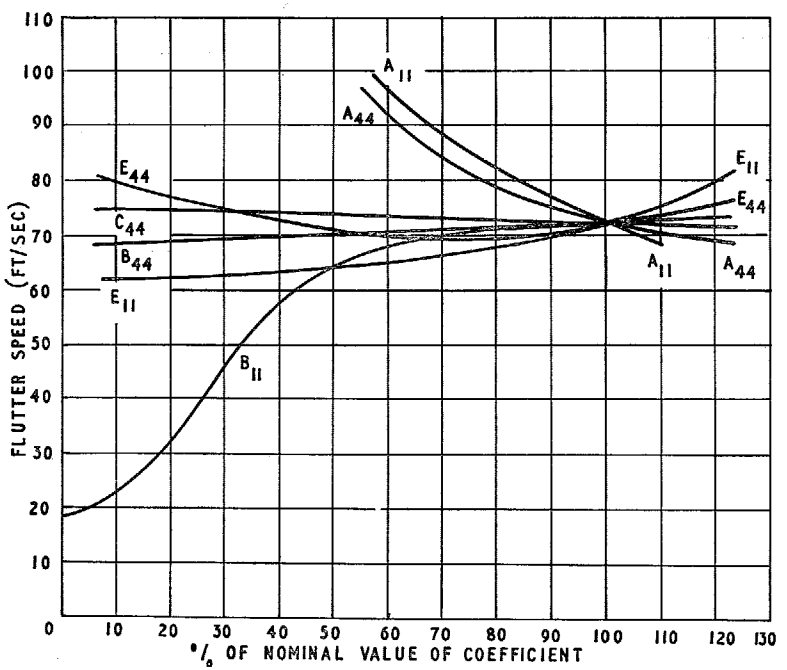

FIG. II.1. Effect of variation of direct coefficients on the flutter speed of the 1–4 binary. Flutter calculations based on arbitrary modes.

Case 4.

(*a*) Wing with original spar stiffness

(*b*) Localised mass { 70 per cent bare wing weight; Spanwise position: 75 per cent semi-span; Chordwise position: T.E.

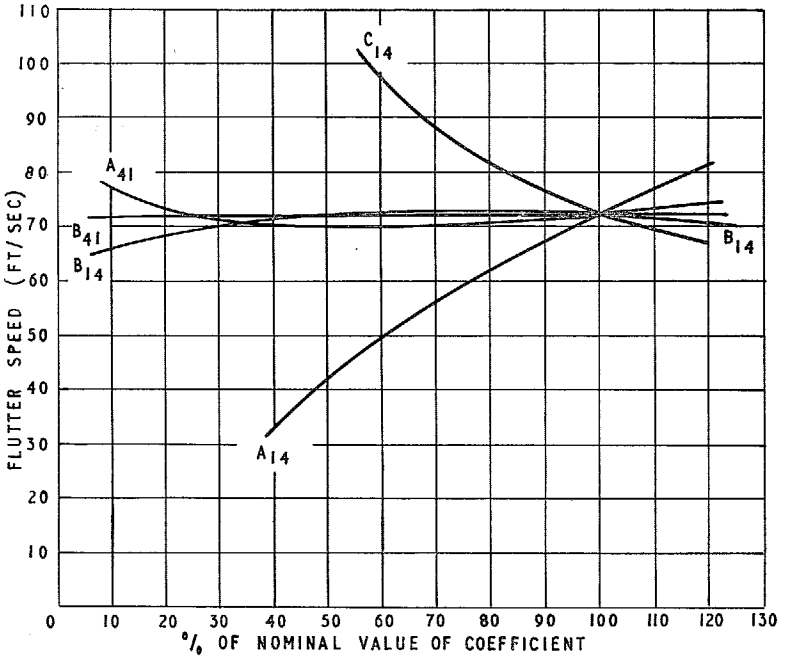

FIG. II.2. Effect of variation of cross-coupling coefficients on the flutter speed of the 1–4 binary. Flutter calculations based on arbitrary modes.

Case 4.

(*a*) Wing with original spar stiffness

(*b*) Localised mass { 70 per cent bare wing weight; Spanwise position: 75 per cent semi-span; Chordwise position: T.E.

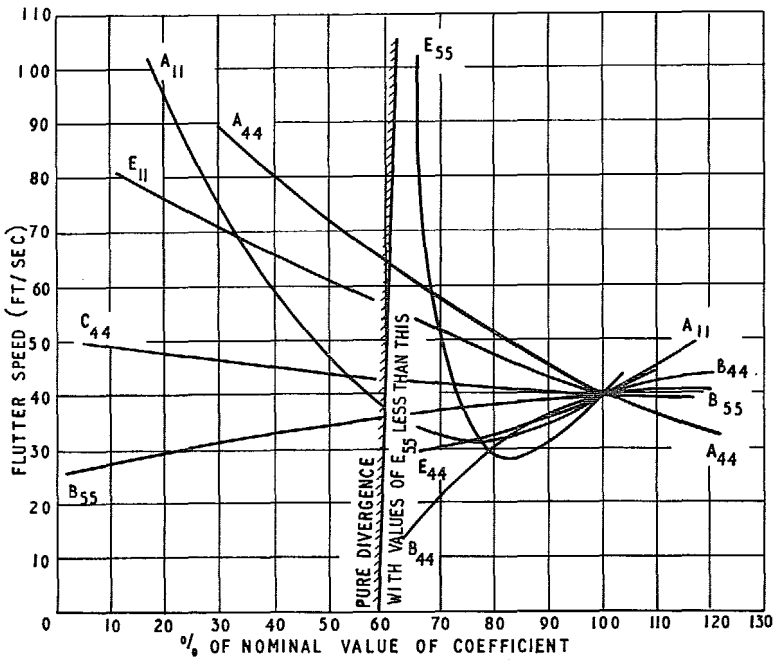

FIG. II.3. Effect of variation of direct coefficients on the flutter speed of the 1–4–5 ternary. Flutter calculations based on arbitrary modes.

Case 6.

(*a*) Wing with original spar stiffness

(*b*) Localised mass { 70 per cent bare wing weight; Spanwise position: Wing-tip; Chordwise position: 40 per cent chord aft of L.E.

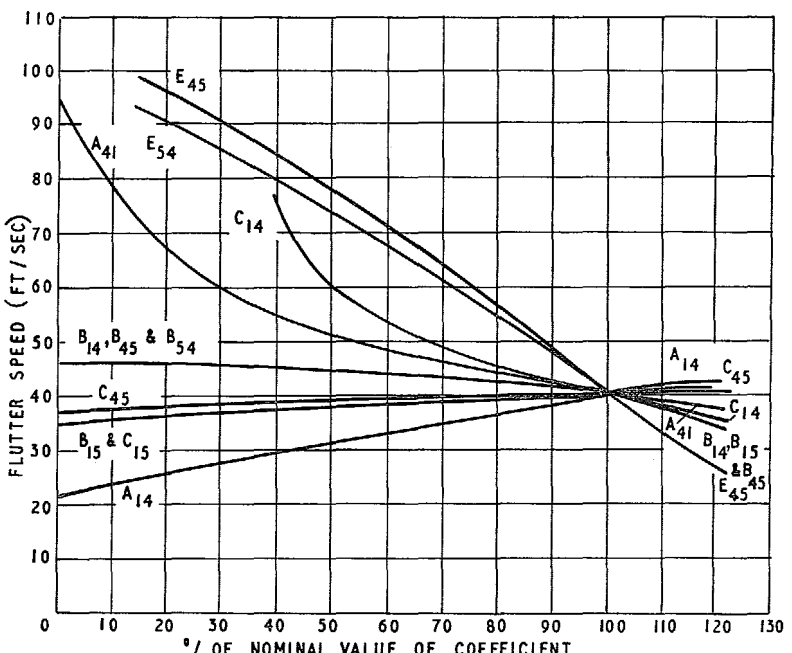

FIG. II.4. Effect of variation of cross-coupling coefficients on the flutter speed of the 1–4–5 ternary. Flutter calculations based on arbitrary modes.

Case 6.

(*a*) Wing with original spar stiffness

(*b*) Localised mass { 70 per cent bare wing weight; Spanwise position: Wing-tip; Chordwise position: 40 per cent aft of L.E.

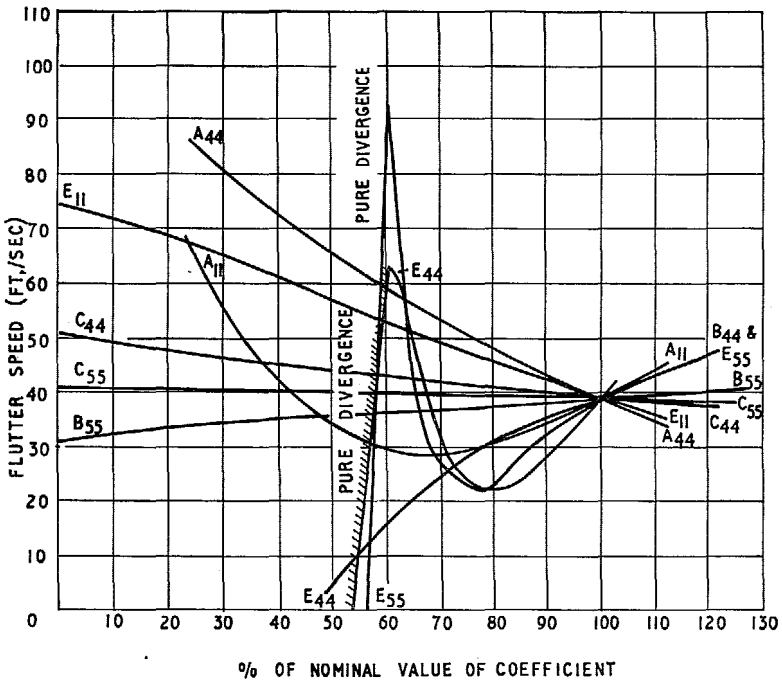

FIG. II.5. Effect of variation of direct coefficients on the flutter speed of the 1–4–5 ternary. Flutter calculations based on arbitrary modes.

Case 6A.

(*a*) Wing with spar modified to simulate cut-out

(*b*) Localised mass { 70 per cent bare wing weight; Spanwise position: Wing-tip; Chordwise position: 40 per cent aft of L.E.

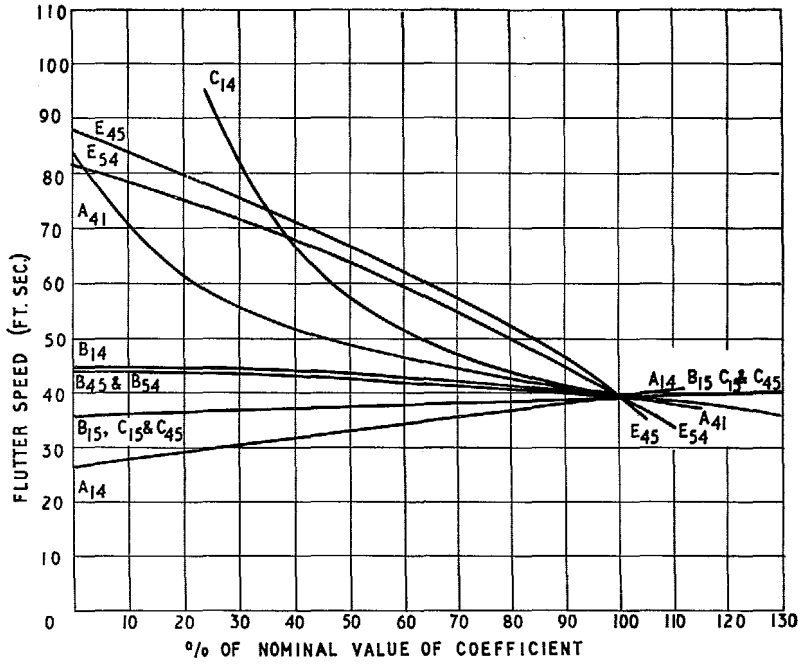

FIG. II.6. Effect of variation of cross-coupling coefficients on the flutter speed of the 1–4–5 ternary. Flutter calculations based on arbitrary modes.

Case 6A.

(*a*) Wing with spar modified to simulate cut-out

(*b*) Localised mass { 70 per cent bare wing weight; Spanwise position: Wing-tip; Chordwise position: 40 per cent aft of L.E.

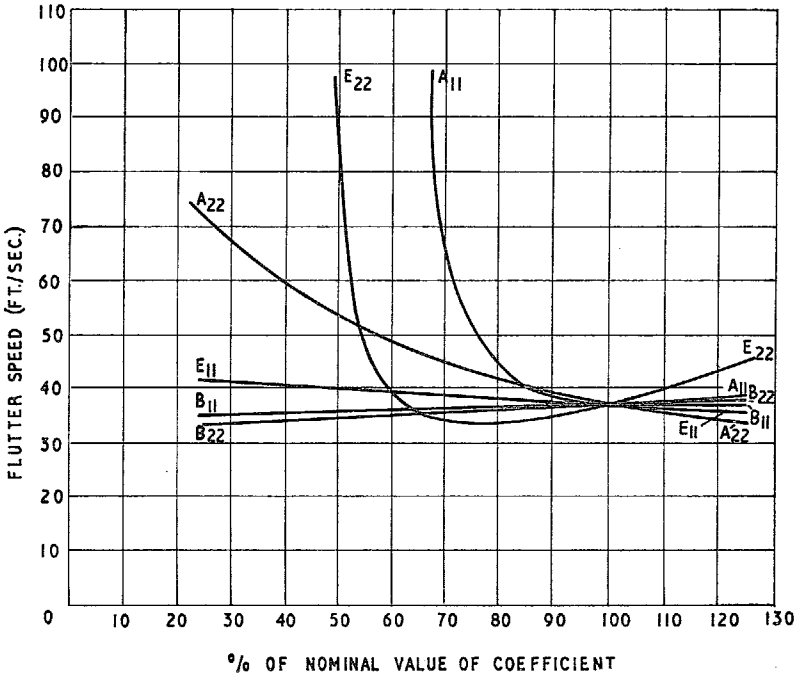

FIG. II.7. Effect of variation of direct coefficients on the flutter speed of the 1–2 binary. Flutter calculations based on resonance modes.

Case 2.

(*a*) Wing with original spar stiffness

(*b*) Localised mass { 70 per cent bare wing weight; Spanwise position: 75 per cent semi-span; Chordwise position: L.E.

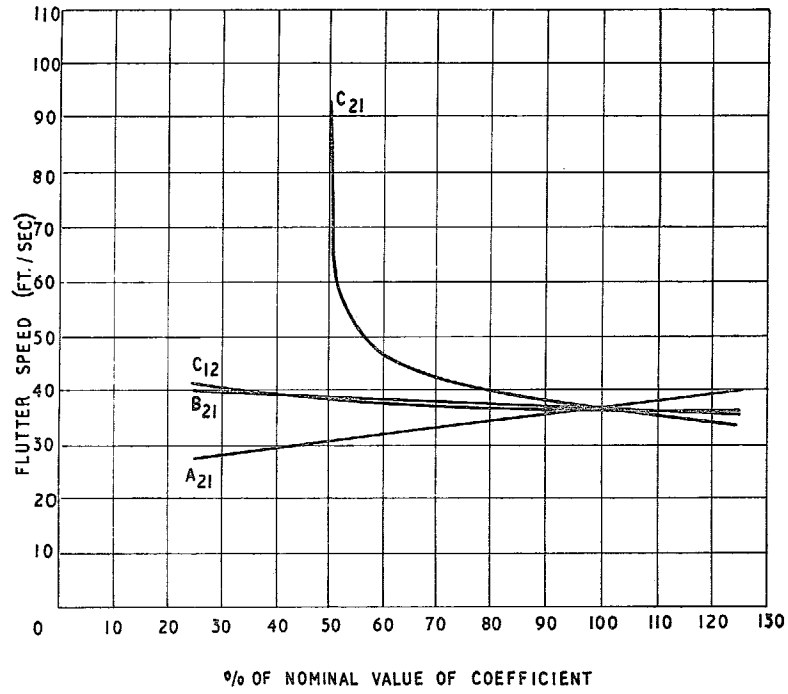

FIG. II.8. Effect of variation of cross-coupling coefficients on the flutter speed of the 1–2 binary. Flutter calculations based on resonance modes.

Case 2.

(*a*) Wing with original spar stiffness

(*b*) Localised mass { 70 per cent bare wing weight; Spanwise position: 75 per cent semi-span; Chordwise position: L.E.

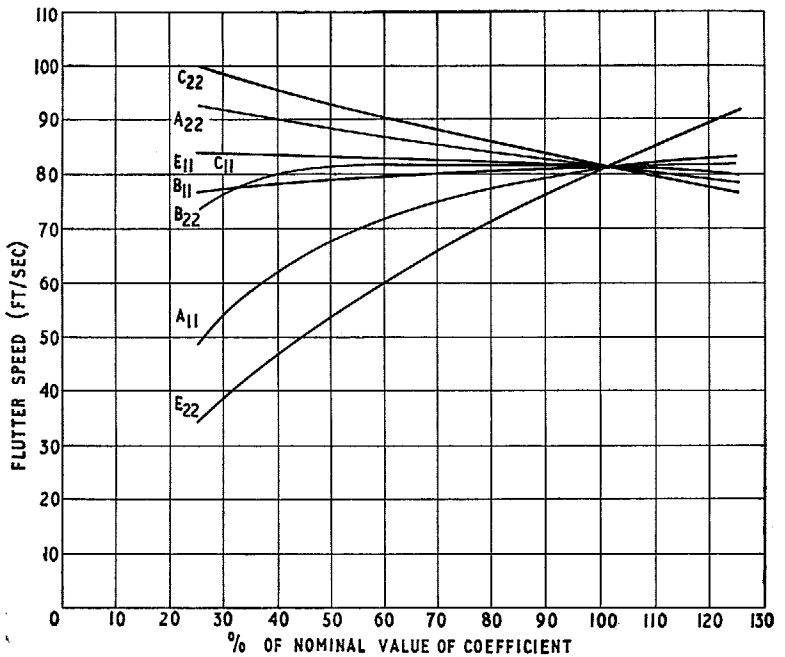

FIG. II.9. Effect of variation of direct coefficients on the flutter speed of the 1–2 binary. Flutter calculations based on resonance modes.

Case 4.

(*a*) Wing with original spar stiffness

(*b*) Localised mass { 70 per cent bare wing weight; Spanwise position: 75 per cent semi-span; Chordwise position: T.E.

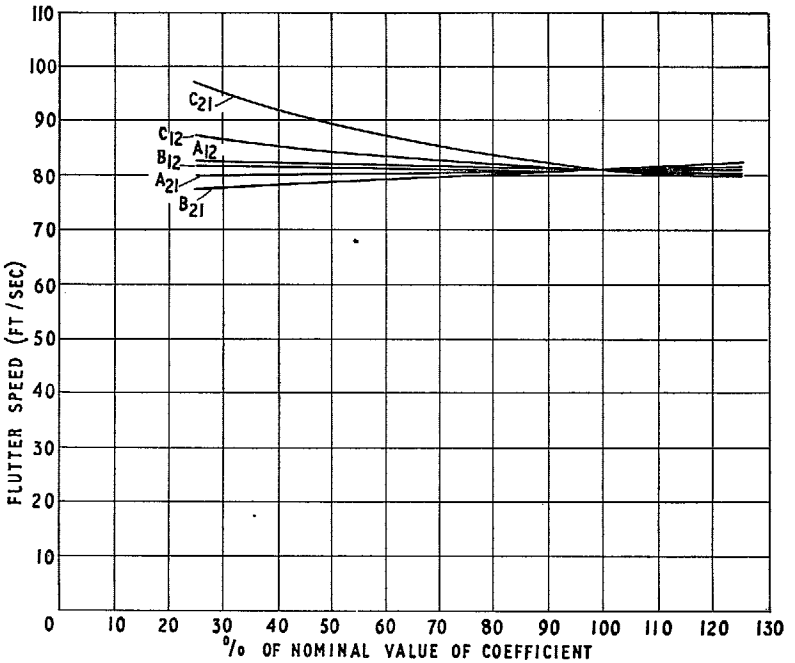

FIG. II.10. Effect of variation of cross-coupling coefficients on the flutter speed of the 1–2 binary. Flutter calculations based on resonance modes.

Case 4.

(*a*) Wing with original spar stiffness

(*b*) Localised mass { 70 per cent bare wing weight; Spanwise position: 75 per cent semi-span; Chordwise position: T.E.

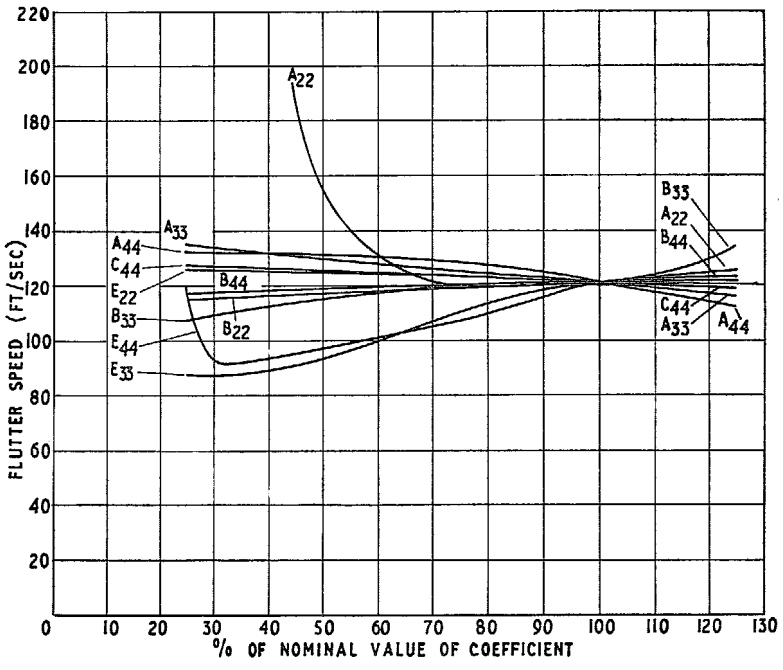

FIG. II.11. Effect on variation of direct coefficients on the flutter speed of the 2–3–4 Ternary. Flutter calculations based on resonance modes.

Case 5.

(*a*) Wing with original spar stiffness

(*b*) Localised mass { 70 per cent bare wing weight; Spanwise position: Wing-tip; Chordwise position: L.E.

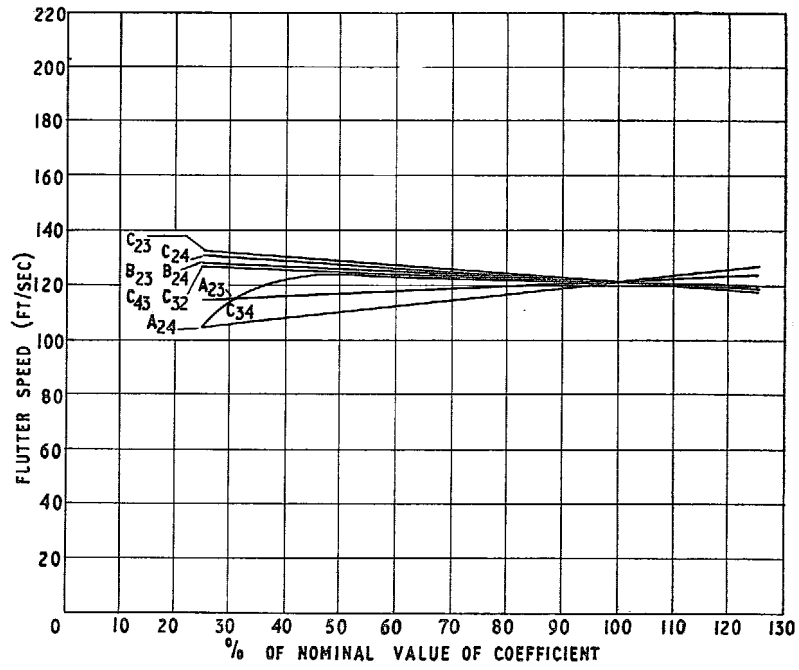

FIG. II.12. Effect of variation of cross-coupling coefficients on the flutter speed of the 2–3–4 ternary. Flutter calculations based on resonance modes.

Case 5.

(*a*) Wing with original spar stiffness

(*b*) Localised mass { 70 per cent bare wing weight; Spanwise position: Wing-tip; Chordwise position: L.E.

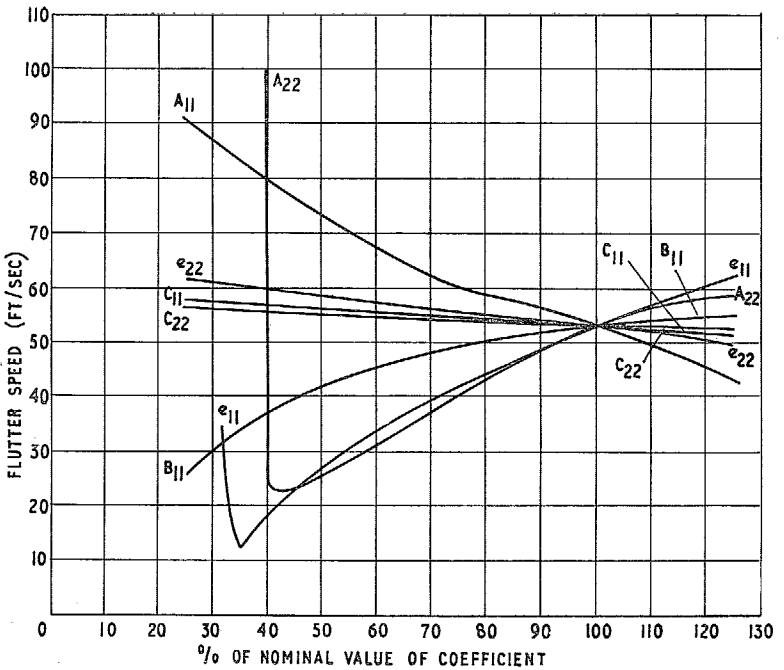

FIG. II.13. Effect of variation of direct coefficients on the flutter speed of the 1–2 binary. Flutter calculations based on resonance modes.

Case 6.

(*a*) Wing with original spar stiffness

(*b*) Localised mass { 70 per cent bare wing weight; Spanwise position: Wing-tip; Chordwise position: 40 per cent aft of L.E.

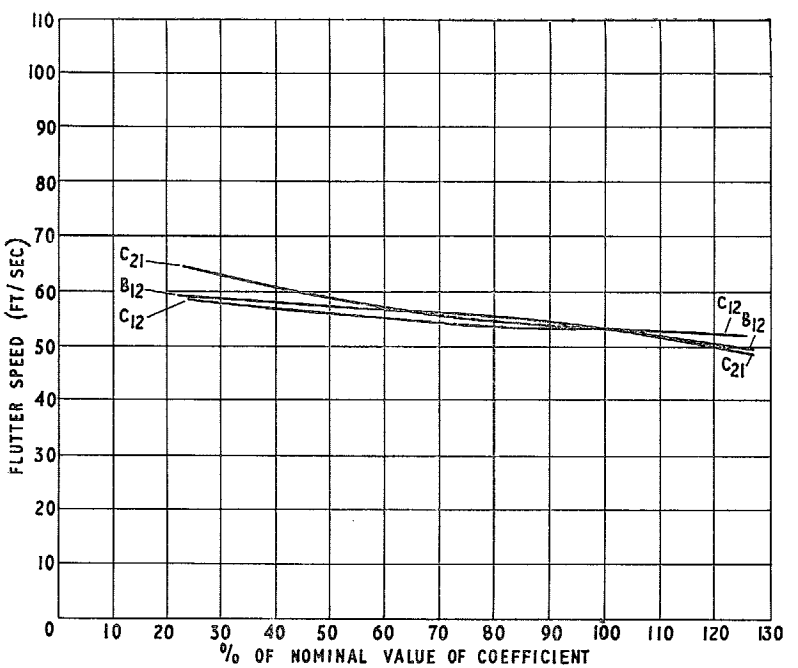

FIG. II.14. Effect of variation of cross-coupling coefficients on the flutter speed of the 1–2 binary. Flutter calculations based on resonance modes.

Case 6.

(*a*) Wing with original spar stiffness

(*b*) Localised mass { 70 per cent bare wing weight; Spanwise position: Wing-tip; Chordwise position: 40 per cent aft of L.E.

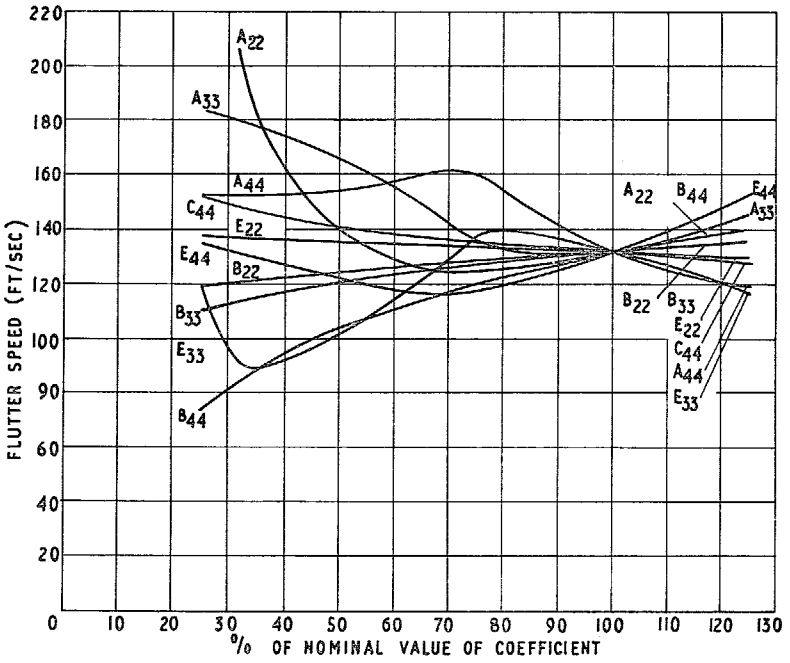

FIG. II.15. Effect of variation of direct coefficients on the flutter speed of the 2–3–4 ternary. Flutter calculations based on resonance modes.

Case 7.

(*a*) Wing with original spar stiffness

(*b*) Localised mass { 70 per cent bare wing weight; Spanwise position: Wing-tip; Chordwise position: T.E.

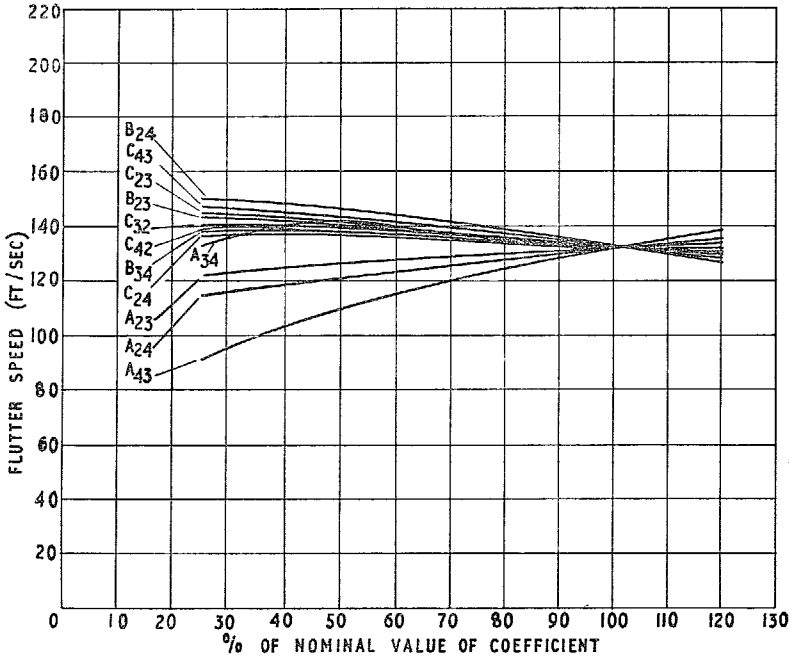

FIG. II.16. Effect of variation of cross-coupling coefficients on the flutter speed of the 2–3–4 ternary. Flutter calculations based on resonance modes.

Case 7.

(*a*) Wing with original spar stiffness

(*b*) Localised mass { 70 per cent bare wing weight; Spanwise position: Wing-tip; Chordwise position: T.E.

Publications of the Aeronautical Research Council

ANNUAL TECHNICAL REPORTS OF THE AERONAUTICAL RESEARCH COUNCIL (BOUND VOLUMES)

1941 Aero and Hydrodynamics, Aerofoils, Airscrews, Engines, Flutter, Stability and Control, Structures. 63*s.* (post 2*s.* 3*d.*)

1942 Vol. I. Aero and Hydrodynamics, Aerofoils, Airscrews, Engines. 75*s.* (post 2*s.* 3*d.*)
Vol. II. Noise, Parachutes, Stability and Control, Structures, Vibration, Wind Tunnels. 47*s.* 6*d.* (post 1*s.* 9*d.*)

1943 Vol. I. Aerodynamics, Aerofoils, Airscrews. 80*s.* (post 2*s.*)
Vol. II. Engines, Flutter, Materials, Parachutes, Performance, Stability and Control, Structures. 90*s.* (post 2*s.* 3*d.*)

1944 Vol. I. Aero and Hydrodynamics, Aerofoils, Aircraft, Airscrews, Controls. 84*s.* (post 2*s.* 6*d.*)
Vol. II. Flutter and Vibration, Materials, Miscellaneous, Navigation, Parachutes, Performance, Plates and Panels, Stability, Structures, Test Equipment, Wind Tunnels. 84*s.* (post 2*s.* 6*d.*)

1945 Vol. I. Aero and Hydrodynamics, Aerofoils. 130*s.* (post 3*s.*)
Vol. II. Aircraft, Airscrews, Controls. 130*s.* (post 3*s.*)
Vol. III. Flutter and Vibration, Instruments, Miscellaneous, Parachutes, Plates and Panels, Propulsion. 130*s.* (post 2*s.* 9*d.*)
Vol. IV. Stability, Structures, Wind Tunnels, Wind Tunnel Technique. 130*s.* (post 2*s.* 9*d.*)

1946 Vol. I. Accidents, Aerodynamics, Aerofoils and Hydrofoils. 168*s.* (post 3*s.* 3*d.*)
Vol. II. Airscrews, Cabin Cooling, Chemical Hazards, Controls, Flames, Flutter, Helicopters, Instruments and Instrumentation, Interference, Jets, Miscellaneous, Parachutes. 168*s.* (post 2*s.* 9*d.*)
Vol. III. Performance, Propulsion, Seaplanes, Stability, Structures, Wind Tunnels. 168*s.* (post 3*s.*)

1947 Vol. I. Aerodynamics, Aerofoils, Aircraft. 168*s.* (post 3*s.* 3*d.*)
Vol. II. Airscrews and Rotors, Controls, Flutter, Materials, Miscellaneous, Parachutes, Propulsion, Seaplanes, Stability, Structures, Take-off and Landing. 168*s.* (post 3*s.* 3*d.*)

Special Volumes

Vol. I. Aero and Hydrodynamics, Aerofoils, Controls, Flutter, Kites, Parachutes, Performance, Propulsion, Stability. 126*s.* (post 2*s.* 6*d.*)
Vol. II. Aero and Hydrodynamics, Aerofoils, Airscrews, Controls, Flutter, Materials, Miscellaneous, Parachutes, Propulsion, Stability, Structures. 147*s.* (post 2*s.* 6*d.*)
Vol. III. Aero and Hydrodynamics, Aerofoils, Airscrews, Controls, Flutter, Kites, Miscellaneous, Parachutes, Propulsion, Seaplanes, Stability, Structures, Test Equipment. 189*s.* (post 3*s.* 3*d.*)

Reviews of the Aeronautical Research Council

1939–48 3*s.* (post 5*d.*) 1949–54 5*s.* (post 5*d.*)

Index to all Reports and Memoranda published in the Annual Technical Reports

1909–1947 R. & M. 2600 6*s.* (post 2*d.*)

Indexes to the Reports and Memoranda of the Aeronautical Research Council

Between Nos. 2351–2449	R. & M. No. 2450 2*s.* (post 2*d.*)
Between Nos. 2451–2549	R. & M. No. 2550 2*s.* 6*d.* (post 2*d.*)
Between Nos. 2551–2649	R. & M. No. 2650 2*s.* 6*d.* (post 2*d.*)
Between Nos. 2651–2749	R. & M. No. 2750 2*s.* 6*d.* (post 2*d.*)
Between Nos. 2751–2849	R. & M. No. 2850 2*s.* 6*d.* (post 2*d.*)
Between Nos. 2851–2949	R. & M. No. 2950 3*s.* (post 2*d.*)
Between Nos. 2951–3049	R. & M. No. 3050 3*s.* 6*d.* (post 2*d.*)

HER MAJESTY'S STATIONERY OFFICE

from the addresses overleaf

© *Crown copyright* 1962

Printed and published by
HER MAJESTY'S STATIONERY OFFICE

To be purchased from
York House, Kingsway, London W.C.2
423 Oxford Street, London W.1
13A Castle Street, Edinburgh 2
109 St. Mary Street, Cardiff
39 King Street, Manchester 2
50 Fairfax Street, Bristol 1
35 Smallbrook, Ringway, Birmingham 5
80 Chichester Street, Belfast 1
or through any bookseller

Printed in England

S.O. Code No. 23-3264